LEVEL II

12

TECHNICAL REPORT S-78-17

FEASIBILITY STUDY OF AN EARTH MELTING PENETRATOR SYSTEM FOR GEOPROSPECTING TUNNEL RIGHT-OF-WAYS

by

D. L. Black
Westinghouse Advanced Energy
Systems Division
Large, Pennsylvania 15025

December 1978
Final Report

Approved For Public Release; Distribution Unlimited

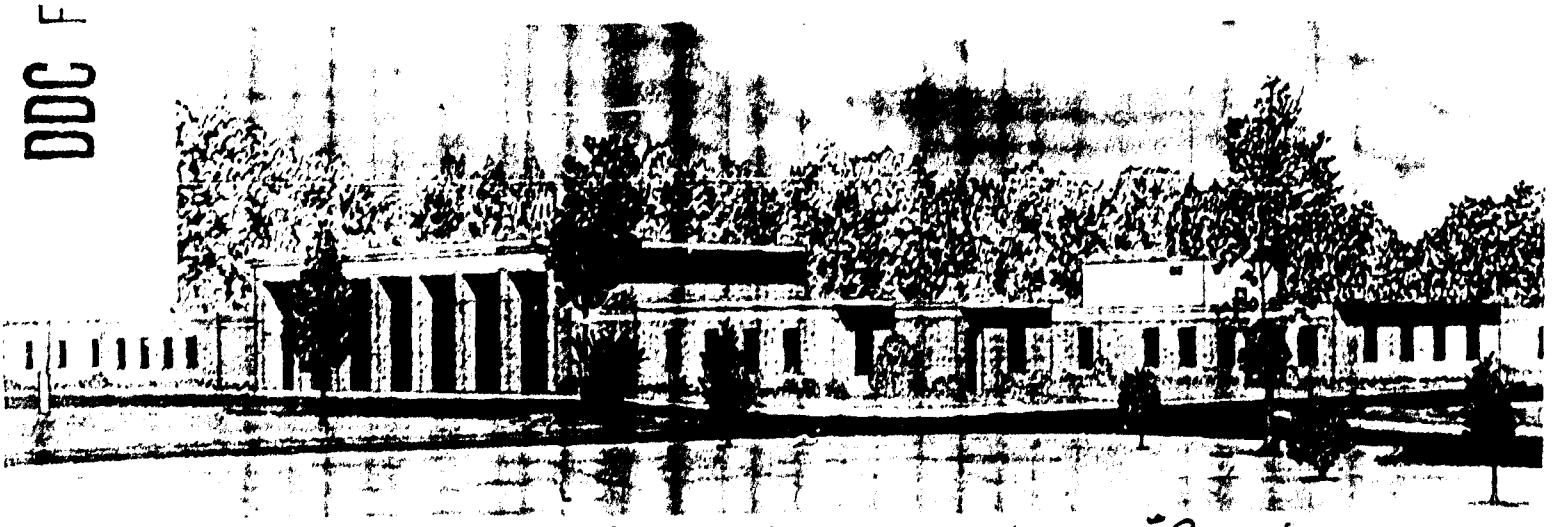

Prepared for Office, Chief of Engineers, U. S. Army
Washington, D. C. 20314

Under Contract No. DACW 39-76-C-0163

Monitored by Geotechnical Laboratory
U. S. Army Engineer Waterways Experiment Station
P. O. Box 631, Vicksburg, Miss. 39180

Destroy this report when no longer needed. Do not return it to the originator.

The findings in this report are not to be construed as an official Department of the Army position unless so designated by other authorized documents.

(18) WES

Unclassified

SECURITY CLASSIFICATION OF THIS PAGE (When Data Entered)

REPORT DOCUMENTATION PAGE	READ INSTRUCTIONS BEFORE COMPLETING FORM
1. REPORT NUMBER (14) Technical Report S-78-17 / 2. GOVT ACCESSION NO.	3. RECIPIENT'S CATALOG NUMBER
(1) 4. TITLE (and Subtitle) FEASIBILITY STUDY OF AN EARTH MELTING PENETRATOR SYSTEM FOR GEOPROSPECTING TUNNEL RIGHT-OF-WAYS,	(9) 5. TYPE OF REPORT & PERIOD COVERED Final report, 6. PERFORMING ORG. REPORT NUMBER 26 Oct 76 – 30 Mar 78.
(10) 7. AUTHOR(s) D. L. Black	(15) 8. CONTRACT OR GRANT NUMBER(s) Contract No. DACW 39-76-C-0163 new
9. PERFORMING ORGANIZATION NAME AND ADDRESS Westinghouse Advanced Energy Systems Division Large, Penn. 15025 No. 411143	10. PROGRAM ELEMENT, PROJECT, TASK AREA & WORK UNIT NUMBERS
11. CONTROLLING OFFICE NAME AND ADDRESS Office, Chief of Engineers, U. S. Army Washington, D. C. 20314	(11) 12. REPORT DATE December 1978 13. NUMBER OF PAGES 146
14. MONITORING AGENCY NAME & ADDRESS (if different from Controlling Office) U. S. Army Engineer Waterways Experiment Station Geotechnical Laboratory P. O. Box 631 Vicksburg, Miss. 39180	15. SECURITY CLASS. (of this report) Unclassified 15a. DECLASSIFICATION/DOWNGRADING SCHEDULE
16. DISTRIBUTION STATEMENT (of this Report) Approved for public release; distribution unlimited. (14) 161 p.	
17. DISTRIBUTION STATEMENT (of the abstract entered in Block 20, if different from Report)	
18. SUPPLEMENTARY NOTES	
19. KEY WORDS (Continue on reverse side if necessary and identify by block number)	

Drilling	Penetration	Soil penetration
Earth melting penetrators	Penetrators	Subsurface exploration
Feasibility studies	Right of way	Tunnels
Geophysical exploration	Rock melting penetrators	Underground openings

H11143

20. ABSTRACT (Continue on reverse side if necessary and identify by block number)

The Earth Melting Penetrator (EMP) is a concept utilizing high-temperature penetrator tips at the leading end of a length of nonrotating stem to melt earth materials in its path and leave an open hole for geologic exploration purposes. The early proof-of-concept testing was performed by the Los Alamos Scientific Laboratory. Westinghouse Corporation Advanced Energy Systems Division developed a conceptual design and cost estimate for a technically feasible EMP system (including heater, core handling, power transmission, and power —

(Continued)

DD FORM 1 JAN 73 1473 EDITION OF 1 NOV 65 IS OBSOLETE

Unclassified

SECURITY CLASSIFICATION OF THIS PAGE (When Data Entered)

20. ABSTRACT: (Continued)

generation subsystems) capable of penetrating a 3-mile long right-of-way path through rock and soil and recovering a 3-in.-diam core from that hole. The heater tip is an annular extended surface tungsten body heated to 2300°C by pyrographite resistance elements. A special annular configuration downhole electrical transformer was designed to convert 1.25 mw of electric power from high voltage-low current transmission mode to low voltage-high current heater mode. A special power generation and control system using paralleling and load sharing between three 680 Hz, 900 kw diesel-powered generators was designed. Tip-steering techniques were established. Several tip-location (guidance) schemes were examined, and it was found that an inertial system would be best but was outside the current state of the art and that a combination electrolitic level-compass scheme would be marginally adequate but technically feasible. Furthermore, providing sufficient (6300 SCFM) air at the tip to preserve components and cool the core would require more power than the electrical system. It would be simple to provide sufficient water (14 gpm), but its proximity to high-level electrical circuits necessitates special design considerations. A downhole propulsion system is described. The EMP system is technically feasible at a total system projected cost of $4,000,000.

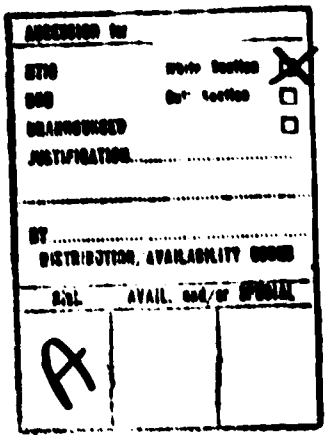

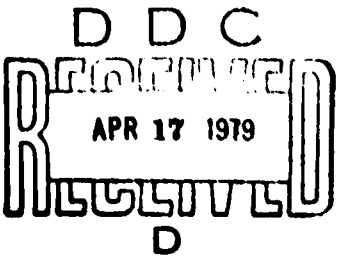

THE CONTENTS OF THIS REPORT ARE NOT TO BE USED FOR ADVERTISING, PUBLICATION, OR PROMOTIONAL PURPOSES. CITATION OF TRADE NAMES DOES NOT CONSTITUTE AN OFFICIAL ENDORSEMENT OR APPROVAL OF THE USE OF SUCH COMMERCIAL PRODUCTS.

PREFACE

This investigation was authorized by the Office of the Chief of Engineers (OCE) under the Civil Works Research Program. The work reported herein was accomplished under Contract No. DACW 39-76-C-0163 between the USAE Waterways Experiment Station, Vicksburg, Mississippi (WES) and Westinghouse Advanced Energy Systems Division, Large, Pennsylvania. Funding was provided in equal parts by the OCE, by the National Science Foundation (NSF), and by the Department of Transportation (DOT). The work was initiated 26 October 1976 and completed 30 March 1978.

The designated Contracting Officer's Representative monitoring the contract work was Mr. James B. Warriner (WES) who also prepared the Requirements Definition, Part III of this report. Acknowledgement is given for critical advice and support to Messrs. Jerry S. Huie and Don C. Banks, Chiefs of the Rock Mechanics Applications Group and the Engineering Geology and Rock Mechanics Division, respectively, of the Geotechnical Laboratory, WES; William W. Hakala, NSF; Russell MacFarland, DOT; Paul Fisher and Wayne McIntosh, OCE; and Robert G. Hanold, Los Alamos Scientific Laboratories, Los Alamos, New Mexico. Commander and Director of WES during the period of the contract was COL J. L. Cannon. Technical Director was Mr. F. R. Brown.

Principal contributors to this study and report include the following:

1. D. L. Black, Project Manager
2. M. Gibbons, Westinghouse Geophysical Instrumentation, Guidance
3. B. R. Krasicki, Air Flow Analysis
4. W. L. Lundberg, Heat Transfer Analysis
5. F. S. Spurrier, Mechanical Design
6. M. Vuchovich, Electrical Design
7. M. K. Wright, Development Plan and Engineering Management

CONTENTS

CONVERSION FACTORS, METRIC (SI) TO U. S. CUSTOMARY AND U. S. CUSTOMARY TO METRIC (SI) UNITS OF MEASUREMENT

Units of measurement used in this report can be converted as follows:

Multiply	By	To Obtain
Metric (SI) to U. S. Customary		
millimeters	0.0394	inches
centimeters	0.3937	inches
meters	3.2808	feet
kilometers	0.6214	miles (U. S. statute)
square centimeters	0.1550	square inches
square meters	10.76	square feet
cubic meters	1.308	cubic yards
cubic decimeters	0.26417	gallons (U. S. liquid)
kilograms	2.205	pounds
metric tons	1.1	tons
Newtons	0.2248	pounds (force)
kilograms per meter	0.6720	pounds per foot
megapascals	145.03894	pounds per square inch
kilograms per cubic meter (mass)	1.68557	pounds per cubic yard
Celsius degrees or Kelvins	9/5	Fahrenheit degrees*
U. S. Customary to Metric (SI)		
inches	2.54	centimeters
feet	0.3048	meters
miles (U. S. statute)	1.609344	kilometers
cubic yards	0.7645549	cubic meters
gallons (U. S. liquid)	3.785412	cubic decimeters
pounds (mass)	0.4535924	kilograms
pounds (force)	4.448	Newtons
pounds per square inch (force)	0.006894757	megapascals
pounds per cubic yard (mass)	0.59327631	kilograms per cubic meter
degrees (angle)	0.01745329	radians

* To obtain Fahrenheit (F) readings from Celsius (C) readings, use the following equation: $F = 9/5(C) + 32$. To obtain Fahrenheit from Kelvin (K), use: $F = 9/5(K - 273.15) + 32$.

PART I. EXECUTIVE SUMMARY

Introduction

1. Westinghouse Advanced Energy Systems Division (AESD) submitted an unsolicited proposal to the Corps of Engineers Waterways Experiment Station (WES) to perform a conceptual design study of a small diameter, long-range hole borer using a rock melting technique. Proof of principle studies on this device, called the "subterrene," were conducted by Los Alamos Scientific Laboratory (LASL) in the 1960s and early 1970s. AESD (formerly Westinghouse Astronuclear Laboratory) also conducted theoretical studies on the fundamental physical processes for the U. S. Department of Transportation. The proposed project was the first phase of a three-phase effort that would eventually result in a field tested prototype geoprospecting earth melting penetrator (EMP). This conceptual design phase was accepted in a joint agreement among the Corps of Engineers, the Department of Transportation, and the National Science Foundation.

2. The proposed design feasibility study is directed to advancing current drilling technology. It is a reasonable next step because feasibility has been shown, performance functions are known, and technology is available to minimize the development efforts. The four objectives of this study are:

a. To produce a conceptual design of a complete drilling system.

b. To determine the limits of capabilities of performance.

c. To complete an economic evaluation.

d. To formulate a detailed development plan for the subsequent phases.

3. The remainder of this section, as well as the body of the report, is organized according to contract work statement or task number. These include:

Task 1 *To develop integrated requirements for extra long reusable* holes (the responsibility for this task was completely fulfilled by the WES).

Task 2 To develop conceptual designs and alternatives based on EMP techniques that have the potential for satisfying the requirements of Task 1.

Task 3 To perform a qualitative assessment of the relative trades among the concepts and parameters identified in Task 2.

Task 4 To provide visual, narrative and analytical descriptions of the reference system concept.

Task 5 To provide a logical development program for advancement of the reference system concept into detailed design, development, fabrication and field testing.

Task 6 To provide technical coordination and project management.

Requirements Definition

4. The system requirements as stated herein were assembled entirely by WES personnel from specifications and recommendations set forth by Engineering Manuals of the Corps of Engineers, the American Society for Testing Materials, the International Society of Rock Mechanics, the Bureau of Mines Reports, and the Bureau of Reclamation Reports. Together, these requirements are intended to represent the best concept of the equipment design features, the necessary characteristics of the EMP created hole, characteristics of the EMP recovered core, and the areas of further investigation into the lithologic effects of tunneling a melted hole into a groundmass.

5. Five potential applications for EMP-created holes listed in order of decreasing projected importance were identified: core sampling recovery, geophysical logging, mechanical/fluid testing, conduits for utilities, and fluid transfer. Consistent with these uses, a quantitative description of EMP requirements was compiled and subdivided into four categories: hole, liner, core/extrudite, and groundmass. A summary of these quantitative requirements is given in Table 1. Those requirements that cannot be expressed quantitatively were excluded from this table and are summarized in the following paragraph.

6. The necessary ground support equipment must obtain sufficient electric power for all operations from commercially available mobile generators, and transformers, compressors, and other large equipment must be highway transportable. Air is the preferred coolant medium because of its universal availability, but water is acceptable. The control and operating console should be capable of real time representation of tip location. Protective equipment must be provided for the possibility of inadvertent steam or other volatile release from the portal area under high pressure.

Table 1

Requirements Summary

DIAMETERS

Hole < 30 cm $^{+10\%}_{-0}$ over 3 meter interval

Core (unmelted) > 5 cm, 15 cm max

LENGTH

Economical over 200 m
< 5000 m

LOCATION ACCURACY

90% probability of being within 5 m radially of projected tunnel centerline at 5000 m

ORIENTATION - EITHER VERTICAL OR HORIZONTAL

THRUST < ~ 2700 kg for 30 cm hole
~ 90 kg/cm in either direction

RATE

5 m/hr

OVERBURDEN

max { - 3000 m in blocky and seamy rock
- 100 m in UNCON (Unconsolidated Soil)
- 10 m minimum + 1000 to 150,000 kg/m^2 surface loading

CORE LENGTH

L/D > 2-1/2 of each piece

Accumulated pieces of L/D > 2-1/2 must be 50% of hole length

Accumulated total recoverable must be 90%

7. The nature of the material comprising the glass liner is important to the correct usage and interpretation of geophysical logs in the hole. This required that an estimate be made of the composition of the liner, as well as its elastic and fluid flow properties and the effect of the liner on measured physical phenomena. Besides the liner, the thermal history of the recoverable core must have a minimal perturbation on the potential mineralogic and hydrologic effects. Exterior to the glass liner in the parent medium, the effects of heat wave propogation on other structures such as utility conduits also must be minimized.

8. The EMP must have a universal penetrating capability. Calculations on its design and performance should be made using all five geologic models derived in the earlier DOT study.

Conceptual Designs

9. Prior to initiating design work, a parametric study on size and performance variables was completed to develop preliminary evaluations of system requirements. These were further divided into geometry, power and thrust, and groundmass effects in an effort to parallel the preceding requirements section. Within the diametral constraints of ID greater than 50 mm and OD less than 300 mm, the power and flow requirements will be minimized for the smallest size penetrator, but down-hole equipment packaging becomes more difficult. For the parametric study it was estimated that 200 mm is the smallest hole diameter that could conceivably accommodate such down-hole equipment as guidance electronics and transformers. Performance calculations, therefore, concentrated on evaluations at 200 and 300 mm diameters with a 50 mm core.

10. The structural requirements of the liner to sustain all overburdens at a depth of 100 m, in addition to specified surface loading, is an independent variable and can be evaluated. Based on a conservative model of the earth overburden, called a condition of "restrained lateral deformation," at the depth of 100 m in UNCON, the required liner thickness/radius ratio is 0.046 as determined by the nominal tensile strength of the glass. Considering surface loading as a hydrostatic column on the UNCON model, the equivalent depth is doubled to 200 meters.

11. The generalized mass balance was derived for the configuration relating the linear geometry to the melted rock and penetrator velocities. These can be related to the internal flow areas of the penetrator head in order to obtain the proper liner thickness. The ratio of the extrudite to penetrator velocity of approximately 20 gives this desired linear thickness within the range of the dimensions and model densities considered.

12. Using the energy and temperature equations developed in the DOT study, the heater power and penetrator surface temperatures were calculated for the two diameters and five geological models as functions of penetrator velocity. The CALCI model has the highest melting point and consumes the most power because nearly 40 percent of its energy is consumed in CO_2 evolution. At the maximum penetration velocity of 1.4 mm/sec, the CALCI model power requirement is 509 kW for the 0.2 m diameter hole, and 1078 kW for the 0.3 m diameter hole. The power required to penetrate at the same velocity through UNCON is approximately half that of CALCI.

13. Although the predictions of heater power are based on LASL test data and are considered reasonably accurate, the prediction of surface temperature by simple analysis is much more difficult. The thermal conductivity of liquid rock is an unknown quantity and significantly increases the uncertainty in the analysis. The parametric evaluation of the surface temperature was performed on the basis of correlations developed in the DOT study and the thermophysical properties developed therein. The results indicate that temperatures in excess of 2300 K, considered to be the maximum operating temperature for the materials under consideration, are exceeded for most operating velocities and geological models, assuming a simple surface geometry and a length to diameter ratio of 1.5. Substantial reduction in operating temperature can be achieved by increasing the L/D ratio and incorporating fins on the exterior surface of the penetrator.

14. The applied thrust load was calculated for all geologic models based on the maximum depth of penetration for 200 m equivalent depth. The results show that the maximum force required is 10^5 newtons including the drag of the stem on the liner.

15. An analysis of the sheet wave penetration into the groundmass was performed using a transient digital computer code. the UNCON and MASIG geological models are, respectively, the least and most conducting respectively, and these were considered. During the time of penetrator passage, the MASIG temperature changes were restricted to an area

within a 20-inch radius of the EMP centerline, and the liner cooling air can withdraw much of the energy added to the earth by the EMP within one hour after passage of the penetrator. During this period the centerline temperature of the core increased only 150°F beyond the ambient for the nominal penetrator temperature and velocity. At the maximum penetration velocity of 1.4 mm/sec the outside surface temperature of the retrievable core reached 1000°F.

16. Two principal changes occur during the passage of the penetrator. First, the groundmass temperature is temporarily elevated; second, a glass liner is formed. Each of these can affect logging results as described in the following paragraphs.

17. Igneous rocks acquire most of their magnetism as they cool through the Curie temperature. Temperature distribution analyses indicate that the 850 K isotherm (Curie temperature) does not extend more than five inches from the penetrator. However, the natural remanent magnetism can be increased up to a factor of 5. In the volume of rock that exceeds this temperature, the factor increases with the age of the rock.

18. Dehydration of the surrounding rock and the rock in the liner will affect the calibration of all neutron logs. Neutron logs will be usable for quantitative analysis in EMP created holes if the instruments are calibrated in an environment that simulates this hole. This recalibration is required because the neutron slowing-down length is increased, which is attributable to the decrease in the macroscopic cross section at epithermal energies caused by the hydrogen being driven from the rock.

19. Seven geophysical logs were investigated to determine the effect of the heated, glass-lined hole. Electrical induction logs, gamma logs, and density logs should be useful. It is doubtful that spontaneous potential logs, guard logs, and electrical logs will produce satisfactory results. The utility of acoustical logs is dependent upon the type of groundmass.

20. Six mechanical design concepts were developed and evaluated, based primarily on the LASL technology, in an effort to keep future development requirements at a minimum. The first concept, a removable core barrel and wire line, made provision for the removal of the undisturbed core, section by section, as penetration proceeded. The inner diameter of the penetrator accommodated a core barrel several feet long into which the core was to be extruded. As the core completely filled the barrel, the release mechanism was activated and the core barrel and core could be withdrawn to the portal by means of a wire line. After removal of the core from the barrel at the portal, the core barrel was then reinserted into the penetrator stem and propelled by compressed air to the penetrator head location to await its reset and refilling.

The penetrator head, machined from tungsten, accommodated 12 cylindrical heaters in equally spaced axial holes around the penetrator axis. Molten rock was fed through a series of holes and grooves machined in the penetrator head to 12 carry-off tubes equally spaced around the penetrator axis. These are connected with an annular carry-off passage in the stem. High pressure air was applied to the outer passage at the portal. It flowed to the penetrator where it entered the injection nozzles at the penetrator end of the carry-off tubes. Molten rock extruding into the carry-off tubes was then solidified and fluidized by the high velocity air emerging from the nozzles and transported pneumatically to the surface.

21. The second concept incorporated a cooling passage arrangement at the inside diameter of the penetrator head to remove heat from the core in an attempt to limit the temperature of the core at its entry into the penetrator bore and thus maximize the diameter of the thermally undisturbed portion of the core. In other aspects, this design was generally similar to concept no. 1.

22. In the third concept, the 12 separate cylindrical heater geometry was replaced by an annular configuration divided into three 120° sectors. This three-sector arrangement was intended to provide the necessary steering capability by appropriate modulation of the power to the three sectors. The location of the heaters in the heater annulus was effected by a system of spring-loaded tungsten electrodes similar to that employed in the previous two concepts.

23. In concept no. 4 the annular heater arrangement was used together with four separate carry-off tubes. In this arrangement the inner diameter of the penetrator was insulated from the centering core by pyrographite tubes and no provision was made for cooling the core. Molten rock was fed to the carry-off tubes through drilled passages from a circumferential groove in the penetrator periphery. This, in turn, received molten rock from the extended surface fins machined axially along the penetrator.

24. The fifth arrangement contained nine heaters with three carry-off tubes. This arrangement provided three independently controllable heating sectors, each of which contained three resistance heater elements, constituting the load of a three-phase circuit Nine transformer modules were accommodated in the stem in three groups of three within the spaces between the three carry-off tubes.

25. Although generally similar to the previous concept, this last design incorporates three large diameter axial holes drilled from the leading edge of the penetrator in line with the carry-off tubes. Provision was made to accommodate the flow of a large portion of the molten rock directly from the leading edge of the penetrator. Thus, the design provided for the flow of molten rock from both ends of the penetrator head.

26. For the electrical design of the EMP, individual studies were made of heater configuration and material, the down-hole stem transformer, the power transmission, and the up-hole surface power supplies.

27. Both tungsten filament and pyrographite heaters were originally considered. However, because heater flux densities must be high to produce the required temperatures and consideration must be given to slight vibrations within close tolerances, wire filament and filament mesh heaters were eliminated. Calculations were made for pyrographite heaters 25.4 mm in diameter and 25.4 cm long for various power and voltage combinations. The ultimate selection of operating voltage for the heaters is a trade between the desire to have a low-voltage and minimum sparking potential in the heater and the desire for high voltage with its low loss in transmission.

28. To minimize large transmission losses for a system length of 5000 m, the possibility of installing step-down transformers in the stem behind the penetrator was investigated. The maximum annular space allowed for the transformers was 8.255 cm. A continuing investigation into transformer design indicated that a transformer could be built to power the heaters, but to meet the diameter envelope each transformer phase would have to be 59 ft long using typical 60 Hz power. Since nine heaters are used and only one three phase transformer could be placed in a stem section, the stem length required to accommodate the transformers alone would be approximately 180 ft. If the frequency of the power is increased, the stem transformer size could be proportionately decreased.

29. At the heater voltages considered, the total current requirement would be in excess of 1000 amperes in order to achieve 1.25 MW. Transmitting currents of this magnitude for 5000 meters would result in extremely high losses in addition to requiring large cable diameters. Considering heater transformer and transmission line characteristics a number six cable was selected, with the source transmission voltage to fall between 2600 and 5000 volts, at a frequency of 680 Hz.

30. Four options for power supplies were developed by considering only self-contained trailer mounted units. These options considered paralleling, load sharing, and synchronizing. The selected option contains three generators sized such that any two generators can supply power to all three heaters. Paralleling and load sharing controls are provided.

31. The problem of accurate guidance through the earth is complicated by the inhomogeneous, hostile, and unpredictable medium. Guidance of the earth melting probe must be approximately 5 feet in 5000 feet or $\pm$ 0.1 percent; data gathering must be nearly continuous. If the guidance system is in the probe, then the guidance package must be insulated from temperatures from 2000 to 2500 K. Several types of systems were investigated with respect to their size and accuracy. These included seismic, magnetic, electromagnetic, optical and inertial. Only the inerted could fulfill the accuracy requirements. However, size, packaging and environment problems were not completely solved. A hybrid possibility includes the inertial guidance system and an arrangement of electrolytic levels and a compass that would give pitch, roll and direction or yaw. This arrangement represents the cheapest available working system, assuming successful interface and test. However, the electrostatic gyro compass must provide continuous yaw data. Therefore, only the inertial navigation system gives continuous real time data on roll, pitch, and yaw within the desired accuracy. Here the major obstacle was size and, although a smaller system exits, data on drift and environmental tolerances are classified.

Cost Evaluation

32. The cost evaluation consists of the rationale for selecting the reference design and some preliminary cost estimates for the entire system. Although all six configurations were deemed feasible, the provision made in concept no. 6 for augmenting the heat flow to the penetrator leading edge by mass transport of the rock made this the most potentially useful design feature and it was therefore retained as a selected concept. Although it is anticipated that propulsion of the penetrator head will be achieved by applying the com-

pressive force to the stem at the portal, a self-contained down-hole propulsion module was also defined conceptually. Because of the added complexity and lower reliability associated with moving parts, this propulsion concept was not given further consideration.

33. A cost estimate was developed for the reference concept description derived primarily from conversations with potential vendors and is in terms of 1977 dollars. A summary of the mechanical and electrical system costs is given in Table 2. A total cost for the system (assuming no government-furnished equipment) is slightly less than $4,000,000. The two largest cost items are three miles of stems and the electrical generator for the heater, which are about $1,000,000 each. Costs do not include trailers for housing personnel, fuel and water trailers, control room trailers, communication system, or general facility interconnections.

Selected Penetrator Design

34. The selected earth melting penetrator configuration is illustrated in Figure 1. The penetrator head is made of tungsten having a melting point of 3683 K which is 800 K above that of molybdenum. Actual operating temperature will be substantially below these melting points. The manufacturer of the tungsten penetrator head involves the initial pressing and sintering of 92 percent density blanks, which must then be further densified by forging. Since available press size is limited, the penetrator head will be comprised of diffusion-bonded laminations. The penetrator head has axial fins machined in its exterior surface. The large diameter hole is machined along its centerline, which accommodates tungsten, pyrographite, and molybdenum rings that together function as the core former. Twelve holes are machined axially in the penetrator. Three of these holes provide a flow path for the molten rock and the other nine are arranged in three equally spaced groups of three holes to accommodate the nine resistance heaters. Each heater consists of a cylindrical stack of pyrographite and graphite discs held in position by compressive force transmitted through a spring-loaded tungsten electrode. The transition tube assembly consists of a molybdenum tube of sufficient length to provide the necessary thermal isolation of the stem from the penetrator. Control thermocouples are also accommodated in drilled holes in the

Table 2

Mechanical System Cost Summary

Penetrator and Transition Sections	
Penetrator head - tungsten (forged)	$ 50,000
Transition tube - molybdenum	5,000
Smaller molybdenum pieces and tubes	1,000
Tungsten electrodes	900
Pyrographite insulation	2,000
Misc. small machined parts	3,000
Carry-Off tubes (molybdenum and SS bronzed)	3,000
Graphite heaters and receptors	5,000
Instrumentation	1,000
Total penetration and transition	$ 70,900
Stem	
Aluminum (21' long)	$ 2,300
Total cost - 5000 m (813 units)	1,900,000
Aluminum (40' long)	2,540
Total cost - 5000 m (406 units)	1,000,000
Stainless steel (20' long)	4,600
Stainless steel (40' long)	5,000

TABLE 2 (Continued)

Electrical System Cost Summary

Description	No. of Units	Total Cost
Heaters	9	$ 5,350
Primary compressor power supply	2	561,110
Facility power supply	1	200,000
Stem transformers	3, 3 Ø	125,000
Heater generator	(Nonrecurring) (Based on 3 units)	521,000
	1st unit	200,000
	2nd unit	170,000
	3rd unit	150,000
a) Regulator for above generator	1st unit	2,000
	2nd unit	1,000
	3rd unit	1,000
Prime mover and trailer for item 5	(Nonrecurring)	20,000
	3	270,000
Switchgear for item 5	(Nonrecurring)	200,000
	3	260,000
Guidance	1	125,000

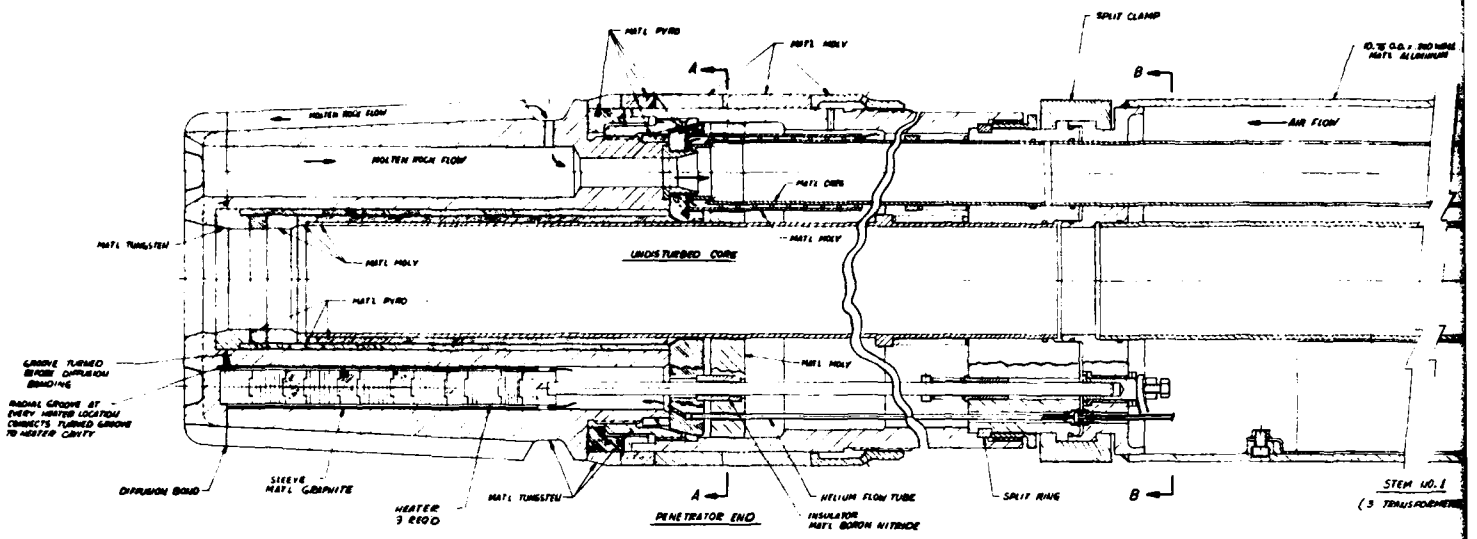

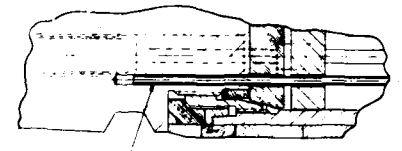

SECTION E-E

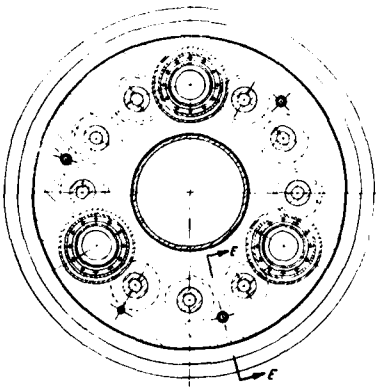

SECTION A-A

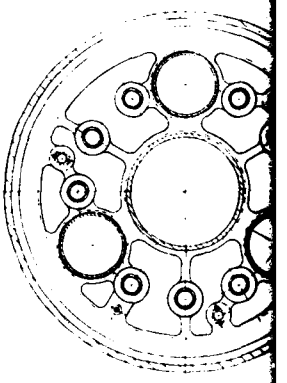

SECTION B-B

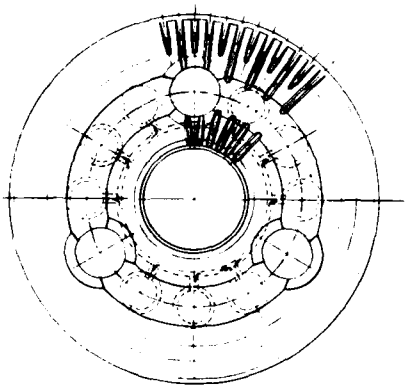

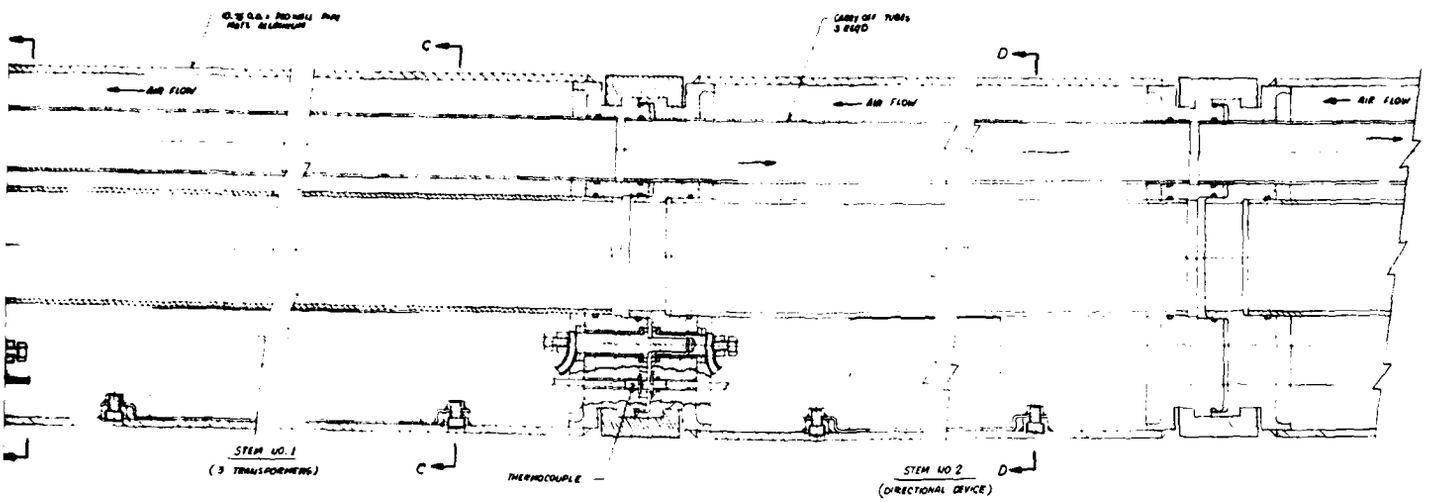

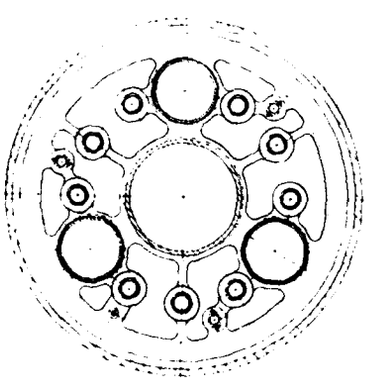

SECTION B-B

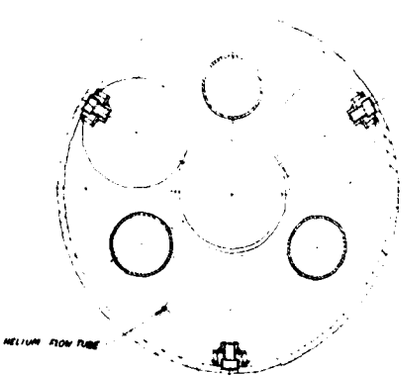

SECTION C-C

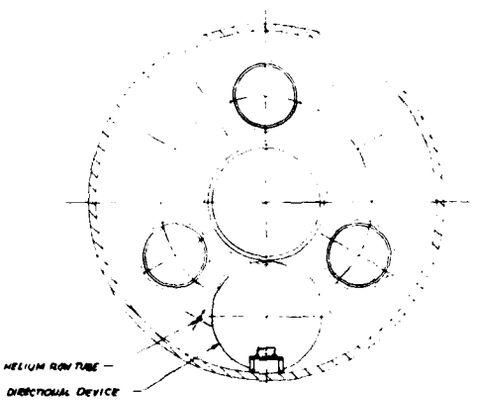

SECTION D-D

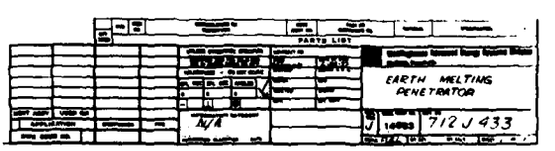

Figure 1. Selected earth melting penetrator configuration

penetrator head. Helium gas is supplied to the heater cavities of the penetrator to provide an inert atmosphere.

35. An assembly of standard stem sections joined end to end by split clamps forms the overall drill string. Specially modified stem sections accommodate transformer modules, guidance equipment, and control boxes. The standard stem section is fabricated from standard sizes of aluminum pipe. The outer casing of 10.75 in. diameter by 0.2 in. thick pipe is welded at each end to machined aluminum end fittings. End fittings provide support for a central 3.5 in. diameter x 0.12 in. thick pipe and 3 1.90 in. diameter x 0.065 in. thick pipes equally spaced around the central pipe. Rubber O-rings are used to seal the smaller tubes to the end fittings and to seal the stem sections to each other. The end fittings also provide support for nine male and female electrical connectors, thermo-couple connectors and the helium line.

36. By using a power source frequency of 680 Hz, the overall transformer stem length was reduced from 180 ft. to 30 ft. The transformer primary and secondary are wound around microlaminations and could be made in small sections about 15 in. long x 3.5 in. in diameter. These small sections are stacked in series like cells in a flashlight until the proper operating voltages are achieved for the primary. All the secondaries are connected in parallel to a common bus for that phase.

37. Generators to provide the power requirements for the system are expected to be 18 in. in diameter and 48 in. long with an estimated weight of 1600 lbs. To produce 680 KV frequency, the generators may have to be turbine driven. Additional generators are required for facility power and air compressor power. Figure 2 shows the system block diagram for the entire electrical family.

38. Power and temperature were calculated for the reference design configuration in all geological models using the same techniques previously described. The maximum power requirement of 909 kW is shown in Figure 3 for the CALCI model at 1.4 mm/sec (5 m/hr) velocity). The maintenance of an operating temperature level less than 2300 K continues to be a problem even with the extended surface geometry (fins). The low thermal conductivity of the UNCON model results in that operating temperature at velocities of 0.4 mm/sec. Doubling the length of the penetrator to 0.61 m would increase its allowable operating velocity to 1.0 mm/sec. Temperatures for all five models are shown in Figure 4 as a function of velocity.

39. An analysis of the air cooling supply was made for the reference conceptual design. The purpose of the air coolant supply is threefold: to provide coolant for internal parts (e.g., guidance baggage); to cool the glass liner until it becomes self supporting; and to provide floatation for the extrudite cooling and removal. Assuming the maximum allowable pipe temperature is 400°F for the aluminum stem configuration, and that the maximum power that can be extracted is 600 kW, the maximum air flow requirement is approximately 8 lb/sec. (6300 SCFM). For a flow of water at pressures greater than 250 psia, only two pounds per sec. (14 gpm) is needed. If steel pipes were used instead of aluminum, air flow rates of 3 to 4 lbs. per sec. could be used because of higher allowable material temperatures.

40. Pressure drop calculations were made to determine the feasibility of supplying this quantity of air to the end of a 5000 meter hole. The conclusion of a series of calculations is that 8 lbs/sec of air cannot be provided to the penetrator head at distances of 5000 meters within a moderate compressor outlet pressure of 1000 psia. In order to obtain sufficient flow area to reduce the pressure drop, a stem OD of approximately 14 in. may be required. This is based on the requirement of at least 2.5 in. diameter carry-off or pneumatic mucking tubes, which in the current design configuration have greater than 1000 psi pressure drop. These pneumatic mucking tubes require a minimum air velocity of 78 ft. per sec. in order to maintain the fluidization of the particles to transport them to the surface.

41. Within the present geometric constraints of a 12 in. diameter and 3 mile hole, the water pressure drop and pressure level (to prevent boiling) are not a problem since only 500 psia pump pressure is required at 14 gpm.

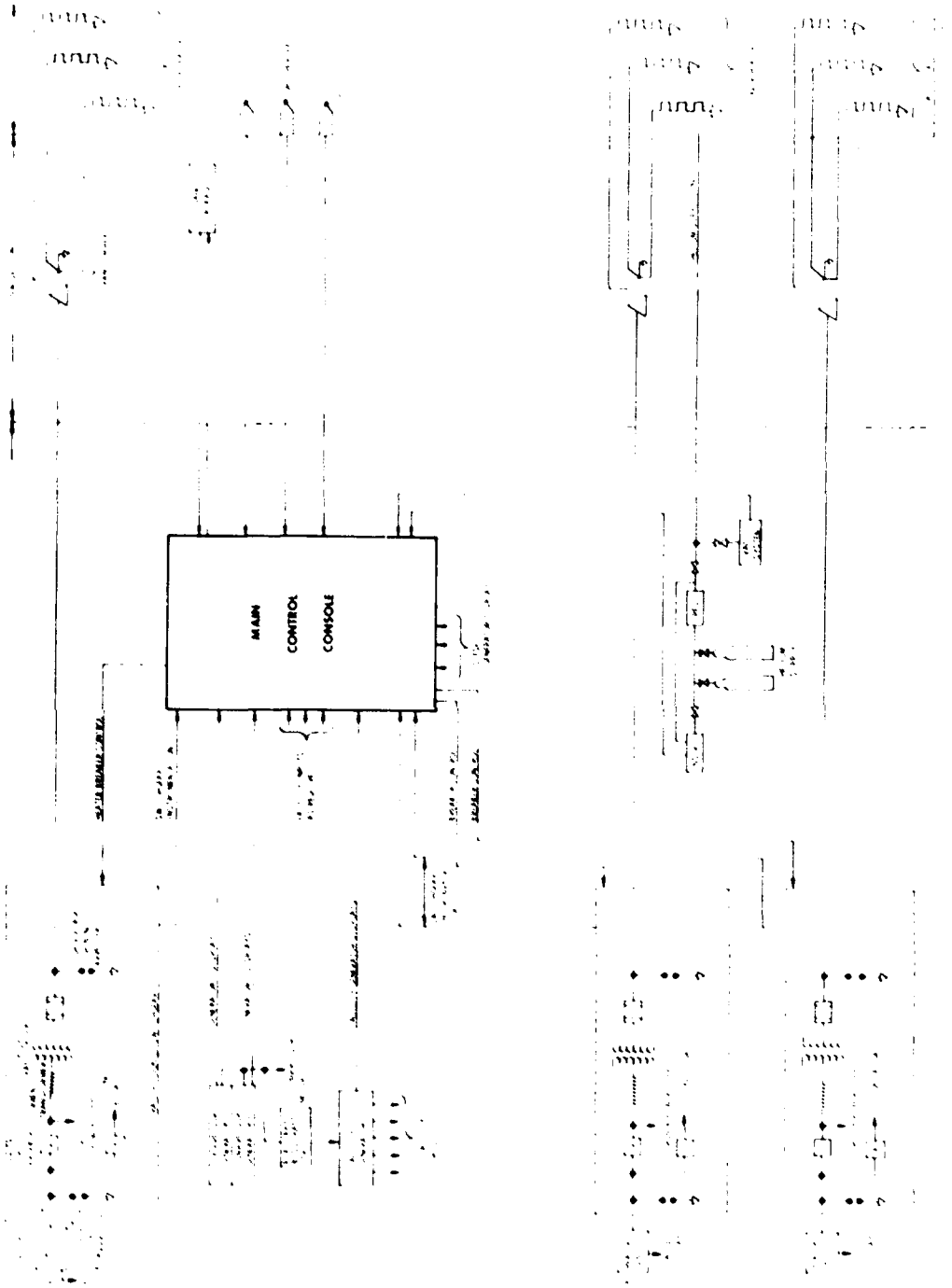

Figure 2. System block diagram for electrical facility

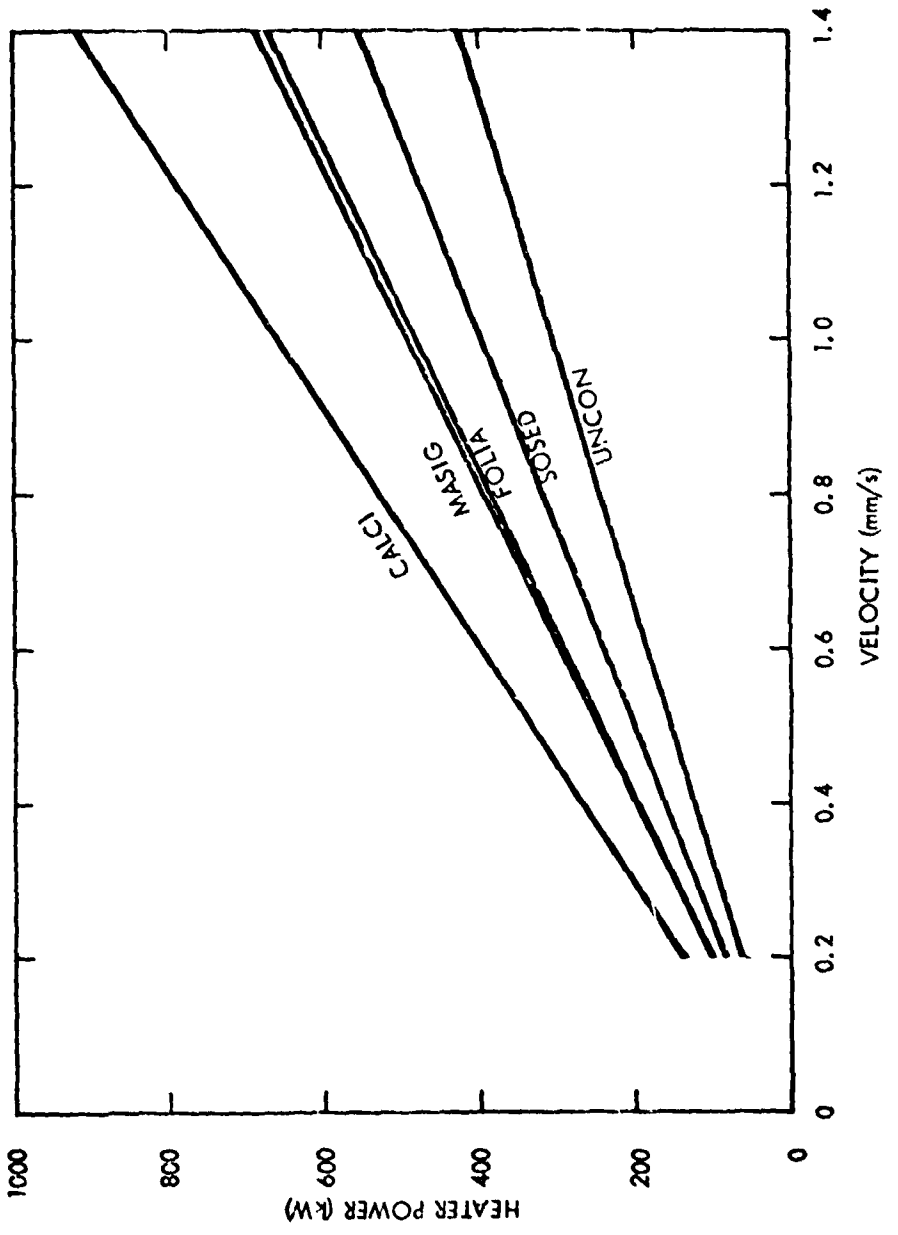

Figure 3. Maximum power requirement of 909 kW for CALCI model

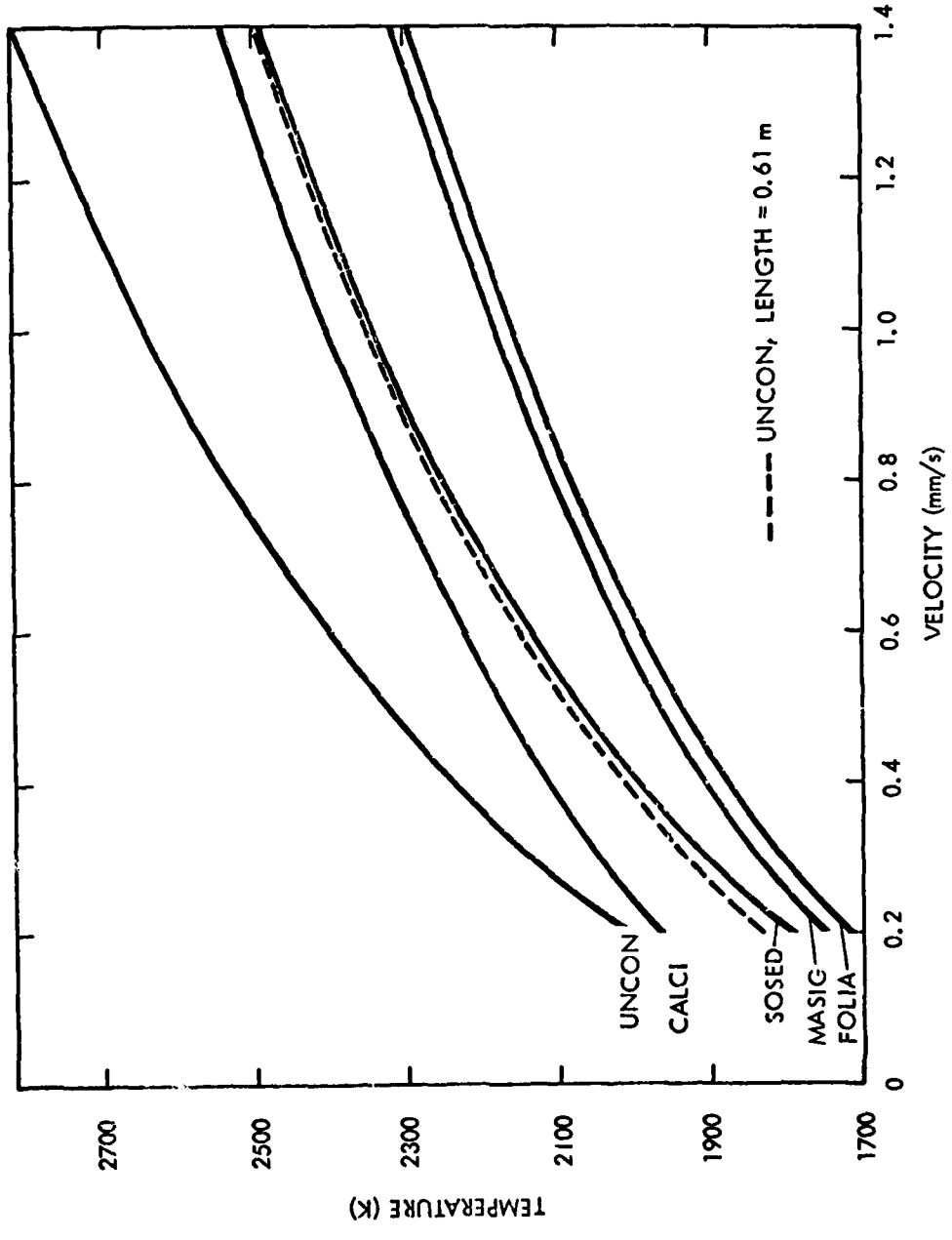

Figure 4. Temperatures for five models as functions of velocity

Development Program

42. With the completion of the Phase I conceptual design study, the details of subsequent phases were prepared consisting of three more phases spanning the next five fiscal years. This development program is summarized by task in the schedule bar chart of Figure 5.

43. The objective of Phase II is to demonstrate a prototype penetrator in the field. Operational performance can be evaluated through demonstration of penetration rate, hole and core formation response to guidance through differential heating, starting, stopping, and retraction evaluations. Six tasks are associated with this phase: heater tests, penetrator design, penetrator fabrication and assembly, fuel test plan, fuel test, and program management and integration.

44. The objective of Phase III is the acquisition of a complete system for checkout and field demonstration in Phase IV. This effort assumes a successful Phase II program and the decision to proceed. Current plans envision the following seven tasks as appropriate to Phase III: experience update, new components assessment, component evaluation, system and component design, fabrication and assembly, system demonstration plan, and program management.

45. Phase IV is the test phase for the hardware required in Phase III. Its relationship to the total program is shown in Figure 5, and it is expected to last one year. It will consist of the following tasks: checkout, demonstration, and program management.

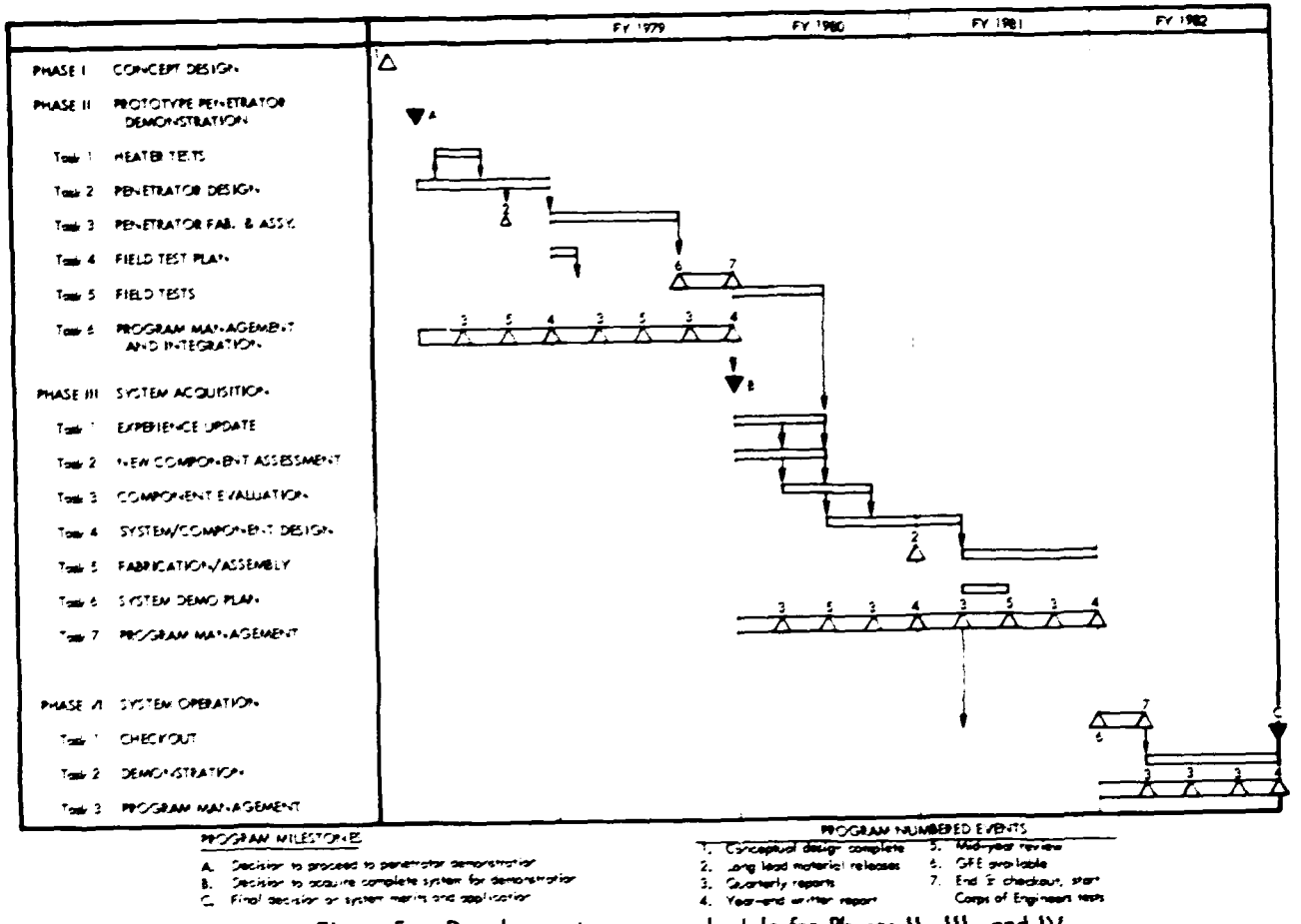

Figure 5. Development program schedule for Phases II, III, and IV

PART II: INTRODUCTION

Background

46. In December 1974 Westinghouse Advanced Energy Systems Division (AESD) submitted an unsolicited proposal (BK-4038-0301) to the Corps of Engineers Waterways Experiment Station (WES) to perform a "... conceptual design study of a small-diameter long-range hole borer using a rock melting technique." The device concept was termed an Earth Melting Penetrator (EMP) and is an outgrowth of empirical proof-of-concept studies conducted by Los Alamos Scientific Laboratory (LASL) in the 1960s and early 1970s on a device LASL called the "Subterrene." At about the same time, additional theoretical studies were conducted by AESD (formerly Westinghouse Astronuclear Laboratory) to describe the fundamental physical processes involved in operation of an EMP. The proposed project was the first phase of a long-term effort by AESD that could eventually result in a field-tested prototype geoprospecting EMP. The three following phases of the effort can be generally described by prototype demonstration, system acquisition and operations. The first phase proposed was accepted in a joint agreement between the Corps of Engineers, Department of Transportation, and National Science Foundation.

47. The earth melting system of producing holes has several features that are different from normal methods of excavating and boring holes:

- A glass casing can be formed to line the bore holes or to case and contain a core.
- The penetrator can be shaped to make a noncircular hole.
- The efficiency of the penetrator increases with increase of the in situ temperature.
- The expected long life of the heated bit can significantly reduce the number of times it must be removed to change penetrators.
- The penetrator does not need to rotate or reciprocate to make holes.
- In porous rock or soils, the melt can be consolidated to form a thick glass casing.

- In high density rocks and structures, the melt can be chilled by the coolant and blown to the surface. Chilled melt-glass cuttings will not decompose at the surface or contaminate surface water.
- In certain formations, the liquid melt can be used to "lithofracture" the formation, and the excess melt is forced into the fractures.

48. The unique features of EMP support a wide range of applications in addition to survey of proposed tunnel routes with the remotely guided and self-propelled coring penetrator proposed in this study. Some of these potential applications are:

- Retrieving glass encased cores from unconsolidated formations
- Melting noncircular transportation tunnels and utilidors with finished glass lining
- Making drainage holes in archeological sites without damaging vibrations
- Punching precision holes in rock or soil for structural anchors
- Sinking glass-lined stabilized holes for foundation piles
- Drilling holes for high explosive shot emplacement without dust
- Completing water wells with in-place, noncorrosive glass casings
- Making fluid and slurry conducting pipe lines
- Sinking large diameter shafts by melting a narrow peripheral kerf
- Drilling oblong holes to confine blasting to a desired cut-off line (curtain drilling)
- Implanting long, accurately profiled urban utility conduits through congested areas without surface disruption
- Making ultradeep core holes for geophysical research
- Drilling in hot rock for geothermal energy or mining resource exploitation

Study Objective

49. Based on the broad applications presented in the preceding section, the Westinghouse Advanced Energy Systems Division proposed a design feasibility study of a complete EMP drilling system. This study is directed to advancing current drilling

technology. It is a reasonable next step since the feasibility of the process has been shown, analytical performance functions are known, and available critical technology is sufficient to minimize the development efforts. The overall project is envisioned in four phases in order to reduce the exposure to risk. The first phase is the conceptual design and evaluation ending in cost and development planning for the follow-on phases of the detailed design, including an experimental demonstration, system acquisition and field evaluations.

50. The objectives of this study are fourfold:

- Conceptual design for a complete drilling system, including penetration, power supply, above ground facilities, cabling, and instrumentation
- Determination of the limits and capabilities of the EMP performance
- Economic evaluation of the EMP
- Formulation of a detailed development plan and cost estimate for carry-on phases

Work Statements

51. The remainder of this report is organized according to contract task number. Of the six tasks, five of them present deliverable items, with the sixth being Program Management. The original tasks as proposed in BK-4038-0301 were reduced in scope, commensurate with available funding. The contracted work statement includes:

Task 1	To develop integrated requirements for extra long reusable holes (the responsibility for this task was completely fulfilled by WES)
Task 2	To develop conceptual designs and alternatives based on EMP techniques that have the potential for satisfying the requirements of Task 1
Task 3	To perform a qualitative assessment of the relative trades among the concepts and parameters identified in Task 2
Task 4	To provide visual, narrative and analytical description of the reference system concept

Task 5 To provide a logical development program for advancement of the reference system concept into detailed design, development, fabrication and field testing

Task 6 To provide technical coordination and project management

PART III: REQUIREMENTS DEFINITION

by

James B. Warriner
Waterways Experiment Station

Background

52. Part III describes the requirements determined by WES for Corps of Engineers usage of an EMP and the hole it will produce. Requirements stated herein were assembled entirely by WES personnel from specifications and recommendations set forth by the Corps Engineering Manuals, the American Society for Testing Materials, the International Society of Rock Mechanics, Bureau of Mines reports, and Bureau of Reclamation reports. Together, these requirements are intended to represent the WES concept of the equipment design features, the necessary characteristics of the EMP-created hole, the characteristics of the EMP-recovered core, and the areas of further investigation into the lithologic effects of tunneling a melted hole into a groundmass.

53. Several additions to and increased emphasis on specific details in the planned work were felt to be necessary. The additions and re-emphasis are, in all cases, in the direction of expanding the flexibility of the tool and using the produced core and hole properties as primary measures of the benefits accrued from EMP usage as compared to the development costs and the use of conventional drilling methods. It will be noted that a requirement for the ability to place vertical holes has been made to increase the flexibility of the final EMP system. Except for the sensors providing penetrator guidance data, no requirements have been formulated to include, as part of the EMP, equipment that will log the hole as it is being made. Essentially no restrictions have been made on the degree of fracturing of the groundmass during penetration. The emphasis on recovered core quantities and the condition of that core has been increased. Emphasis on determining the changes occurring in the penetrated groundmass has been increased, primarily in the

areas of effects on geophysically logged properties. A device which could penetrate earth and rock accurately over long distances would be of no real benefit if neither a representative testable core could be recovered nor meaningful logs could be made. The final product of the effort to develop a geoprospecting EMP is not merely the physical system, although it is a necessary milestone, but rather involves the ability to economically obtain complete and meaningful geologic data along extra long subsurface paths.

54. The following paragraphs give quantitative description of the EMP requirements, subdivided into four categories of hole, liner, core/extrudite and groundmass.

Hole

Diameter specifications

55. The minimum hole diameter required for optimum use of in situ stress and strength testing methods, for pressuremeter testing, and for use of small diameter geophysical logging tools is 7.6 cm. The minimum diameter quoted in Section 3.1.1 of the proposal is 10.2 cm. Both of these limits must be controlled by the core diameter requirements (Section 3.1) since the Corps of Engineers considers the recovered core to be one of the most important products of the exploratory EMP. The minimum diameter of unmelted core required is 5 cm. Thus, the minimum hole diameter will be 5 cm, plus the glass core encapsulation annular thickness, plus the annular thickness of the EMP coring tip and melt shaping surfaces. One of the tips fabricated by LASL was a universal extruding penetrator having an OD of 11.4 cm and ID of 6.4 cm with a penetrator wall thickness of 2.5 cm. These dimensions suggest a minimum hole diameter allowing 5 cm of core diameter and 1 cm of encapsulation is such that $5 + 1 + 1 + 2.5 + 2.5 = 12$ cm.

56. The maximum hole diameter of 30 cm will allow passage of virtually all available geophysical logging probes and yet is small enough to prevent the hole effect from degrading the quality of the logs.

57. Allowable variations of hole diameter are plus 10 percent and minus 0 percent of the nominal diameter over 3-meter intervals.

Hole length specifications

58. There is no effective restriction on minimum hole length save the cost and effort of equipment setup and operation. Conventional drilling technology is capable of producing horizontal boreholes 50 to 100 meters or more in length, and for vertical boreholes in

lengths up to 150 or 200 meters which are quite economical. The EMP system design is tentatively specified to be sufficiently economical in setup and operation such that costs for a 200-meter horizontal melted hole will be comparable with costs for conventional vertical drilling to explore a 200-meter horizontal right-of-way.

59. The maximum length of an exploratory EMP hole was defined in Section 3.1.1 of the proposal as 3 miles (approximately 5000 meters). This is about twice the length of the Eisenhower Highway Tunnel in Colorado and about one-half the length of the railroad relocation tunnel near Libby, Montana. Because a 5000-meter EMP hole could have been melted from both portals of the latter example (a condition typical of virtually all transportation tunnels), it is apparent that the proposed maximum length of the EMP hole is appropriate as a final requirement.

Location accuracy specifications

60. The location of the operating EMP tip should be known and controlled such that there is at least a 90 percent probability of being within 5 meters radially from the projected tunnel right-of-way centerline over the entire maximum range of 5000 meters. Uncertainties in locating the EMP tip must be randomly distributed; that is, there should be no systematic deviation in hole location such as might be caused by consistent dropping of the tip in the gravity field.

61. Location data must originate at the tip and control applied from the portal in the same time frame. Whether the control is applied directly to the EMP assembly and tool string from the portal or indirectly through signal transmission to the operating tip assembly is immaterial to Corps of Engineers usage, but it is expected that the former type of method will prove to be more cost-effective.

Orientation (slant angle)

62. Military applications of the EMP as an exploratory tool fall within the mission of the Corps of Engineers. The proposed length (5000 meters) and high degree of location accuracy required of the EMP holes make the device attractive for use in site examination for deep-seated facilities. In addition to the horizontal orientation of tunnel right-of-way exploratory holes, one requirement associated with this application stipulates that the EMP must be able to operate vertically within the same tolerances

stated elsewhere (diameter: Section 1.1, length: Section 1.2, accuracy: Section 1.3, penetration rate: Section 1.5). Intermediate hole slant angles between vertical and horizontal are not required.

Required thrust/penetration ratio

63. The maximum thrust required to advance the EMP of approximately 90 kg per cm of hole diameter will be commensurate with that available from conventional mobile drilling units. For a minimum hole diameter of 12 cm, the requirement will be about 1100 kg. For a maximum hole diameter of 30 cm, the required thrust will be about 2700 kg.

64. The most flexible type of EMP design is one which has a self-contained, electrically driven thrusting assembly. This type is preferable to hydraulic units since power can be obtained from the melting assembly. Because the associated cost of this design detail may prevent its implementation, the major design effort should proceed in the direction of thrusting by means of a stiff string of stems extending from the portal while, at the same time, a preliminary subtask is undertaken to determine the feasibility of electrically driven thrusters. Reverse thrusting will be necessary for tool extraction and will be most easily accomplished if the primary thrusting utilizes a stiff stem. In any event, even if thrusting and retraction is applied downhole, a backup retraction system operating from the portal through the stem must be provided for emergency retrieval. The reverse thrust (retraction) capability should be comparable in magnitude to the forward thrust capability, that is, up to approximately 2700 kg tension. Penetration rates have been shown to be dependent primarily on the applied thermal power and thrust force, secondarily on porewater quantities, and minimally on material types to be penetrated. To avoid melting tip replacement and assuming the past research conclusion of a 1000-hr tip life to be achievable, then a 5000-meter hole must be advanced at the rate of 5 meters per hour of operation or greater. This rate of advancement is less than that of conventional equipment in soft ground but greater by the same order of magnitude factor in very hard rock.

Required/available supporting activity

65. The EMP is assumed to be electrically powered and is required to derive sufficient electric power for all operations from commercially available mobile generators. These generators must be highway transportable either on a single chassis or a semi-trailer truck.

66. The coolant used for rock melt cool-down control and EMP subassembly cooling must be readily available in remote localities. Air would be best from a standpoint of availability; water would be adequate if supplied at a high enough volume rate to prevent steam generation or if the steam generated could be used to propel core and extrudite out of the hole; and tanked nitrogen gas would be the most inconvenient of previously suggested coolants from the standpoint of availability.

67. Helium has been used in the past as an inert anti-corrosion bath for the heaters and is satisfactory if the EMP tip assembly is sealed and does not require frequent purging with the inert gas. The reaction required for thrusting must be easily transportable. Since the required thrusts should be modest, either dead weight or grouted rock or soil anchors can be used for vertical and horizontal holes.

68. All subsystems associated with the EMP and its operation must be transportable by trucks. Subassemblies such as cable and stem sections should be of sizes and weights that can be carried by several men or at least by a light duty truck-mounted hoist.

69. The control and operating consoles should be capable of real-time representation of tip location relative to its nominal projected path, should allow the operator to maintain manual control of all phases of the penetration operation, should continuously record both location data and control commands, and should provide a single-command initiation of the emergency retraction sequence of operations to prevent loss of the tool or danger to the workers. All system electrical connections must be fail-safe protected for safety during stem section attachment. Protective equipment must be provided for the possibility of inadvertent steam or other volatile release from the portal area under high pressure.

Uses of EMP created holes

70. The following is a list, in order of decreasing projected importance to applied civil engineering, of probable applications for EMP-created holes.

a. Core sampling recovery. Despite the advent and increasing application of in situ mechanical and geophysical measurement techniques, the core recovered from underground exploration remains the mainstay of geologic and rock mechanics characterization. Recovered core must be disturbed as little as possible from

its in situ condition, must be available for direct examination for lithologic and structural characteristics, and must be of an appropriate size to allow meaningful extrapolation of laboratory test interpretations to the subsurface environment.

b. Geophysical logging. The EMP-created hole must provide an environment conducive to the application and accurate interpretation of various geophysical logging methods. The glass liner and thermal alterations to the groundmass peculiar to a melted hole must be examined in minute detail so that their effects on geophysical logs can be minimized or incorporated into the data interpretation. This application is second in importance only to direct examination of recovered core and may, in the near future, surpass core testing in the opinion of design engineers.

c. Mechanical/fluid testing. Included within this category of applications are in situ elastic property measurements such as hydofracturing stress measurements, borehole jack strength and stress measurements, and in situ fluid permeability measurements. The deformation properties and structural integrity of the liner are of greatest importance to this category of applications.

d. Conduits for utilities. These applications make direct use of the EMP-created hole as a final product rather than as a preliminary step in large-scale entries into the earth. The most important characteristics of the hole in this category of applications will be length, diameter, and cost-effectiveness.

e. Fluid transfer. This category is closely related to the above with the added requirement for liner integrity. Specific applications are access holes to geothermal energy sources or recovery of and transportation of geologic fluids such as water and hydrocarbons.

Liner

Physico-chemical nature of liner material

71. The nature of the material comprising the glass liner remaining after EMP penetration of the various modeled geologic materials is of importance to the correct usage and interpretation of geophysical logs in the hole. Specific areas of required theoretical research are the electrical properties, the nuclear radiation properties, and the vulnerability of the liner material to chemical alteration. The electrical properties of interest are resistivity and dielectric constant. Nuclear radiation properties are inherent

gamma and neutron spectra and capture cross sections of thermal and epithermal neutrons. Chemical alterations of the liner material in aerial, aqueous, and mineralized geothermal fluid environments must be researched for applications to fluid transport. Proof of EMP feasibility and concomitant design and fabrication will result in requirements for empirical verification of the theoretical representations of liner properties.

Structural integrity requirements

72. The required structural integrity of the EMP hole liner will vary according to the application. The shortest life required before blockage is that for core recovery only. The life span would only be the time required for hole creation and tool recovery, on the order of 1000 hr. Insertion and recovery of geophysical and/or mechanical testing tools effectively doubles the required life span to 1000 hr after hole completion. In the latter instance, the high probability of hole destruction by the action of mechanical testing must be considered. The longest required life span is in applications such as conduit passages or fluid transport and is on the order of magnitude of 100,000 hr or 100 times the minimum life span. For such long life spans, the use of hole reinforcement or placed liners seems at first glance to be feasible but is beyond the scope of the current study.

73. Maximum overburden thicknesses acting on the liner structure are assumed to be 3000 meters in blocky and seamy (Terzaghi's definition) rock and 100 meters in soil type materials (UNCON). Minimum overburden thickness is 10 meters in all material. In the calculations involving the minimum overburden thickness, localized surface loadings ranging from 1000 to 150,000 kilograms per square meter must be included.

Elastic properties of the liner

74. Elastic properties of the liner materials resulting from the modeled geologic materials must be known for input into structural integrity studies and for determination of the liner's effect on geophysical acoustic logging and in situ mechanical testing data. Desired acoustic properties include compressive and shear wave velocities, wave amplitude attenuation parameters, and the degree of attachment of the liner to the ground mass in terms of acoustic wave impedance mismatching. Other elastic properties necessary are the various deformation moduli and Poisson's ratios.

Fluid flow properties of liner

75. The intact and crack permeabilities of EMP hole glass liners are required for determination of EMP applicability to in situ groundmass permeability testing and to fluid transportation conduits. In the event that liner permeabilities are too low for valid groundmass hydrologic testing in the EMP hole, the measured "leakiness" of the liner can be used to determine the degree of cracking in the liner itself for input into structural stability of the EMP hole.

Liner effects on geophysical log data

76. To properly use geophysical logs in EMP holes, the effect of the glass liner on the measured physical phenomena must be known. It is anticipated that minimal and correctable effects will be noted in acoustic logging. Because much electrical logging relies on current conduction through ionic aqueous solutions, the degree of liner cracking and, thus, communication with the groundmass will greatly affect these frequently used logging methods. Electro-magnetic radiation and induction electrical logs are expected to show little degradation resulting from the glass liner. Likewise, nuclear radiation logs are not expected to be degraded. These hypotheses must, however, be verified.

Core/Extrudite

Core diameter requirements

77. Based on standards for rock testing established by the Corps of Engineers, American Society for Testing Materials, and International Society of Rock Mechanics, the minimum diameter of rock core for laboratory testing is NX-sized or approximately 5.4 cm. Corps of Engineers soil testing procedures recommended the following minimum diameters:

Unit weight	3 in. (7.6 cm)
Permeability	3 in. (7.6 cm)
Consolidation	5 in. (12.7 cm)
Triaxial compression	5 in. (12.7 cm)
Unconfined compression	3 in. (7.6 cm)
Direct shear	5 in. (12.7 cm)

78. However, NX-sized soil core samples are commonly, if not routinely, tested. Therefore, 5.4 cm is the minimum required diameter of the unmelted portion of core to be recovered by the EMP. The largest core diameter recommended by the Corps is 6 in. (15.2 cm), primarily because of capacity limitations inherent to all except specially constructed test equipment. The maximum unmelted core diameter limitation is thus 15 cm.

79. Limitations on minimum and maximum encapsulation are not fixed, although the encapsulation must be adequate to allow recovery of intact specimens of granular, noncohesive soil (UNCON).

Thermal gradient restrictions in core

80. Thermal conditions to which the recovered core is subjected must be investigated for the entire period from approach of the EMP tip through passage to the cool ambient temperature recovery. Maximum temperature levels at radii from the axis out to the melted portion or encapsulation must be determined, the time intervals for temperatures of various proposed penetration rates established, and the probable mineralogic and hydrologic effects within the core caused by these temperatures estimated for each of the geologic material models.

Usable lengths of core segments

81. Laboratory testing standards require minimum core sample lengths of two times the test specimen diameter. Therefore, the minimum acceptable length of recovered segments from the EMP in any geologic material will be 2-1/2 times the diameter of the unmelted internal portion of the recovered core.

Recovery of core/extrudite

82. The core is to be recovered in a manner comparable to conventional wireline techniques in that the core recovery will not require pulling the entire string of stem and melter assemblies from the hole. Pneumatic propulsion of the core to the portal is acceptable.

83. The minimum proportion of testable core, that is the total accumulated length of core segments greater than 2-1/2 times the unmelted internal portion is to be 50 percent of the total length of the hole. The total accumulated length of recovered

core including core segments shorter than 2-1/2 times the unmelted portion is to be 90 percent of the total length of the hole. These requirements are for all modeled geologic materials.

84. These recovery proportion requirements are undoubtedly demanding but are necessary both because of the current importance of core examination for reliable subsurface condition interpretation and because the core segments lost in recovery are most frequently from the precise intervals most critical for the design and construction of economical and stable tunnels. While the ideal capability may be unattainable, it would approach 100 percent core recovery.

Groundmass

Induced fracturing/surface upheaval

85. Because of the large ratio between the minimum ground cover thickness and the EMP hole diameter, surficial deformation is anticipated to be negligible or nonexistent.

86. The degree of melt pressure induced fracturing will not be restricted for this design study although analyses and, eventually, empirical studies will be required to define the relationships between applied thrust, melt pressure, and the quantitative description of the resultant earth and rock fractures for the EMP design.

Thermal gradients in groundmass

87. Amplified analyses of the thermal gradients and time variations of these gradients in the groundmass surrounding the glass liner are required for all modeled geologic materials. These analyses will be applied to the determination of the physico-chemical alterations to the groundmass lithology due to the passage of the EMP. The affects of these alterations on the responses of the various geophysical logging methods and mechanical and hydrologic test methods will be determined. Some of the specific phenomena to be addressed are electrical resistivity and dielectric constant changes, changes in the groundmass gamma and neutron emitted spectra, changes in thermal and epithermal neutron capture cross sections, changes in

remanent magnetism and permitivity, changes in elastic deformation parameters pertaining both to acoustic logging and in situ mechanical testing, and the temporary and permanent alteration to the groundmass hydrologic conditions. These analyses are to be considered of paramount importance to the exploratory applications of the EMP and the benefits derived therefrom.

Materials to be penetrated

88. The models of geologic materials utilized in the earlier DOT study (Reference 1) are adequate, with the exception of UNCON. That model should be altered, or its application should be further detailed, to include two soil fractions that are quite common and one stratigraphic configuration that is nearly universal. The UNCON model should include a clay mineral fraction to range from that applied in SOSED up to 100 percent by weight. Variations of UNCON and SOSED, especially the former, should include an organic fraction of 1 to 5 percent by weight. Earlier studies make no mention of the response of an organic fraction in the melt, solidified liner, or neighboring heated groundmass. While the majority of organic soils lie at shallow depth, less than the specified minimum ground cover thickness, there is significant occurrence of this type of soil at depths below 10 meters in the form of marine clays, cyclothem sedimentary sequences, and valley alluvia. The variation of stratigraphic configuration that must be addressed is a layer or lens several meters thick of nearly pure quartz sand located within UNCON or SOSED. This stratigraphic configuration is almost universal in valley alluvium and fairly common in glacial deposits. Because of the very high melting temperatures required to penetrate pure quartz sand, it would be unfortunate to halt EMP advancement in a given long exploratory hole because of a relatively short length of path through a point bar or outwash channel deposit. The possibility of melt flow from heterogenous lithologies acting as a natural flux for pure quartz sand layers of finite dimensions should be investigated quantitatively.

89. The existence of effective flux additives and the feasibility of their application around the melting tip must be determined as an improvement to the EMP's efficiency.

PART IV: CONCEPTUAL DESIGNS

System Performance Analysis

90. Prior to initiating design work, a parametric study on size and performance variables was completed to develop preliminary evaluations of system requirements. These have been subdivided into geometry, power and thrust, and groundmass effects in an effort to parallel the preceding section.

Geometry

91. Within the diametral constraints of OD < 300 mm and ID > 50 mm, melt power will be minimized for the smallest size penetrator but downhole equipment packaging becomes more difficult. For the parametric study, it was estimated that 200 mm is the smallest hole diameter that could conceivably accommodate equipment such as guidance electronics. Therefore, when calculations could not be performed nondimensionally, two diameters, 200 and 300 mm (8 and 12 in.), were selected as the basis for calculations.

92. The required liner thickness to support the overburden can be calculated as a function of depth from surface and type of overburden. The maximum required depth of 100 m was selected to be met for all situations. Techniques and assumptions of the calculations for liner thickness are contained in Reference 1. Five geologic property models will be used throughout this report. Their composition and thermomechanical property values are also derived in Reference 1.

93. Without considering any surface loading, calculations were performed for the UNCON and MASIG models, the least and most dense, respectively.

94. For the UNCON geologic model, the condition of restrained lateral deformation was selected for calculation. It assumes the earth settlement about the glass liner is such that it returns to the overburden condition which existed prior to hole formation and that the overburden has no tensile strength. The equation for maximum permissible depth is

$$C_{max} = \frac{\left(S - s\right)\left[1 - \left(\frac{r_h}{r_l}\right)^2\right]}{2\,\rho_e\left\{\left[\frac{1 + \left(\frac{r_h}{r_l}\right)^2}{1 - \left(\frac{r_h}{r_l}\right)^2}\right]\left(1 - \frac{\nu}{1-\nu}\right) \mp \frac{1}{2}\left(1 + \frac{\nu}{1-\nu}\right)\right\}}$$

where the negative sign is for tension, the positive sign is for compression and

C_{max}	=	depth from surface to tunnel centerline
S	=	tensile or compressive strength
s	=	stress from a primary load
ρ_e	=	earth or overburden density
ν	=	overburden Poisson's ratio
r_h	=	liner or hole inside diameter
r_l	=	liner outside diameter

95. The compressive strength of the glass is 206 MPa (30,000 psi), and the tensile strength is 13.8 MPa (2000 psi). For a Poisson's ratio of 0.45 and dry and wet densities of 1.5 and 1.9 Mg/m^3, the allowable depth was calculated as a function of thickness to hole radius ratio (δ_o/r_h). Figure 6 shows that the allowable depth is determined by tensile strength and, at 100-m depth, the nominal (S_t = 2000 psi) thickness/radius is 0.046. A factor of four reduction in strength (S_t = 500 psi) increases δ_o/r_h to 0.083.

96. The above does not include the effect of local surface loadings. The maximum additional equivalent depth in dry UNCON is $\frac{150{,}000\ kg/m^2}{1{,}500\ kg/m^3}$, or 100 m. The liner must then withstand an overburden equal to a 200-m depth in the worst case. A more realistic value can be calculated by the method given by Hetenyi (Reference 2). At 10 m deep (minimum specification) and 150,000 kg/m^2 load on 1 m^2, the equivalent load on the liner is reduced to only 860 kg/m^2. For conservative design practice, the thickness ratio at 200 m will be used in all following calculations.

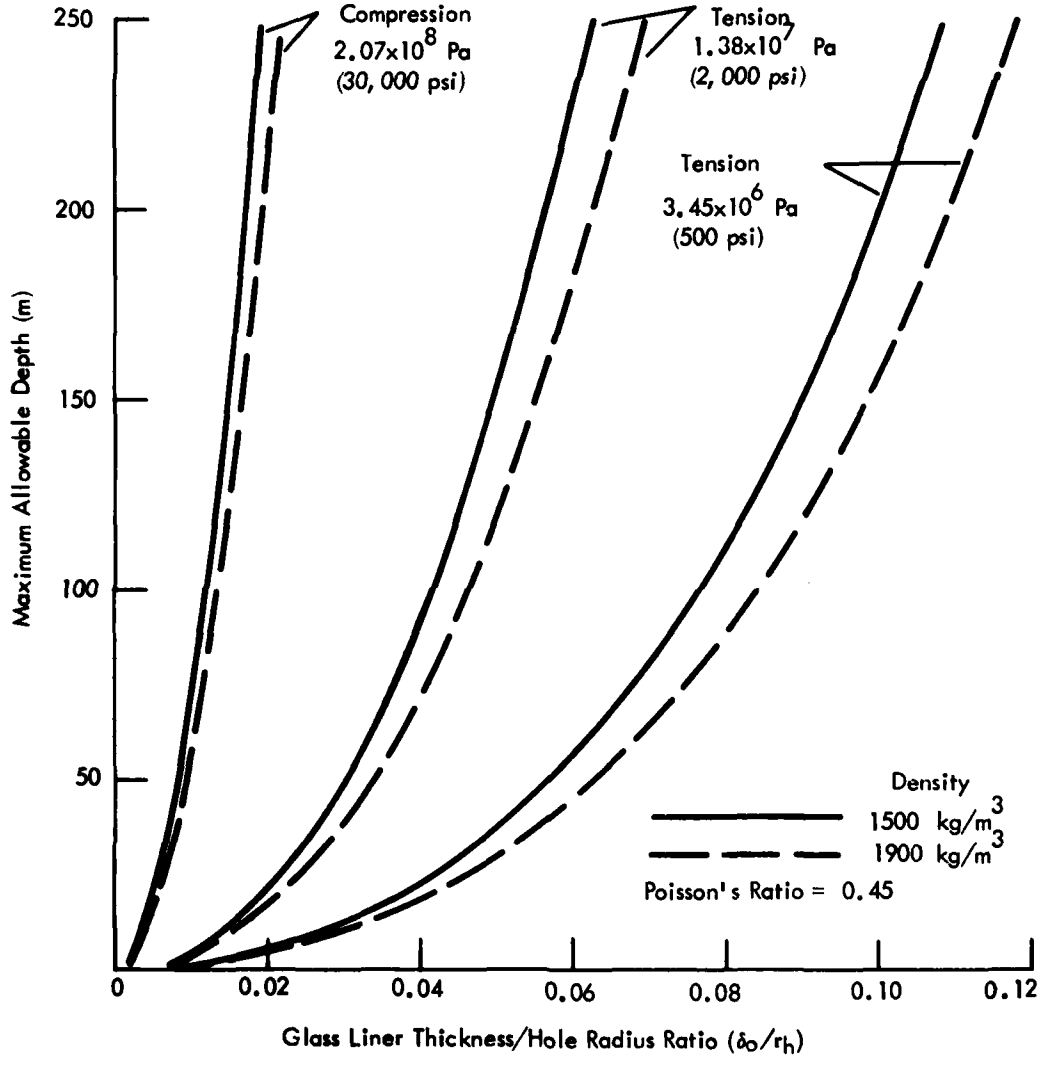

Figure 6. Allowable depth in UNCON for different glass liner strength criteria

97. Similar analyses were performed for SOSED and MASIG overburdens which are in the order of decreasing Poisson's ratio. In these cases, the assumption of zero tensile strength of the overburden is too severe, producing the requirement of thickness/radius ratio of up to 0.3 at a 200-m depth. An equivalent tensile strength of "blocky and seamy" overburden at a 3000-m depth is required to evaluate liner thickness on a realistic basis. This is true for the scale of the tunnel relative to the depth in a competent formation. For a full-size tunnel, this assumption would not be valid. However, for 300-mm dimensions, the overburden does possess some tensile strength. Thus, the UNCON model becomes the limiting case establishing the liner thickness requirement.

98. To determine the relationship between the liner geometry, melted rock and penetrator velocities, a generalized mass balance was derived for the configuration and nomenclature of Figure 7. The resultant equation is

$$\frac{\delta_o}{r_h} = \sqrt{\left[\left(1 - \frac{\rho_g}{\rho_e}\right)\left(\frac{r_c}{r_h}\right)^2 + \left(\frac{r_c + \delta}{r_h}\right)^2\left(\frac{\rho_g}{\rho_e} - \left(\frac{\rho_m U_i}{\rho_e U_p}\right)\right) + \left(\frac{\rho_m U_o}{\rho_e U_p} - \frac{\rho_g}{\rho_e}\right)\frac{\rho_m U_o}{\rho_e U_p}\left(\frac{r_{po}}{r_h}\right)^2 + \left(\frac{\rho_m U_i}{\rho_e U_p}\right)\left(\frac{r_{pi}}{r_h}\right)^2\right]} \Big/ \left(1 - \rho_g/\rho_e\right) - 1$$

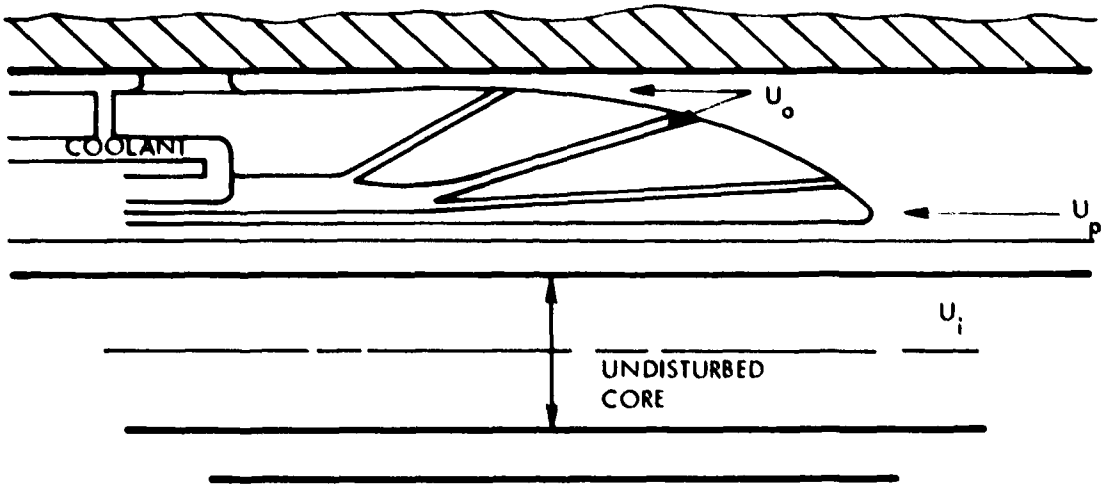

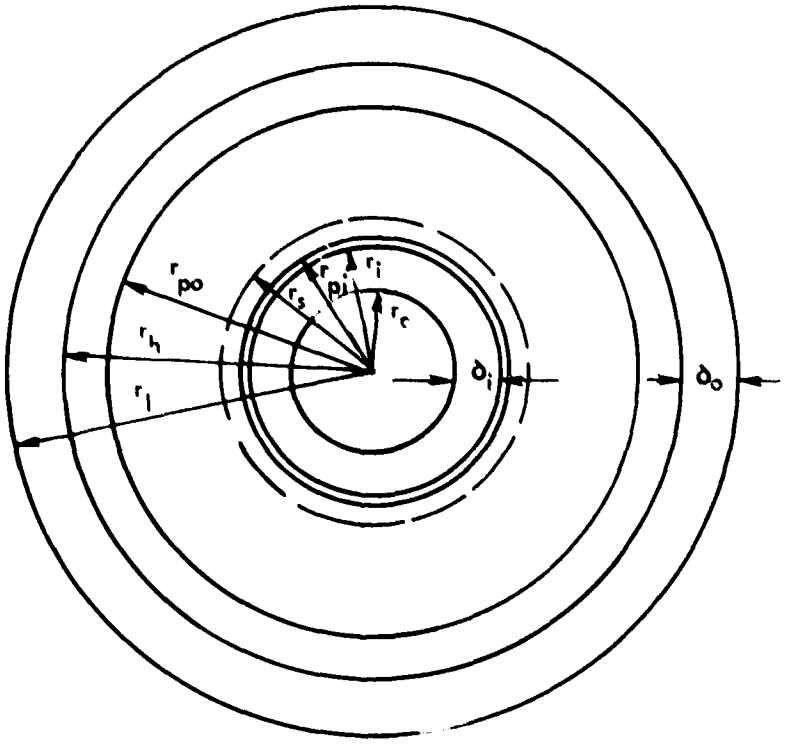

Figure 7. Penetrator schematic

where

δ_o = liner thickness

ρ_g = glass liner density

ρ_m = melt density

99. A mass balance parametric study on dimensions, geologic model, penetration velocity and extrudite velocity was made to size the device consistent with its requirements. The results of this study indicated that a ratio of extrudite to penetrator velocity of approximately 20 gives the desired liner thickness within the range of dimensions and model densities.

Power and Thrust

100. Using the energy equations and model properties developed in Reference 1, the heater power and penetrator surface temperatures were calculated for two diameters and five geologic models as a function of penetrator velocity. The power equation is:

$$q = C \delta_e \rho_e C_p U_p (T_m - T_\infty) + \frac{k_{eff} A_m (T_m - T_\infty)}{2 (r_h + \delta_o)} +$$

$$S_m \rho_e U_p \left[C_p (T_m - T_\infty) + \frac{1}{2} C_m (T_{max} - T_m) + \lambda \right]$$

where

q = heater power

C = mean circumference of melt/earth interface

δ_e = effective heat penetration depth

C_p = earth specific heat

T_m = melt temperature

k_{eff} = effective thermal conductivity

A_m = surface area of melt/earth interface

T_∞ = ambient earth temperature

S_m = cross-sectional area of melt

C_m = specific heat of melt

T_{max} = penetrator surface temperature

λ = latent heat of fusion

101. The first two terms represent dynamic (moving) and static heat losses to the unmelted rock. Figures 8 and 9 show the power requirements for 200-and 300-mm diameter holes for velocities up to 1.4 mm/sec (5 m/hr). Thus, the maximum power of 1050 kW is for CALCI. Heaters are to be sized to deliver up to 1200 kW to meet the requirement of 5 m/hr in any media. Figure 10 shows the amount of power required to melt and also the power lost to the surroundings in the process, as reflected by the previous equation for the CALCI model. If there were no requirement to penetrate CALCI, power could be reduced by nearly 25 percent to MASIG.

102. The above predictions on heater power are based on LASL test data and are considered reasonably accurate. The prediction of surface temperature by a simple analysis is much more difficult. The thermal conductivity of liquid rock (k_{eff}) is an unknown quantity and significantly increases uncertainty in analysis, as indicated in Reference 3. Several new attempts at liquid conductivity were investigated but all gave low values. One example, shown in Figure 11 for MASIG, is extrapolated from the basalt study of Reference 4 and the mantle conductivity calculations of Reference 5. However, the use of the liquid model with the heat transfer model of Reference 1 does not correlate with LASL measured penetrator surface temperatures in basalt. The surface temperature equation used to calculate surface temperature curves as shown in Figures 12 and 13 is:

$$T_{max} = \sqrt[5]{T_m^5 + \frac{5\delta_o}{\beta A_m}\left(q - \frac{1}{2} q_{sh}\right)}$$

where

q_{sh} = melt superheat

β = constant in liquid thermal conductivity equation

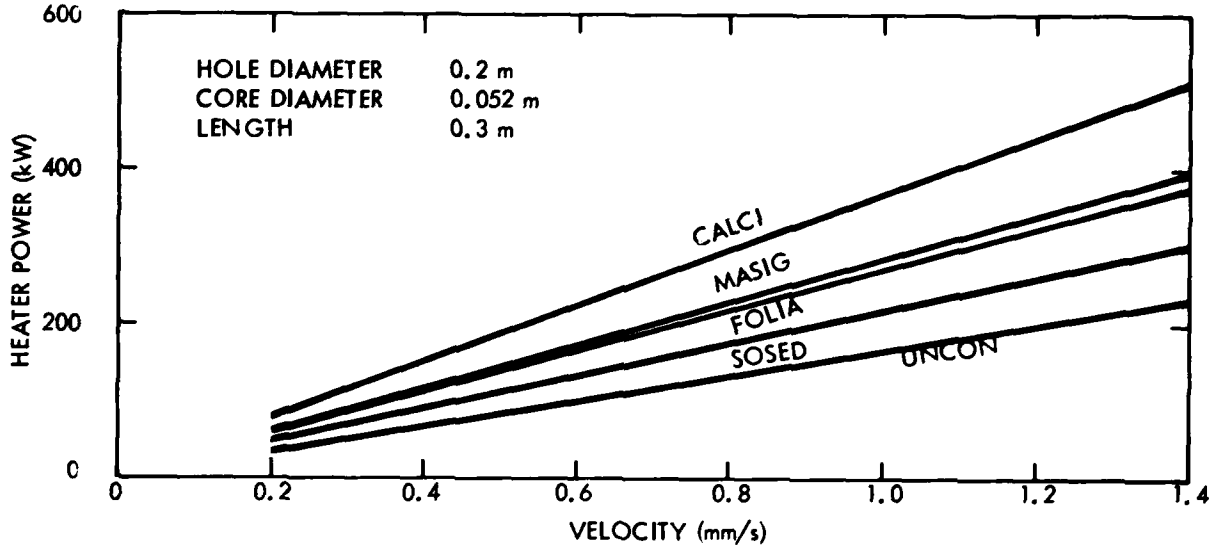

Figure 8. Heater power for 0.2 m hole diameter

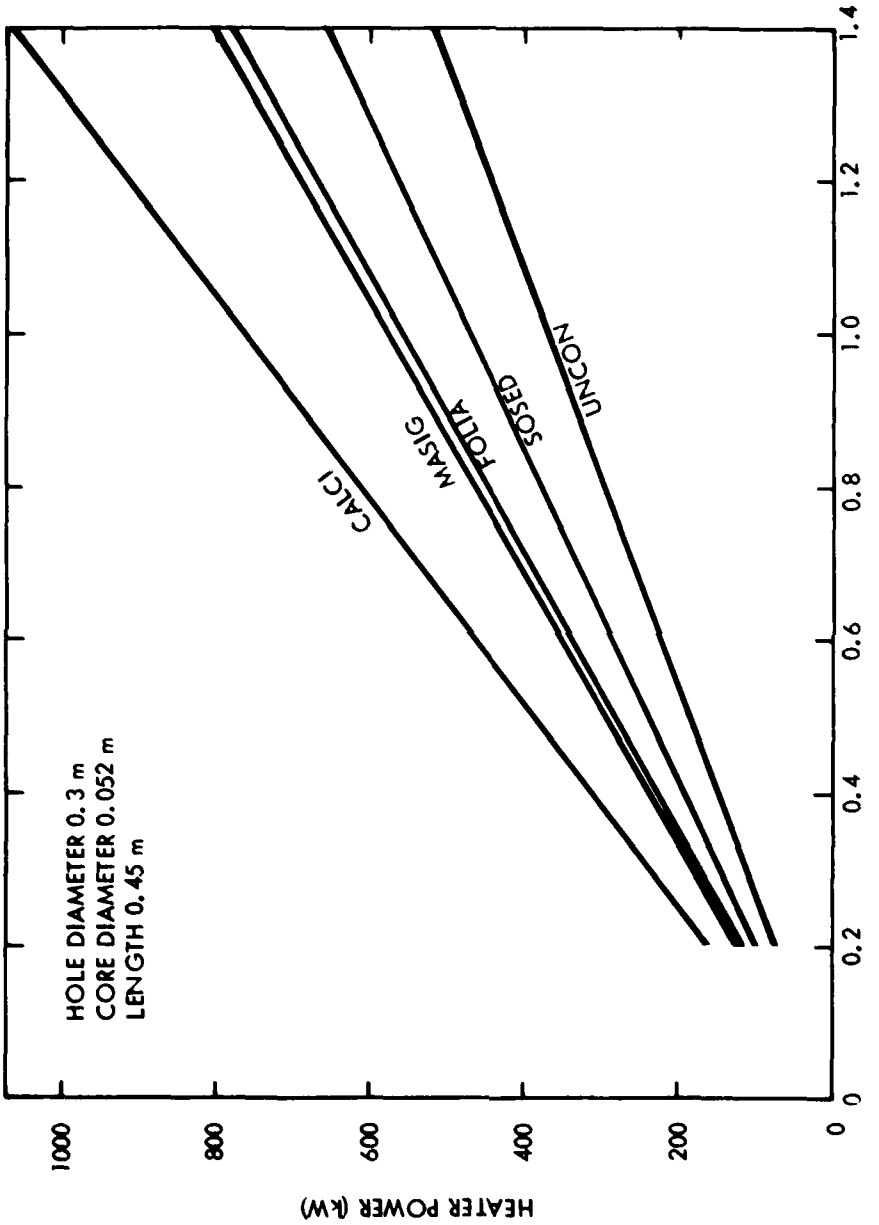

Figure 9. Heater power for 0.3 m hole diameter

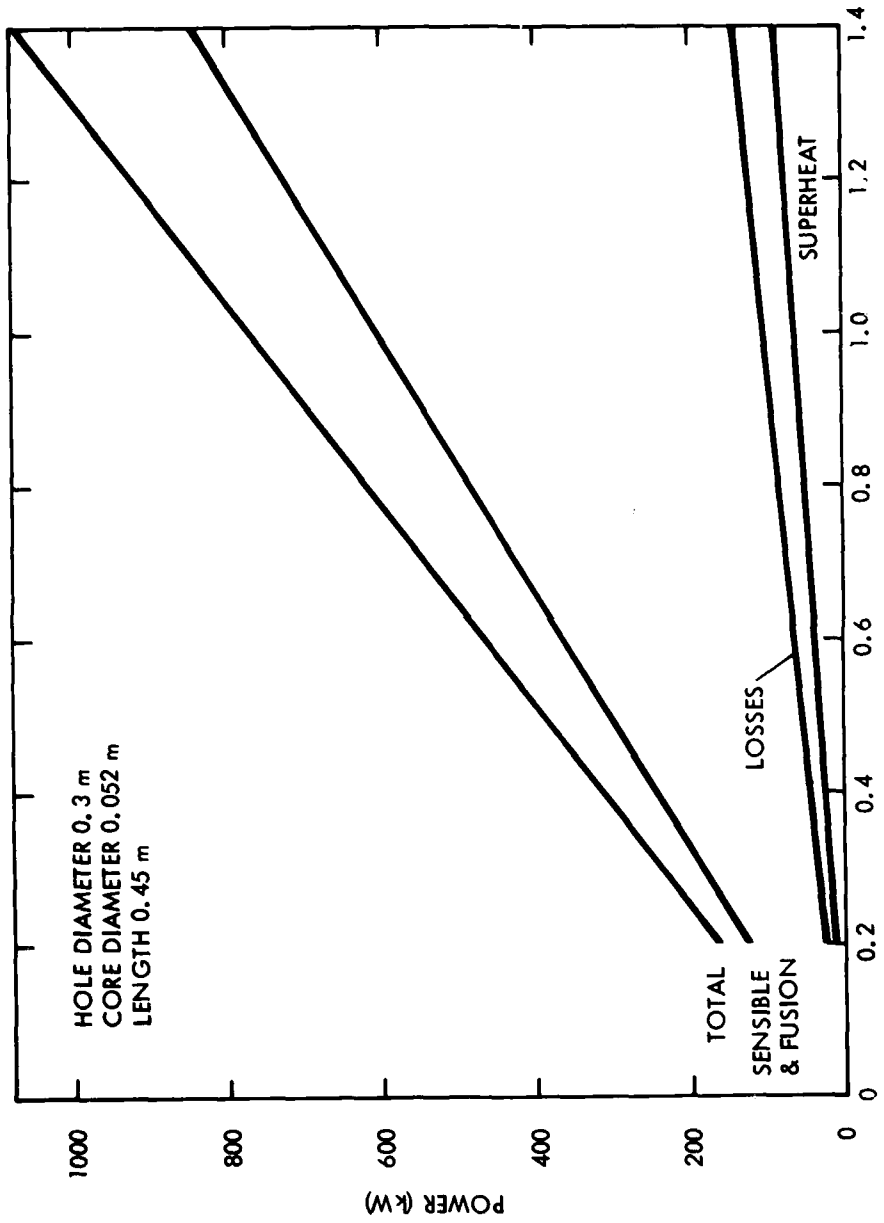

Figure 10. Terms in the power equation for CALCI

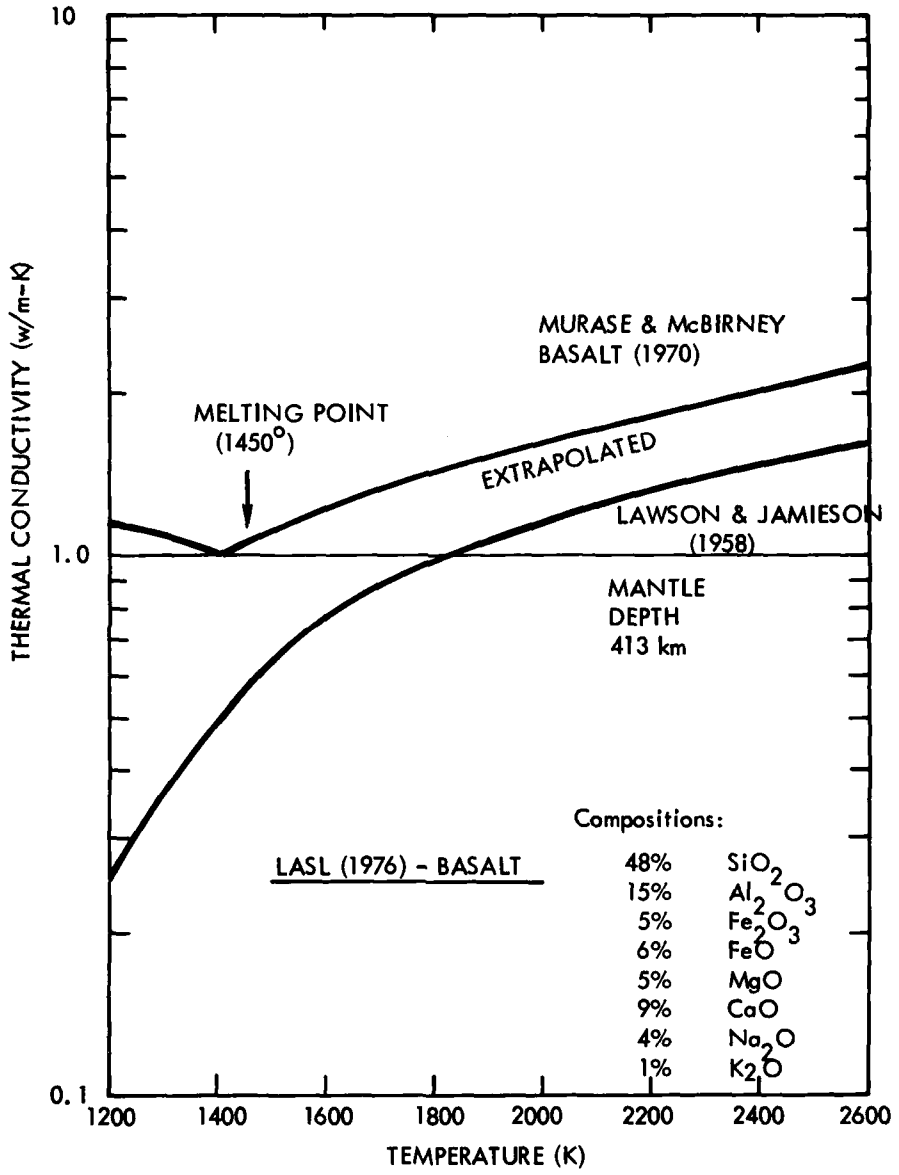

Figure 11. Liquid conductivity model for MASIG

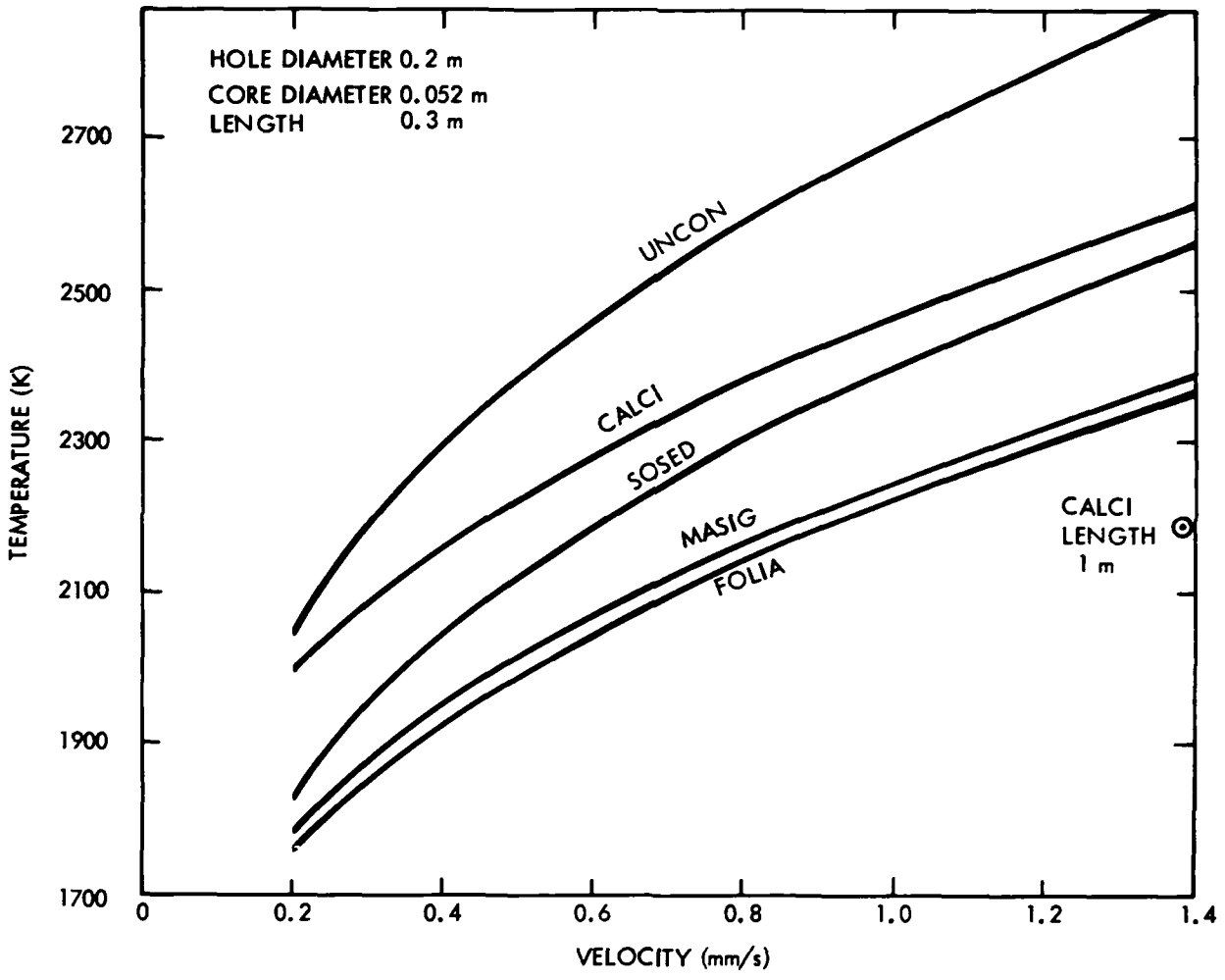

Figure 12. Surface temperature of a 0.2 m diameter penetrator

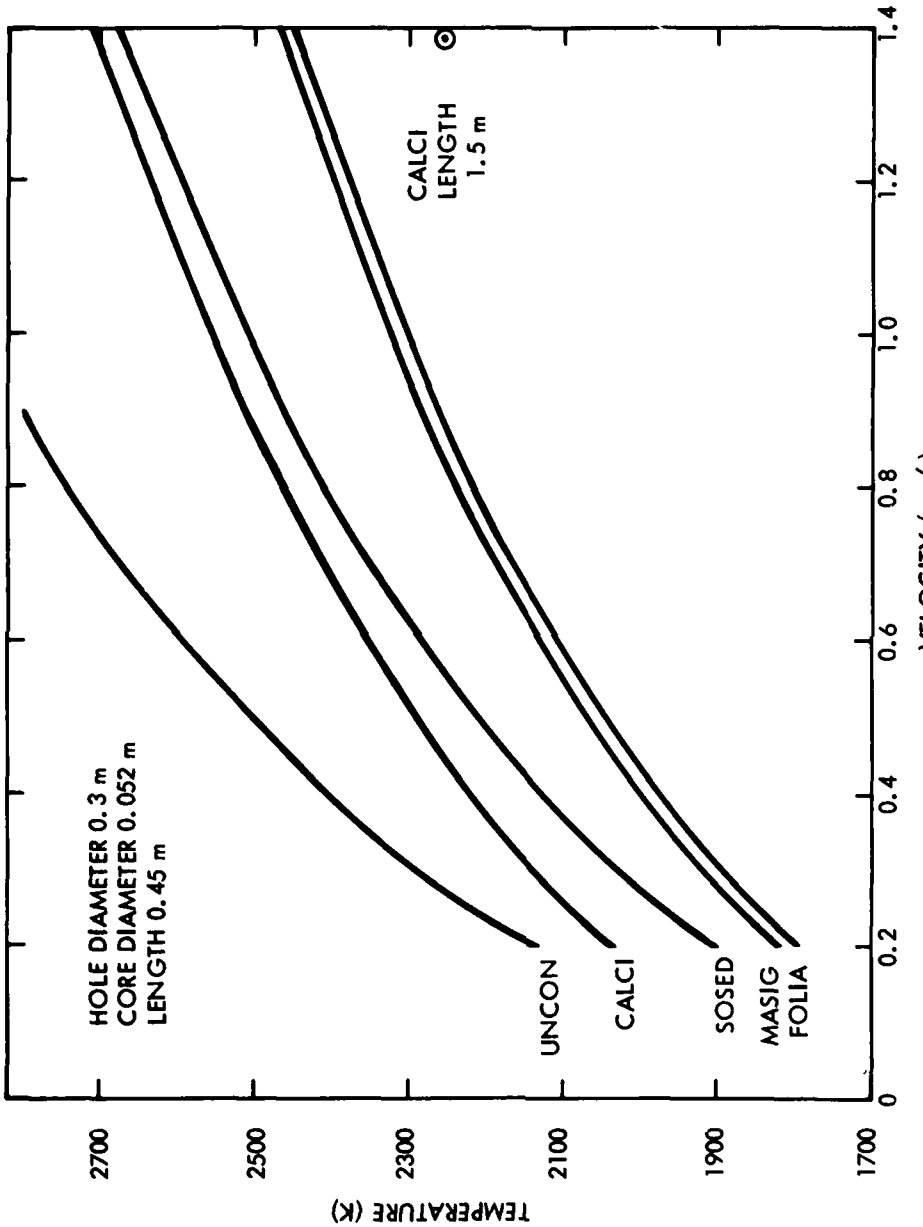

Figure 13. Surface temperature of a 0.3 m diameter penetrator

103. From these curves, it becomes obvious that the surface temperature is the velocity limiting parameter in the system. A single point calculation was made for the CALCI model at an increased L/D of 5 rather than 1.5 as on the curves. This value yields an increased surface area for approximately the same power, although increased surface area slightly increases losses and reduces the temperature by nearly 400 K. An extended surface configuration (fins) can be used to reduce the temperature and is presented in the discussion of design selection.

104. Refractory metals such as tungsten, molybdenum, tantalum, and niobium and a few carbide, nitride, and boride compounds are the only practical candidate materials for 2300°C application. There is severe corrosion by molten earth at higher temperatures. Also, the silicide coatings developed to prevent the elevated temperature corrosion of refractory metals would be readily dissolved by molten earth. If the temperature calculations are reasonably accurate, it will be difficult to meet all the requirements of tip lifetime and penetrator velocity in any media.

105. The applied thrust load calculation, neglecting stem drag, is based on an equation in Reference 1.

$$F = \pi(r_{po}^2 - r_s^2)\left[\rho_e C_{max} + \frac{3\mu_m U_p r_{po}^2}{2 g_c \delta_o^2 \sin\theta} + \frac{2 r_{po} \mu_m U_p \cot\theta}{g_c \delta_o^2}\right]$$

$$+ \frac{\pi \mu_o U_p B^3}{8}\left[4 r_s^4 \ln\left(\frac{r_s}{r_c}\right) - 3 r_s^2 - r_c^2 (r_s^2 - r_c^2)\right]$$

$$+ \frac{4\pi r_{po} \mu_c U_p L_c}{g_c \delta_o}$$

where

F = applied thrust load

μ_m = melt viscosity

θ = half angle of the penetrator head

μ_o = temperature coefficient of viscosity

B = constant of temperature distribution

μ_c = viscosity at cooldown transition temperature

L_c = length of cooldown section

g_c = gravitational constant

106. Results for three of the five models are shown in Figure 14. Excluding stem drop, a maximum force of 10^5N (23,000 lb) is required.

Groundmass

107. Effects of the penetrator on the hole and its use were emphasized by the requirements. The first is the effect of the deposited heat on properties of the unmelted earth and the second is this effect on the validity of present logging measurements.

Heat Wave Penetration

108. A transient analysis was performed to estimate the extent of temperature perturbations in the earth surrounding the path of the EMP. Of main interest were the radial distances from the EMP at which earth temperature changes will be caused by the penetrator and the time periods required. Considerations such as these are important in situations involving earth melting in the vicinity of buried cables and power lines, water lines, etc. The earth heatup calculations were also used to provide estimates of the heat transfer rate between the cylindrical surface of the EMP and the surrounding earth, to correlate with previous simple analytical expressions.

109. The analysis applied an earth heat transfer model in the form of a circular disk, composed of concentric, ring-shaped elements or nodes. As shown in Figure 15, the earth material surrounding the penetrator was represented by 58 nodes. During the computer simulation of the problem, each node was assigned an initial temperature, material thermal properties and values of volume, cross-sectional area and heat conduction length. The 5.0-in. radius of the penetrator/earth interface was established by the diameter of the penetrator, which was assumed to be 10 in.

110. The earth heat transfer model is one-dimensional in the radial direction. The one-dimensional feature provides the analysis with some conservatism during heatup and cooldown since heat dissipation cannot occur parallel to the penetrator axis. The model also introduces some nonconservative effects since the nodes cannot preheat prior to the arrival of the penetrator or continue to heat after the penetrator has passed. While these

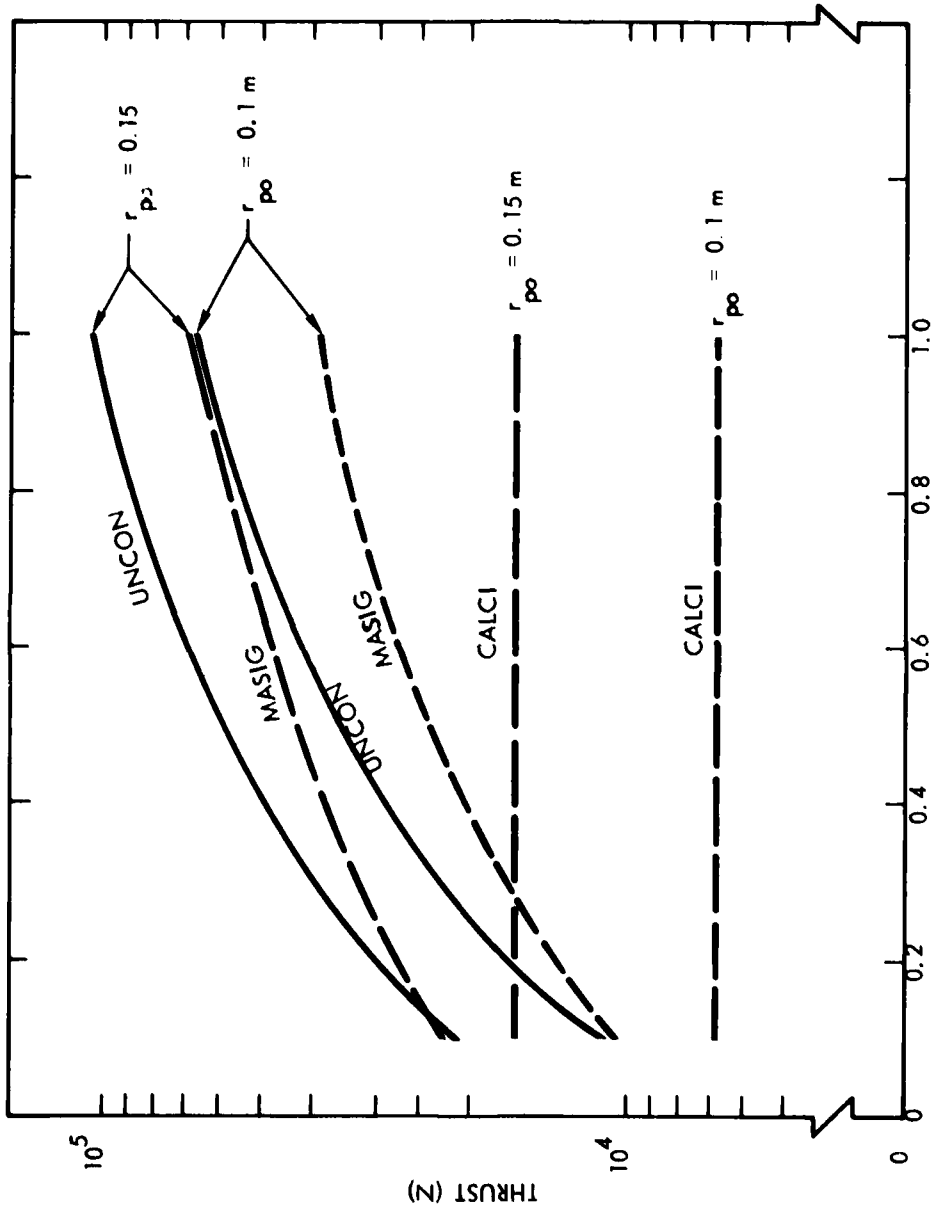

Figure 14. Required penetrator thrust at maximum depth

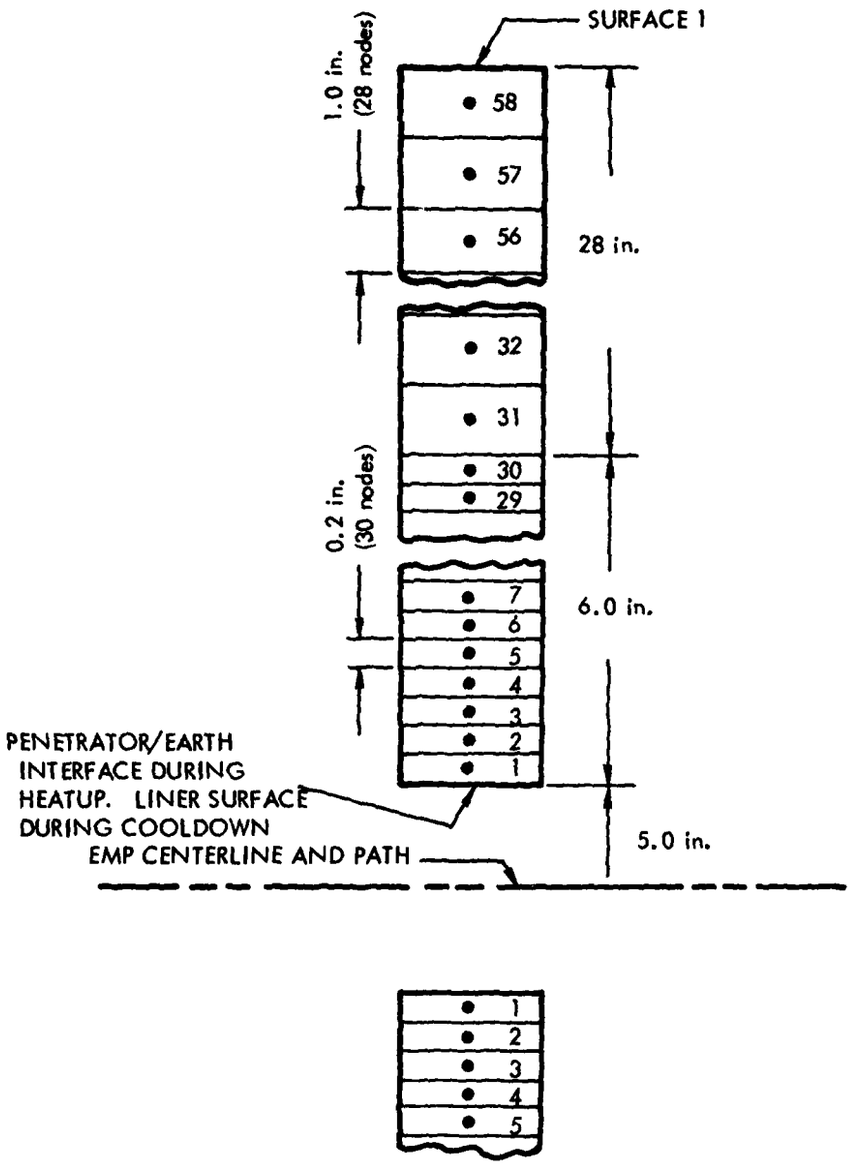

Figure 15. Earth heat transfer model

nonconservative effects are not believed to be significant, they should be examined in future analyses utilizing a two-dimensional earth heat transfer model.

111. In the computer simulation of this problem, the initial steady-state temperature of all nodes was 100°F. At time zero, the temperature of the penetrator/earth interface was step changed to 2222 K (3540°F) to simulate the arrival of the penetrator. That temperature was maintained for 650 seconds, which approximately simulates the passing of a 12 in. penetrator moving at 0.5 mm/sec (or a 24 in. penetrator moving at 1.0 mm/sec, etc.). For $\tau > 650$ seconds, the constant temperature constraint on the interface was removed and heat transfer was permitted between the interface* and liner cooling air. The cooling air was assumed to flow at 400°F and 1.0 lb/sec in the annular space between the liner and the penetrator stem. The assumed thickness and area of this flow path were 0.125 in and 0.0297 ft^2, respectively. This information and the air flow data lead to a film heat transfer coefficient of 104 Btu/hr ft^2 F, which was assigned to the liner surface during the earth cooldown period ($\tau > 650$ sec). The film coefficient was evaluated using the following expression, recommended in Reference 17 for use in analyzing gas flow in annular spaces:

$$h = 0.024\, C_a \frac{G^{0.8}}{D^{0.2}}$$

where

h = film heat transfer coefficient, Btu/hr ft^2 F

C_a = air specific heat ≈ 0.245 Btu/lb-F

G = air flow mass velocity

D = annulus clearance = 0.125 in.

112. Throughout the problem simulation, the temperature of model Surface 1 (Figure 15) was maintained at 100°F. That assumption did not affect the analysis since, for all cases considered, earth temperature variations did not occur in the outermost nodes.

* The penetrator/earth interface becomes the surface of the molten tunnel liner after the penetrator has passed.

113. Earth temperature distribution calculations were performed for two geological models - MASIG and UNCON. Material properties employed in the calculations are presented in Table 3. Specific heat data were obtained from Table 5-1c of Reference 1. The spikes in the specific heat tables approximate the constant temperature melting process that was assumed to occur at 2240°F. Thermal conductivity data are based on the 600 K values presented in Table 5-1b of Reference 1. Thermal conductivities at other temperatures were obtained by passing curves through the 600 K points following the temperature dependency trends exhibited by other rock and glass materials.

114. Predicted cooldown temperature profiles for MASIG and UNCON are presented in Figures 16 and 17. The profiles for time = 0.0 apply to the endpoint of the 650-second heatup period. At that time, the figures show melt thicknesses (at 2240°F) of 1.3 in for MASIG and 0.6 in for UNCON. The relatively large melt thickness and the more extensive temperature propagation in MASIG are due to the high thermal conductivity values exhibited by that material. The figures also indicate that much of the energy added to the earth by the penetrator will have been withdrawn by liner cooling air 1 hour after the penetrator has passed. During that time, all variations in the earth temperature occurred within a 14 in radius of the liner (or within a 20 in radius of the EMP centerline). For longer cooldown times, the temperature of the liner cooling air will exert increasing influence on the earth temperature distribution. This is demonstrated in Figures 16 and 17 by the 1.0-and 5.0-hr cooldown profiles. If high cooling air temperatures cannot be avoided and if earth temperature perturbations must be restricted, the EMP could be purposely operated on an alternating melting/cooling cycle. Periodically de-energizing the penetrator heaters while maintaining the flow of liner cooling air would reduce the air temperature and that of the surrounding earth. After an appropriate cooldown time, the heaters would again be energized to resume melting. Optimum melting and cooling cycle times could be predicted using analyses such as the one described herein.

115. Additional MASIG cooldown profiles are presented in Figures 18 and 19. Those calculations show radial temperature propagations which tend to be slightly less extensive than those in Figure 16 since they apply to a lower penetrator surface temperature (Figure 18) or to a shorter heatup period (Figure 19).

Table 3

Material Properties

Temperature (°F)	Specific Heat (Btu/lb F) MASIG	UNCON	Thermal Conductivity (Btu/hr ft-F) MASIG	UNCON
80	0.302	0.319	0.98	0.16
620	0.302	0.319	1.27	0.19
1340	0.302	0.319	1.88	0.26
1831	0.302	0.319	2.72	0.34
1849	0.269	0.274	2.72	0.34
2240	0.269	0.274	3.70	0.46
2242	9.80	8.47	3.70	0.46
2256	9.80	8.47	3.70	0.46
2258	0.239	0.363	3.70	0.46
2371	0.239	0.363	4.10	0.51
3140	0.239	0.363	7.46	1.01
4040	0.239	0.363	14.45	2.08
4940	0.239	0.363	28.90	4.33

Density:

MASIG 174.5 lb/ft^3 (1% porosity)

UNCON 118.6 lb/ft^3 (40% porosity)*

* Due to porosity, the UNCON density will increase appreciably when melting occurs. Effects of the density change have not been considered in the analyses performed to date.

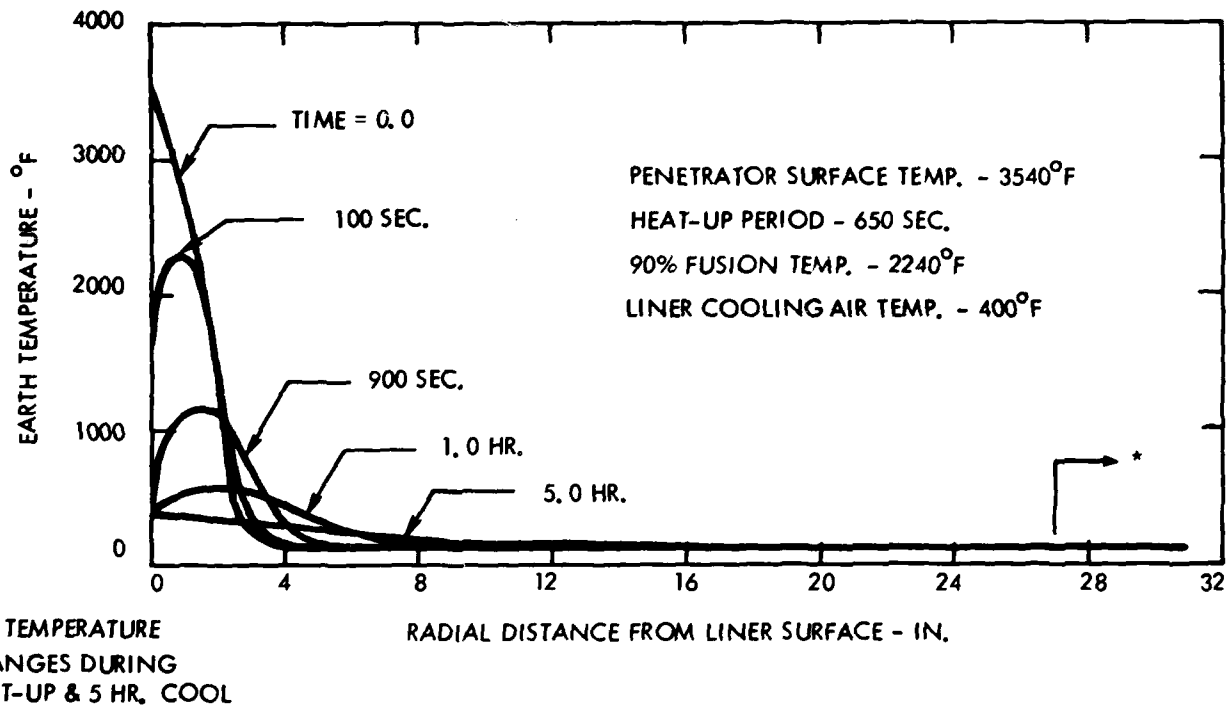

Figure 16. MASIG cooldown temperature profiles at 2222 K (3540°F) and 0.5 mm/sec.

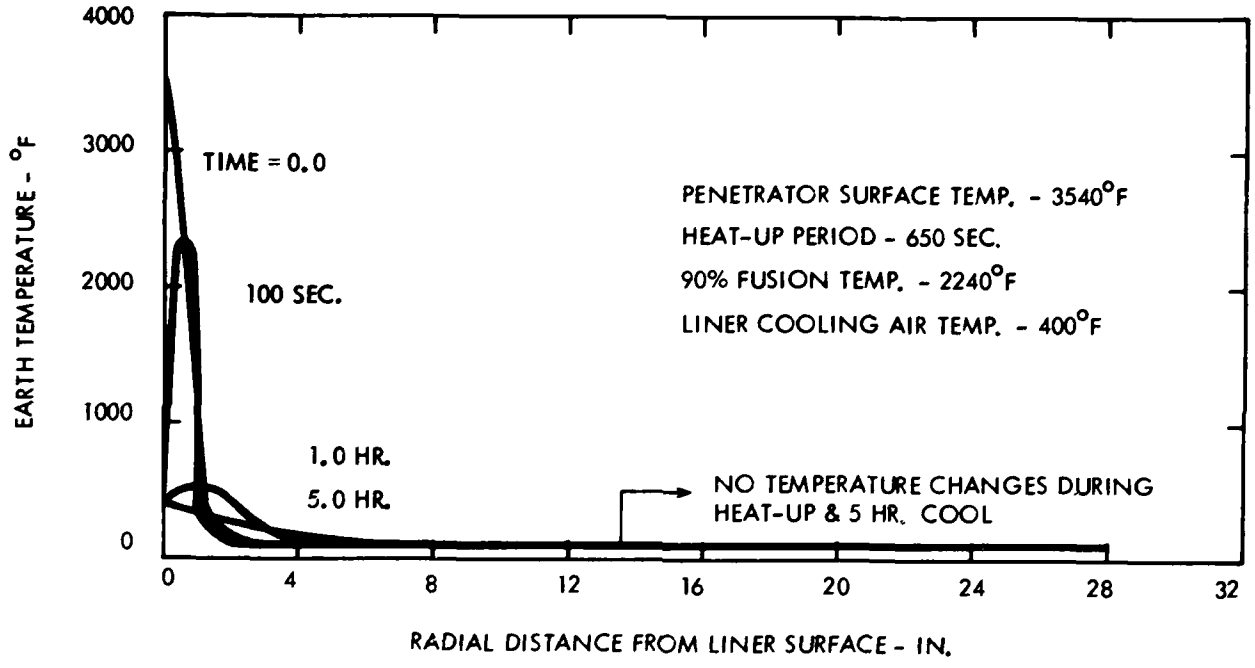

Figure 17. UNCON cooldown temperature profiles at 2222 K (3540°F) and 0.5 mm/sec.

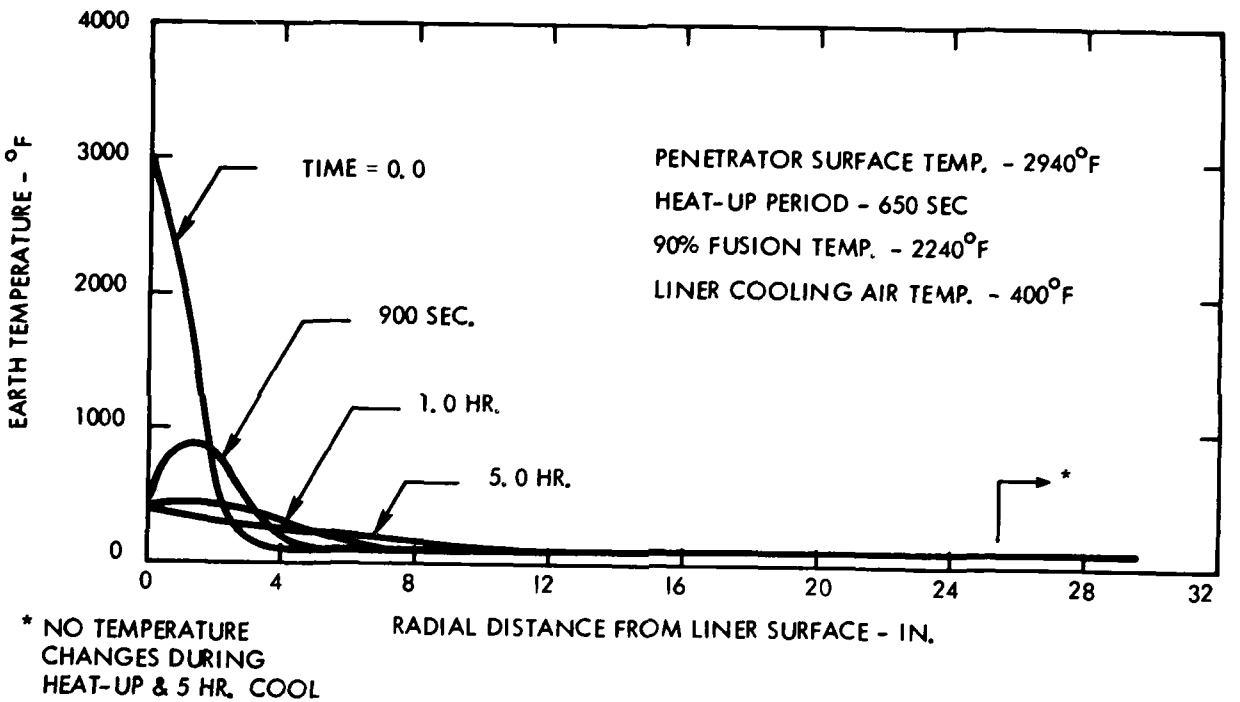

Figure 18. MASIG cooldown temperature profiles at 1889 K (2940°F) and 0.5 mm/sec.

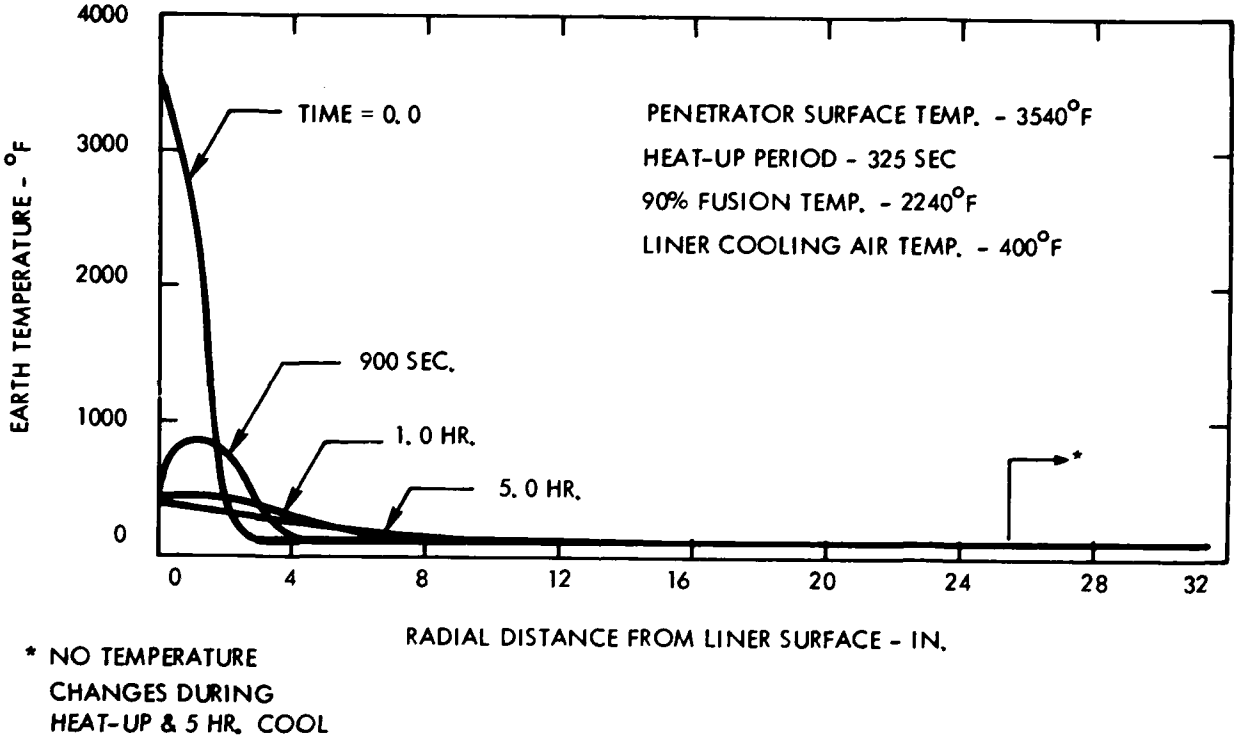

Figure 19. MASIG cooldown temperature profiles at 2222 K (3540°F) and 1.0 mm/sec.

116. The same type of calculation was performed for the core. The model included the resistance of the pyrographite insulation and the molybdenum sheath, while it had no active air cooling. Thus, it presents a worst-case condition. The centerline temperature of the core increased only 150°F beyond the ambient for the nominal penetrator temperature at the time of passage. If cooling air is provided, it can be limited to only slightly greater temperatures. The surface temperature of the core is substantially higher, indicated in Figure 20. The insulation thickness controls this temperature.

117. The earth heatup calculations can also be used to estimate the heat flux distribution along the length of the penetrator cylindrical surface and the total heat transfer rate at that surface. The heat transfer data can be applied in selecting a proper value for the liner cooling air flow rate. Penetrator heat flux distributions for several cases are shown in Figure 21. The distributions were obtained using the one-dimensional earth heatup calculations described above. To illustrate the method, consider the 650-second heatup period case. During that period, the predicted heat flux at the penetrator/earth interface at 325 seconds would represent the penetrator surface heat flux for an $\frac{X}{L}$ value of 0.50. Thus, in general, the penetrator surface heat flux from the one-dimensional heatup calculations at time = t is equal to that at an $\frac{X}{L}$ value of $\frac{t}{\tau}$ where τ is the duration of the heatup period.

118. Additional information is presented in Table 4 to permit a comparison of the heat transfer rate through the cylindrical side surface of the penetrator with the power requirement at the front surface, Q_F. The quantity Q_F was estimated using density and heat content data from Tables 5-1b and 5-1c of Reference 1 and contains only the energy required to achieve melting. Therefore;

$$Q_F = HU_p A_m \sigma_e \times 2.778 \times 10^{-4} \left(\frac{\text{watts-hr}}{\text{Joule}}\right) \times 3600 \left(\frac{\text{sec}}{\text{hr}}\right) \times \frac{1}{10^6} \left(\frac{\text{Megawatts}}{\text{watt}}\right)$$

$$Q_F = 1.0 \times 10^{-6} HU_p A_m \sigma_e$$

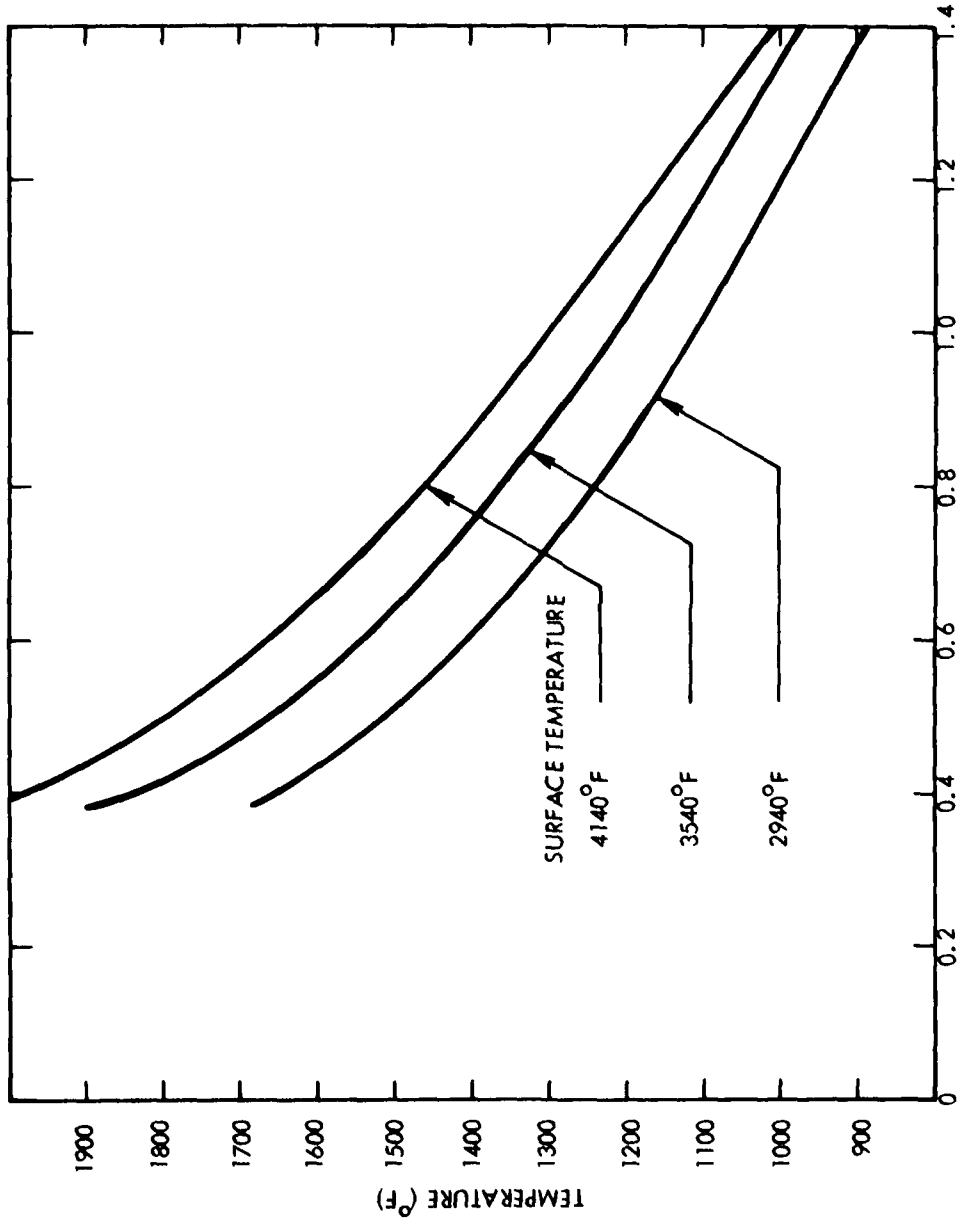

Figure 20. Maximum core surface temperature

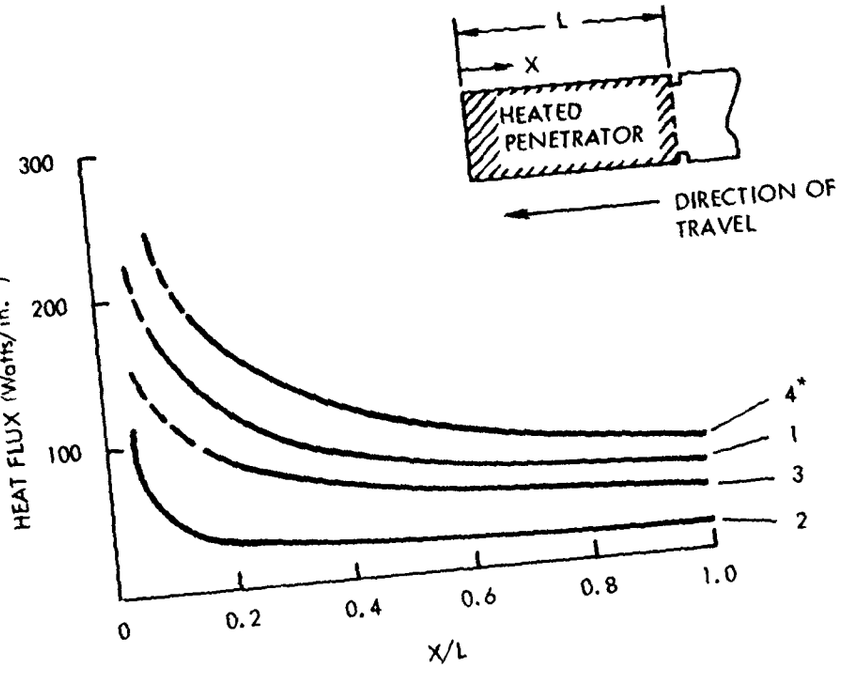

*see Table 4

Figure 21. Penetrator cylindrical surface heat flux distributions

Table 4

Penetrator Heat Transfer Characteristics

Earth Material	1* MASIG	2 UNCON	3 MASIG	4 MASIG
Penetrator Transit Time (sec)**	650	650	650	325
Penetrator Surface Temperature (°F)	3540	3540	2940	3540
Penetrator Side Surface Heat Transfer Rate (MW)†	0.12	0.05	0.09	0.16
Approximate Penetration Rate (mm/sec)	0.5	0.5	0.5	1.0
Front Surface Heat Transfer Rate (MW)	0.15	0.10	0.15	0.30
Total Penetrator Power Level (MW)	0.27	0.15	0.24	0.46

* Refers to the curve in Figure 21 with the same identifying number

** Time required to move a distance equal to the heated length of the penetrator

† For this calculation, the penetrator heated length was assumed to be 12.0 in. Further, the penetrator side surface area was enlarged to 100.0 in.^{2} per in. to account for extended surfaces

where

H = earth heat content required for melting - Joules/gm

U_p = penetration rate - mm/sec

A_m = melt cross-sectional area - mm^2

σ_e = earth density - gm/mm^3

Q_F = front surface power requirement - MW

As an example, consider the conditions for Curve 4 in Figure 21. In that case,

H = 1856 Joules/gm

V = 1.0 mm/sec

A = $\frac{\pi}{4}$ $(11.0^2 - 3.0^2)$ = 88.0 in^2 = 56,770 mm^2

ρ = 2.8×10^{-3} gm/mm^3

Therefore,

$$Q_F = (1.0 \times 10^{-6})\ (1856)\ (1.0)\ (56,770)\ (2.8 \times 10^{-3})$$

$$Q_F = 0.30 \text{ MW}$$

and the total penetrator power requirement (excluding heat losses to the stem region) would be 0.51 MW.

119. In summary, the primary purpose of this section involves prediction of the transient temperature distribution in the earth surrounding the path of the EMP. The UNCON and MASIG geological models were considered and the analysis shows that temperature variations will occur at larger radial distances from the penetrator for MASIG material because of its relatively large thermal conductivity. The analysis also shows that liner cooling air can withdraw much of the energy added to the earth by the EMP within 1 hour after passage of the penetrator. During that time, the MASIG temperature changes were restricted to a 20-in. radius of the EMP centerline. For longer cooldown periods, the temperature of the liner cooling air will control the earth temperatures in the vicinity of the EMP. If high cooling air temperatures cannot be avoided and if the earth temperature perturbations are to be restricted in a certain EMP application, it may be necessary to operate the penetrator with a periodic melting/cooling cycle.

Hole Logging

120. Two principal changes occur in the passage of the penetrator. First, the groundmass temperature is temporarily elevated and, second, a glass liner is formed. Each of these can effect logging results as described in the following discussions.

Remanent magnetism

121. Most rocks owe their magnetism to their content of various iron oxides and to their solid solution with titanium oxides. Igneous rocks acquire most of their magnetism as they cool through the Curie temperature. The intensity of this thermo-magnetic remanence is dependent on the age of the rock (Reference 6). The Curie temperature is a function of composition, but for many rocks is approximately 850 K (Reference 7). Previous temperature distribution curves indicate that the 850 K isotherm does not extend more than 5 inches from the penetrator. However, Reference 6 indicates that the natural remanent magnetization can be increased by up to a factor of 5 in the volume of rock that exceeds the Curie temperature, the older the rock, the bigger the factor.

Neutron logs

122. Neutron sources that are used in well logging emit high energy neutrons. Neutron detectors that are used in well logging are most sensitive to low energy neutrons in the thermal (0.025 eV) and low eV range.

123. Consequently, neutron logging instruments are always sensitive to the neutron scattering properties of the materials near the neutron source. The scattering properties that are important are the neutron scattering cross section of the nuclei and the mass of the scattering nuclei. The larger the scattering cross section for fast neutrons, the more frequent the collisions. Hydrogen has the highest scattering cross section of all nuclei.

124. The mass of the nucleus is important in determining the amount of energy a neutron loses in a collision with a nucleus. The lower the mass, the higher the energy loss. Consequently, hydrogen is the most effective atom involved in slowing down neutrons from the originating energy in the MeV range to the detection range of a few eV or less. For this reason, neutron logging is most often used for determination of the hydrogen present in rocks. Since hydrogen is found in the pore spaces, in the form of water or hydrocarbons, the response of the logging system is primarily a function of porosity if the geologic material is fully saturated.

125. Recent theoretical calculations of the slowing down length, L_s, required to slow neutrons down from the fast neutron emission energy to 0.215 eV have been made. The results are consistent with experimental measurements when graphite, water, and Si_2O are used as the slowing down media. Hence, these calculations should be realistic for sandstone, limestone, and dolomite. They clearly demonstrate that the loss of water from the rocks increases the slowing down distance by a factor of about 3 (i.e., from about 7.2 cm to about 19.2 cm) for a Ra Be source.

126. Inasmuch as the passage of the EMP will completely dehydrate the rock that is in the glass liner, and will partially dehydrate the surrounding rock, it is evident that the effect of the EMP will be to increase the effective slowing down length for neutrons in the material that surrounds the hole. This increase is caused by a reduction in the macroscopic scattering cross section of the rock.

127. As noted in the preceding paragraphs, the dominant change in the operation of a neutron log is likely to occur in the slowing down properties of the rock. This is proportioned to the epithermal scattering cross section and is inversely proportional to the nuclear mass. As water is driven out of the rocks, the epithermal macroscopic scattering cross section for the rock will decrease somewhat. The loss in the Z = 1 hydrogen nuclei should be more important than the decrease in the scattering cross section.

128. Some neutron logs depend on the macroscopic capture cross sections of hydrogen to detect the amount of hydrogen present. The passage of the EMP will cause dehydration of the glass liner and partial dehydration of the surrounding rock. Hence, the thermal macroscopic cross section of the rock will decrease.

129. Epithermal neutron inelastic scattering cross sections are used in instruments that measure the carbon to oxygen ratio in rocks. Dehydration of the rock will not affect these cross sections as such. However, the C is connected with a hydrocarbon and the O with water. High rock temperatures will drive out water and hydrocarbons. Hence, the C/O ratio will not be the same as it would have been prior to the passage of the EMP.

130. Epithermal neutron capture cross sections might be used with 14-MeV neutron sources to identify minerals by activation techniques. Dehydration will not change the cross sections. However, the loss of water and hydrocarbons from the rock will allow the

fast neutrons to penetrate further into the rock. This means that a given concentration of a chemical element in a rock will give a larger signal in a rockmass that has been heated by the EMP than would be obtained from the same groundmass around an unheated hole of the same size.

131. Based on these findings, the following conclusions can be made regarding neutron logs:

a. Dehydration of the rock in the liner and in the surrounding rock will affect the calibration of all neutron logs.

b. Neutron logs will be usable for quantitative analyses in EMP created holes only if the instruments are calibrated in an environment that simulates that around the EMP created hole. This statement includes the requirement that sufficient time must elapse between hole formation and the measurements to permit local fluids driven out by the heating transient to return to the pores in the rock.

c. The dominant change in the operation of the neutron logs will be caused by the dehydration of the rock. This change results in an increase in the neutron slowing down length in the rock.

d. Changes in macroscopic cross sections for the rock occur in the thermal and epithermal ranges because of hydrogen being driven out of the rock. The increase in the neutron slowing down length is attributable to the decrease in the macroscopic cross section at epithermal energies.

Geophysical logs

132. Seven geophysical logs were investigated to determine the effect of the heated glass lined hole. Assuming that the liner has not been partially removed, the following conclusions can be drawn from that study and should be verified by experiment:

a. The effect of the liner on electrical induction logs will lead to only small errors (less than 10 percent) in the measurement of the electrical conductivity of surrounding rock. This statement assumes that sufficient time has elapsed after passage of the EMP for fluids to return to pores in the formations.

b. It seems doubtful that spontaneous potential logs can be used in EMP created holes because the glass liner will not permit a good electron conducting path between the mud in the hole and the surrounding formation.

c. Guard logs will not be usable in EMP created holes because the glass liner will not permit a good electrical conducting path between the mud and the formation. Even if there are cracks in the glass liner, the conducting area will be small and unknown.

d. Electrical logs will not be usable in glass lined holes because of the poor electrical flow paths through cracks in the liner.

e. The density log should be useful in EMP created holes, provided that the time allowed is sufficient for fluids to return to the pores of the rock immediately around the glass liner. The density log investigates a region about 6 inches deep measured from the ID of the liner. The liner will have little effect on the density measurements as long as the thickness of the glass is a small fraction of 6 inches.

f. The glass liner will not significantly affect the operation of the gamma log.

g. Acoustical logs through unconsolidated (UNCON) materials will be substantially affected by the glass liner because the first arrival signal passes through the region close to the surface of the hole.

h. Acoustical logs through MASIG, FOLIA, and CALCI may not be significantly affected by the presence of the glass liner.

Mechanical Design

133. Early in the contract year, a design study program was conducted to determine the best possible configuration for the earth melting penetrator. As a result, several design concepts were defined and analyzed. The most promising configuration was then selected for further development. The selected design is discussed in detail in Part VI.

Concept No. 1 - removable core barrel and wireline

134. The first concept to be defined made provision for the removal of the undisturbed core section-by-section as penetration proceeded. This design is illustrated in Figure 22.

135. The inner diameter of the penetrator accommodated a core barrel several feet long into which the core was to be extruded as penetration proceeded. As soon as

the core completely filled the core barrel, a release mechanism would be activated and the core barrel and core would be withdrawn to the portal by means of a wireline. Activation of the release mechanism would be via the wireline tension or could be effected directly through contact with the end of the core. The latter alternative, used with a wireline maintained constantly under tension, would eliminate the need for instrumentation to signal contact of the core end with the bottom of the core barrel. After removal of the core from the barrel at the portal, the core barrel would be reinserted into the penetrator stem and propelled by compressed air to the penetrator head location to await its next refilling.

136. The penetrator head, machined from tungsten, accommodated 12 cylindrical heaters in equally spaced axial holes around the penetrator axis. The heaters were made up of stacked washers of pyrolytic graphite and were located in their holes by means of spring loaded tungsten electrodes, along which direct current was supplied from transformers in the stem. The molten rock was fed through a series of holes and grooves, machined in the penetrator head, to twelve carry-off tubes equally spaced around the penetrator axis. The 12 carry-off tubes connected with an annular carry-off passage in the stem. The annular passage had to be interrupted at the stem section joint to provide structural support for the inner diameter of the stem. The narrow annular carry-off passage made available an uninterrupted annular space around it in the stem which was capable of accommodating a guidance sensor up to 2 inches in diameter or transformer modules of similar size.

137. High pressure air was supplied to the outer passage at the portal and flowed to the penetrator where it entered the injection nozzles at the penetrator end of the carry-off tubes. Molten rock, extruding into the carry-off tubes, was then broken up into fine particles by the high velocity air emerging from the nozzles and transported pneumatically to the portal.

138. A portion of the high pressure air supplied to the outer annular passage was allowed to exhaust through a number of holes in the hole former area to cool the transition from the penetrator to the stem. Insulation, in the form of pyrolytic graphite rings, was employed to limit the heat conducted into the stem. A gradation of material temperature capability was employed between the tungsten penetrator head and the aluminum stem,

10 1/2 DIA. MULTIPLE HEATERS – MULTIPLE CARRY-OFF TUBES

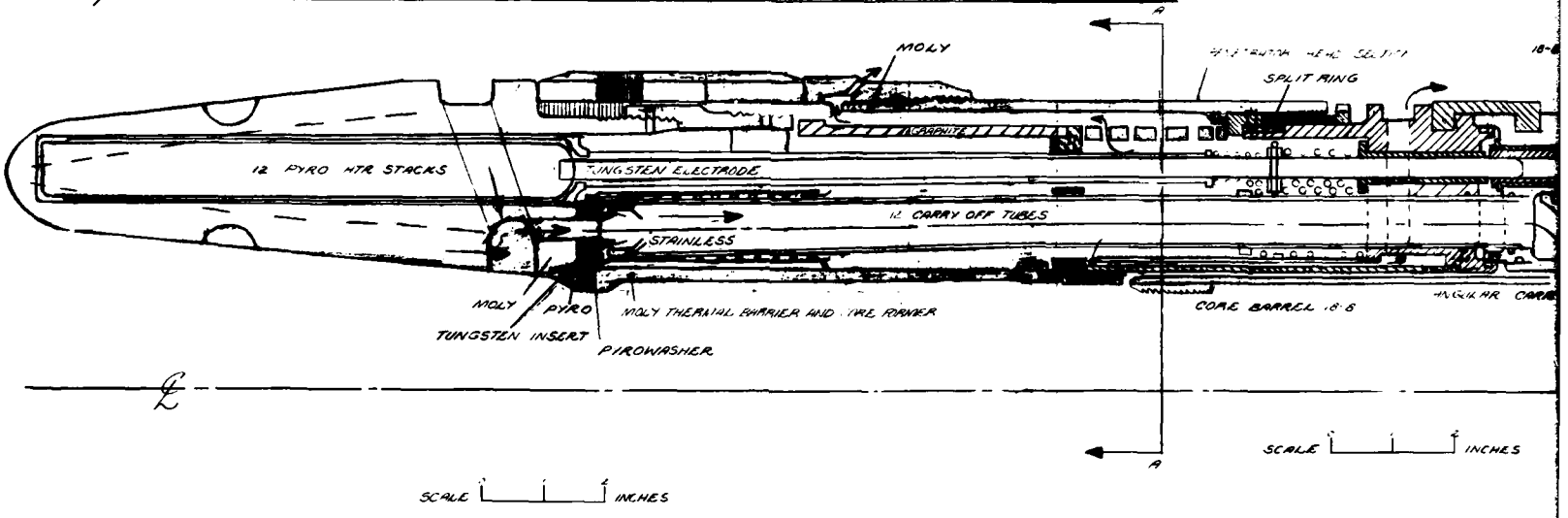

CONCEPT# 1

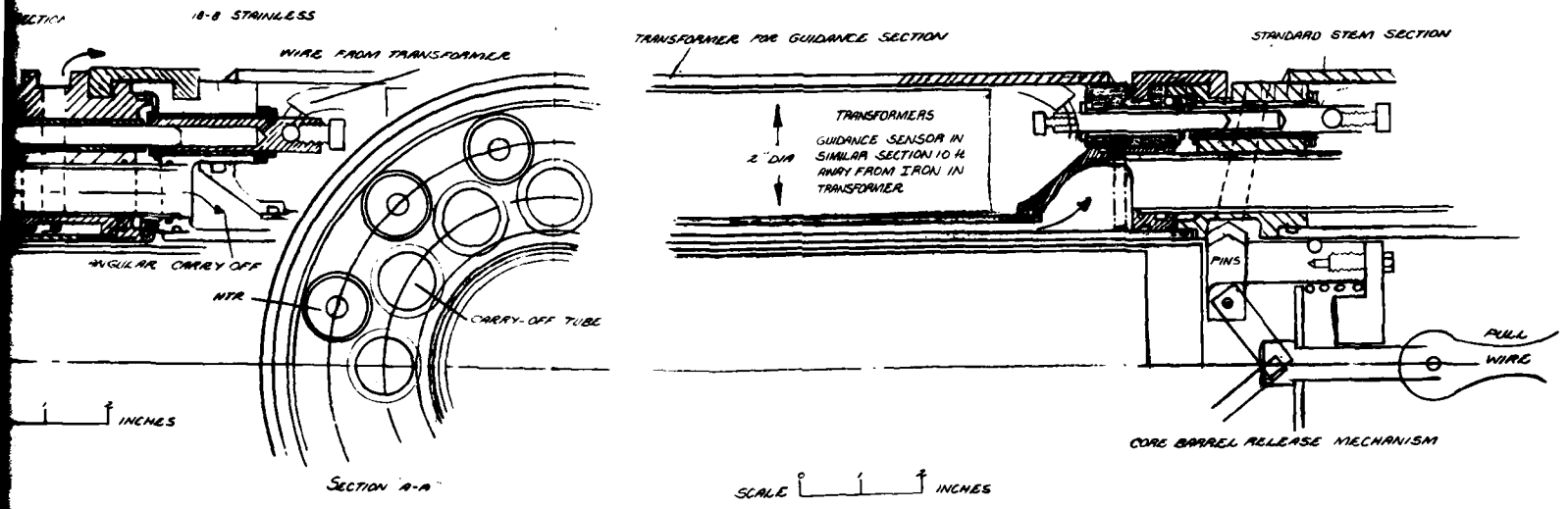

Figure 22. Concept No. 1 Removable Core Barrel and Wireline

consistent with the local temperature environment expected. The transition pieces immediately adjacent to the penetrator head were made of molybdenum. The stem sections local to the penetrator were made of 18-8 stainless steel and the standard stem sections remote from the heated rock area were made of aluminum.

139. Coil springs were used to accommodate the thermal expansion of the graphite heaters, electrodes, carry-off tubes and the penetrator inner diameter.

140. Split clamps were used to join the penetrator head to the adjacent stem section and to join together sections of the stem. The split clamps consisted of simple turned rings, saw cut in half diametrally. The split clamps were to be placed in position in grooves machined in the ends of the adjacent stem sections thus clamping the sections together. A simple bolt and threaded hole arrangement would be used to hold the split clamps together after installation

141. A system of male and female plug terminals was used at each stem-to-stem joint to transfer the electrical connections across the joint and facilitate simple axial plug-in connection of the stem sections. Rubber O-rings were used to seal the carry-off tubes and stem section flow passages at the joints.

Concept No. 2 - cooled inner diameter

142. The second concept incorporated a cooling passage arrangement at the inside diameter of the penetrator head to remove heat from the core in an attempt to limit the temperature of the core at entry into the penetrator bore and thus maximize the diameter of the "thermally undisturbed" portion of the core. This design is illustrated in Figure 23. Air entered a narrow annular passage at the penetrator inner diameter and flowed axially to the region of the penetrator tip. The air then reversed its flow direction and returned along an additional annular passage surrounding the first. The air was then exhausted to the borehole through a series of holes drilled in the transition section of the penetrator. The double annular flow passage arrangement was insulated from the penetrator head by concentric tubes of insulation material.

143. In other respects, the design of Concept No. 2 was generally similar to that of Concept No. 1 and incorporated 12 graphite resistance heaters and 12 carry-off tubes. The core barrel and wireline core withdrawal arrangement was omitted, however.

The penetrator head incorporated a finned exterior surface to promote the transfer of heat from the penetrator head to the rock.

Concept No. 3 - annular heater and carry-off tubes

144. In this arrangement, the 12 separate cylindrical heater geometry was replaced by an annular configuration divided into three 120-degree sectors. The concept is illustrated in Figure 24. The three-sector arrangement was intended to provide the necessary steering capability by appropriate modulation of the power to the three sectors. The location of the heaters in the heater annulus was effected by a system of spring loaded tungsten electrodes similar to that employed in Concepts No. 1 and No. 2.

145. An annular carry-off tube geometry employed in this design also provided some cooling of the core as it entered the penetrator inner diameter. Air flowing along the outer annulus of the stem was fed into the outer of two narrow annular passages around the inner diameter of the penetrator. In the region of the leading edge of the penetrator, the air was injected into the inner annular passage in the reverse direction through a narrow annular nozzle and, at this point, contacted the molten rock being extruded from the extended surface channels of the penetrator head into the carry-off passage.

146. The high velocity annular air jet then sheared the molten rock stream, breaking it up into small particles, and transported the rock to the portal along the inner annular flow passage.

Concept No. 4 - annular heater with four carry-off tubes

147. In Concept No. 4, the annular heater arrangement was used together with four separate carry-off tubes. The annular heater was divided into four 90-degree sectors, each sector being located in the heater annulus by two spring loaded tungsten electrodes, one on each side of each carry-off tube. The design is illustrated in Figure 25.

148. For this arrangement, the inner diameter of the penetrator was insulated from the entering core by pyrographite insulation tubes and no provision was made for cooling the core. The molten rock was fed to the carry-off tubes through drilled passages from a circumferential groove in the penetrator periphery which, in turn, received molten rock from the extended surface fins machined axially along the outer diameter of the penetrator.

MULTIPLE HEATER/MULTIPLE CARRY-OFF TUBE CONCEPT W

COOLED I/D TO TRY TO LIMIT HEAT-UP OF CORE ROCK

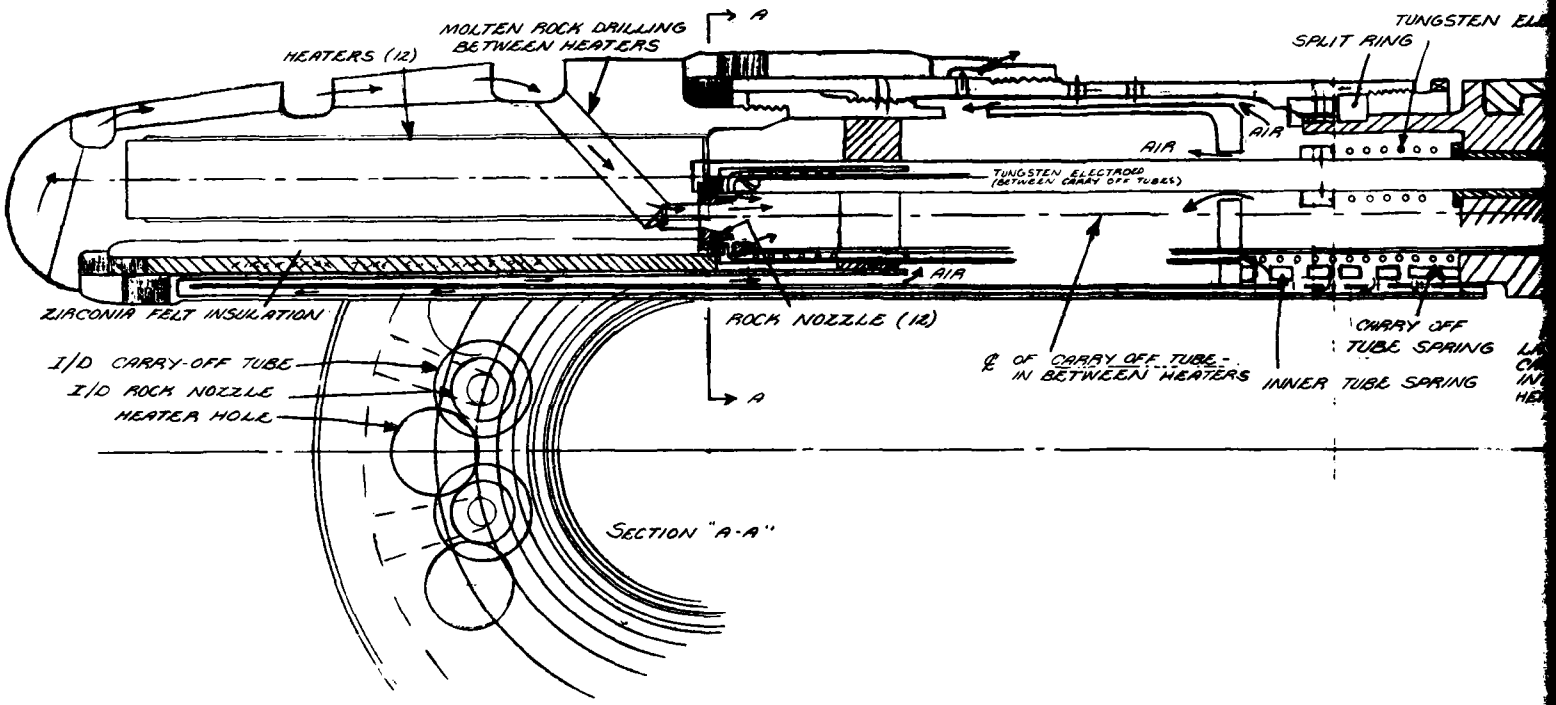

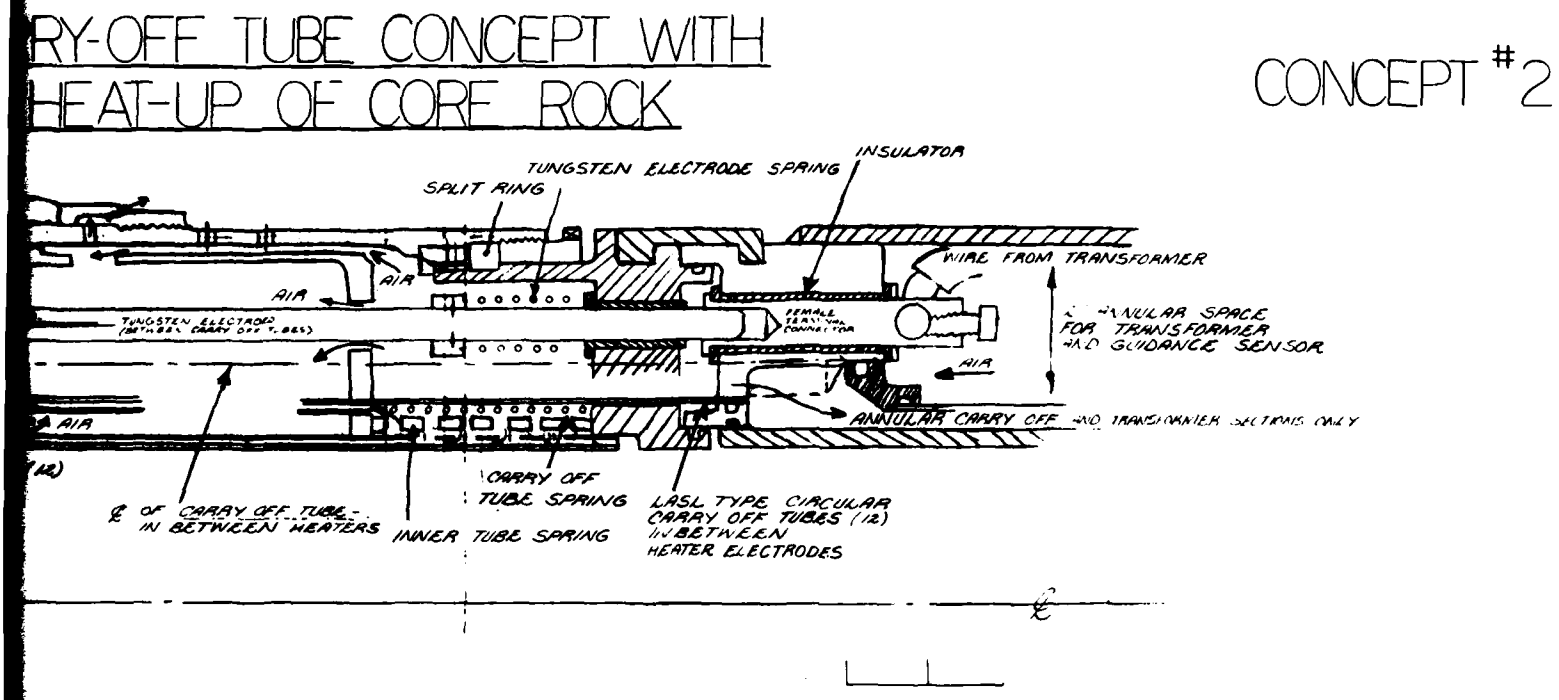

Figure 23. Concept No. 2 cooled inner diameter

1/3 ANNULAR HEATER— ANNULAR CARRY OFF-TUBES EXTENDED SURFACE CONCEPT

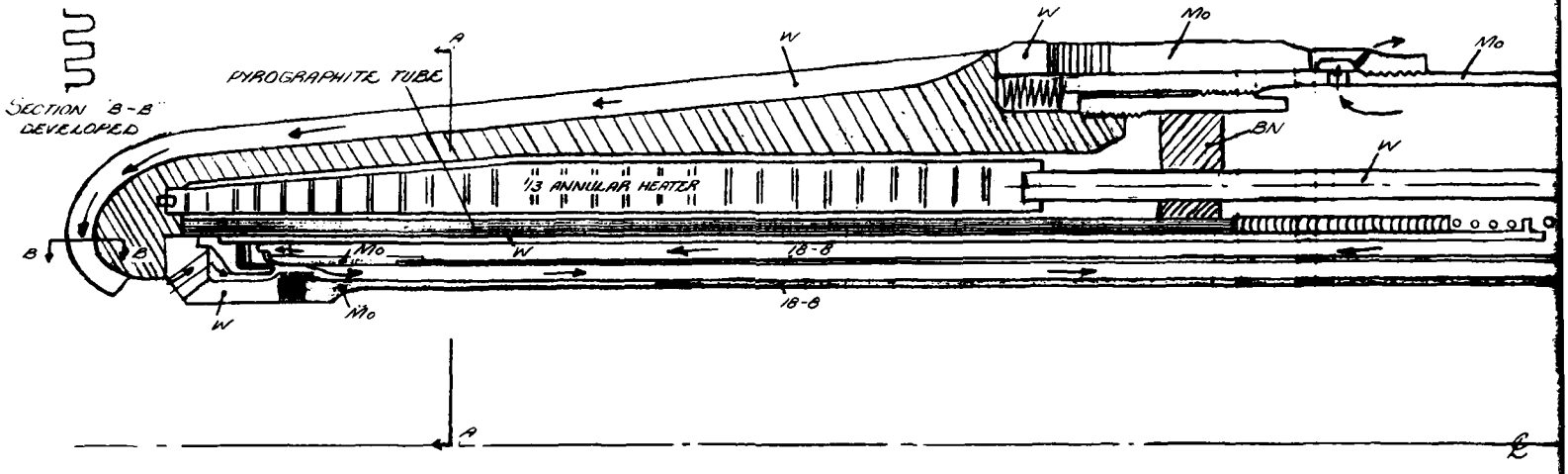

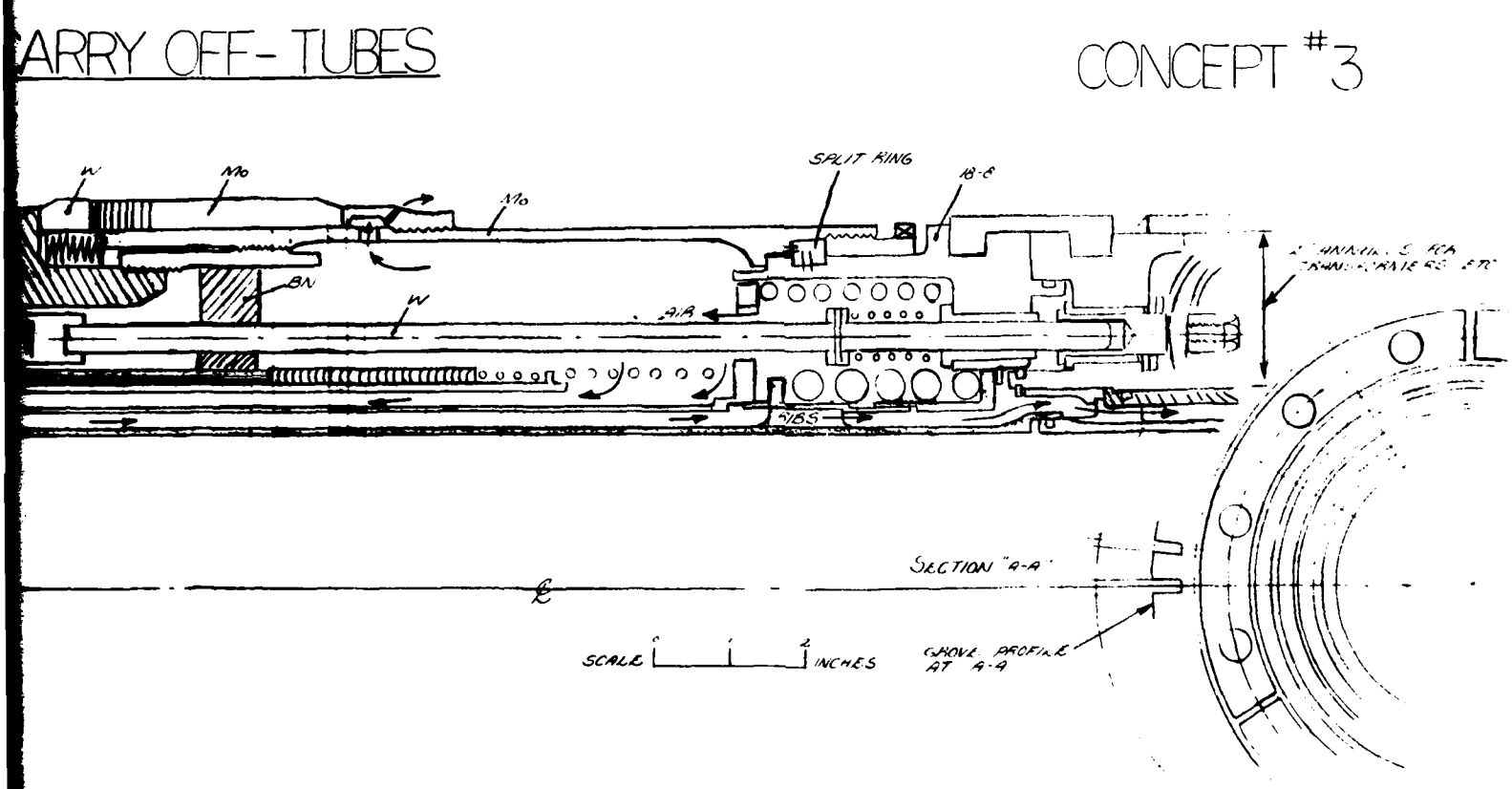

Figure 24. Concept No. 3 annular heater and carry-off

¼ ANNULAR HEATER — 4 ENLARGED CARRY OFF - TUBES

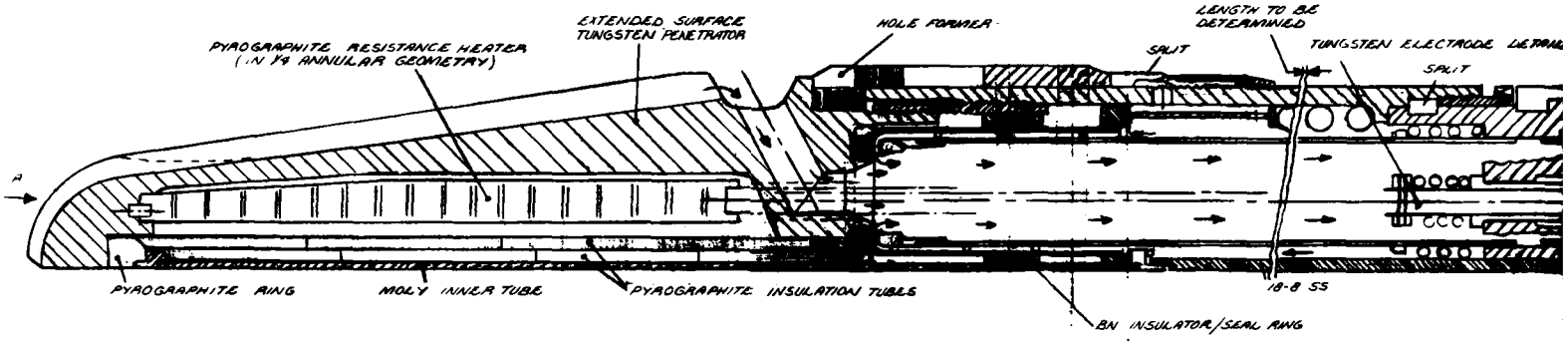

SCALE 0 1 2 INCHES

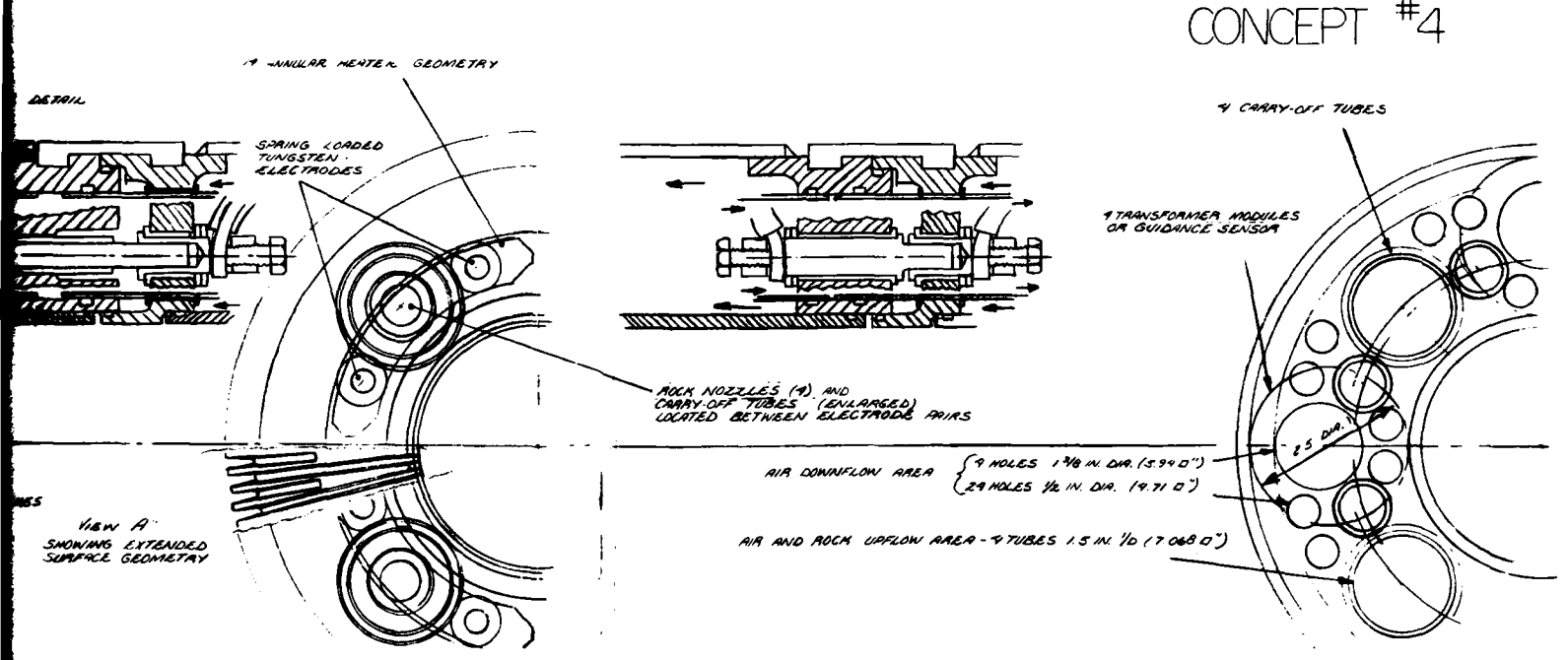

Figure 25. Concept No. 4 annular heater and four carry-off tubes

Concept No. 5 - nine heaters with three carry-off tubes

149. This arrangement provided three independently controllable heating sectors, each of which contained three resistance heater elements constituting the load of a three-phase circuit. Thus, each heater was connected via its spring loaded tungsten electrode, male and female interstem connectors and wiring to the secondary winding of one of the three transformer modules of a three-phase circuit. The nine transformer modules were accommodated in the stem in three groups of three in the spaces between the three carry-off tubes. The molten rock was fed to the carry-off tubes via drilled passages from a circumferential groove machined into the finned periphery of the penetrator in a similar manner to that of Concept No. 4. Concept No. 5 is illustrated in Figure 26.

Concept No. 6 - similar to Concept No. 5 but with rock flow into penetrator leading edge

150. Although generally similar to Concept No. 5, this design incorporated three large diameter axial holes, drilled from the leading edge of the penetrator in line with the carry-off tubes. Concept No. 6 is illustrated in Figure 27. Provision was thus made to accommodate the flow of a large portion of the molten rock directly from the leading edge of the penetrator to the carry-off tubes. Smaller holes were drilled radially into the axial holes from a circumferential groove machined into the penetrator head at the end remote from the leading edge. These holes were intended to channel rock flowing into the annular groove from the extended surface fins into the carry-off tube flow path. Thus, the design provided for the flow of molten rock from both ends of the penetrator head. However, consideration of the required rates of rock removal at various locations on the penetrator suggested that the radial holes might not be desirable.

151. The required rate of rock removal directly ahead of the penetrator leading edge must equal the advance rate into the rock. The corresponding rate of rock removal on the outer periphery is greatly reduced by the oblique angle presented by the surface to the direction of motion. Thus, the advance rate is limited by the rate of heat transfer at the leading edge. Some improvement can be made by concentrating the heating at the leading edge by appropriately increasing the heater resistance in this region. However, the temperature limitations of the penetrator material must be observed and heat transfer

rates are limited by the low coefficient of heat transfer to the rock prevailing in the melting region. If the heat transfer coefficient in the leading edge region could be increased by forcing a high velocity flow of rock across the melting region, some improvement in heat transfer should be obtainable. To this end, rock might be melted on the peripheral surface at a low rate of removal and forced to flow to the leading edge where it would provide a high velocity flow stream across the melting face and also transport heat from the peripheral surface to the leading edge by mass transfer. The development of such a heat transfer mechanism would be a worthwhile goal of an experimental program.

Electrical Design

Heaters

152. As shown in Figure 27, nine heaters will be mounted within the penetrator. Various heater types were considered. These included tungsten filament and graphite type heaters. Since heater flux densities are high to produce the required temperatures and considerations given to slight vibration within close tolerances, wire filament and filament mesh heaters were eliminated because of heater "sag."

153. A number of suppliers were contacted to determine the characteristics of graphite materials available for heater construction. Two of the suppliers produce a fine grain-high purity graphite material that could be used. One of these two suppliers has capability for a pyrolytic graphite coating on fine grain graphite. The third supplier produces pyrolytic graphite up to 0.5-inch thick for normal production. Special runs have been made up to a 3-inch depth; however, this is not a typical run and the material is quite expensive. Table 5 shows the physical property information received from the various suppliers of graphite. There is a difference between extrapolated data from LASL and the vendor "C" data (Columns B and C of Table 6).

154. Since graphite heaters require high currents and relatively low voltages, only pyrolytic graphite heaters are being considered because of its resistivity characteristics.

9-HEATERS – 3 PER CIRCUIT (120° SECTOR) — 9 TRANSFORMER MODULES — 3 CARRY OFF-TUBES
1 PER PHASE (3φ) 1 PER PHASE (3φ)

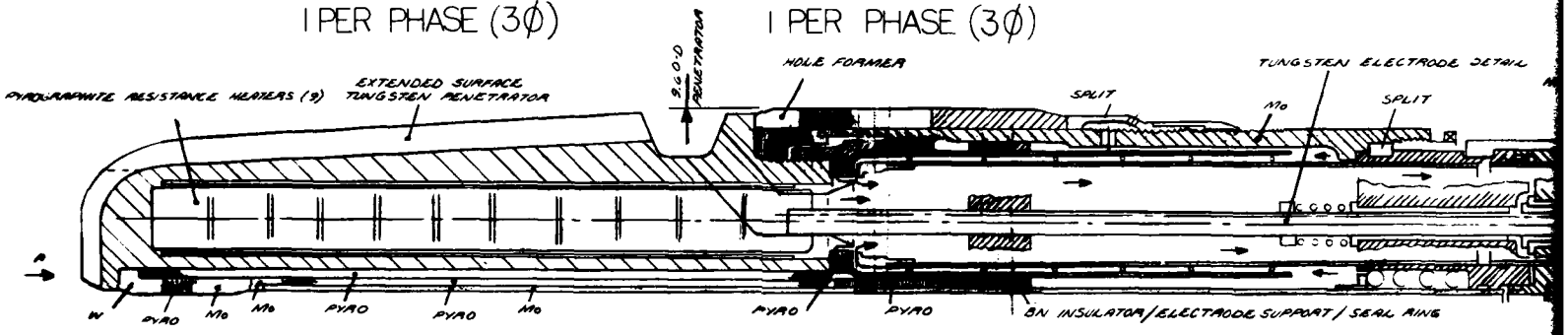

FLOW AREA / 120° SECTOR

DOWN FLOW AREA

2 HOLES	1/16	.177 □"
2 HOLES	1/16	.79 □"
3 HOLES	1/2	.59 □"
		3.10 □"

UPFLOW AREA

1.53 DIA.	1.83 □"

FF-TUBES

CONCEPT # 5

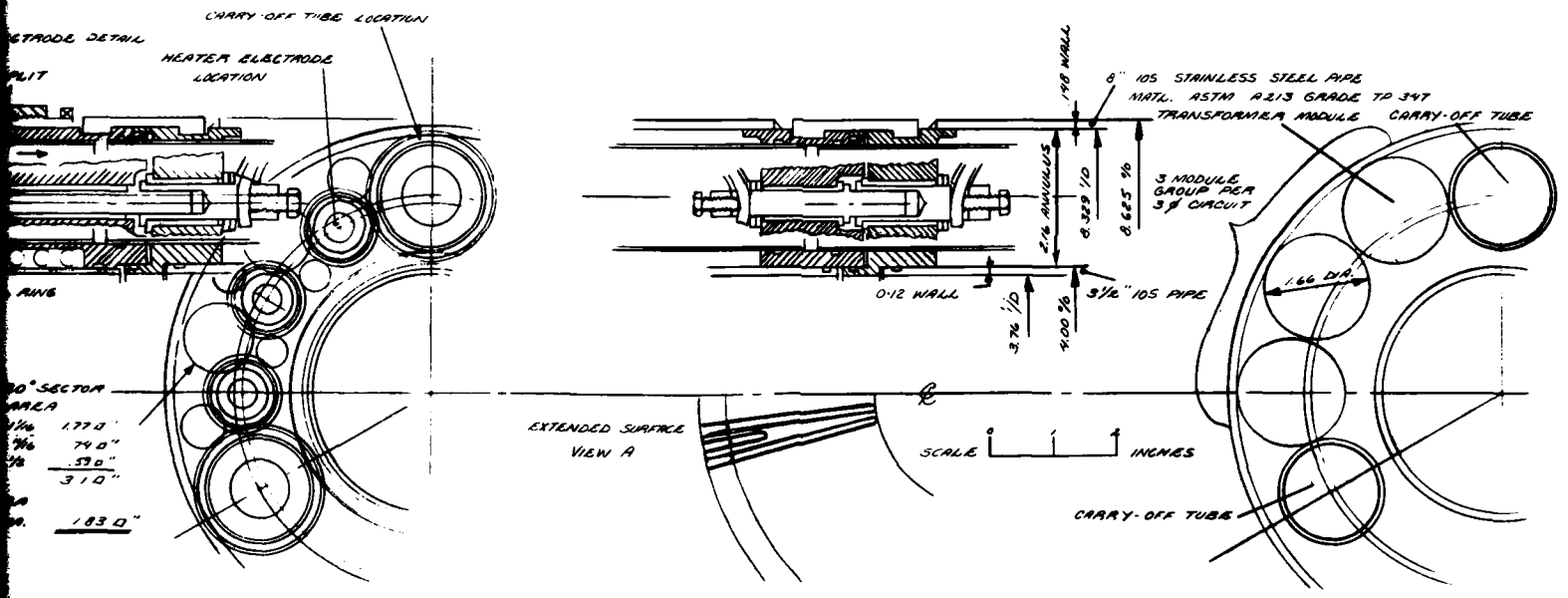

Figure 26. Concept No. 5 nine heaters with three carry-off tubes

2

9.2" DIAMETER PENETRATOR — 8" PIPE STEM

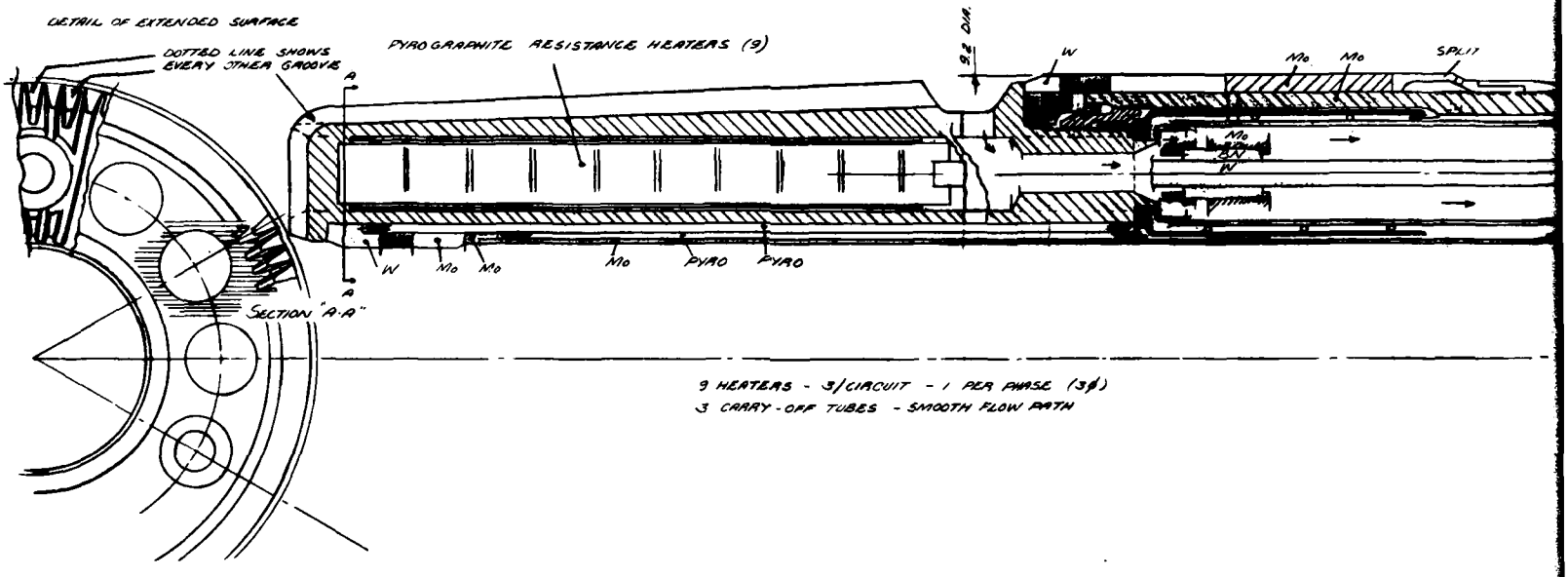

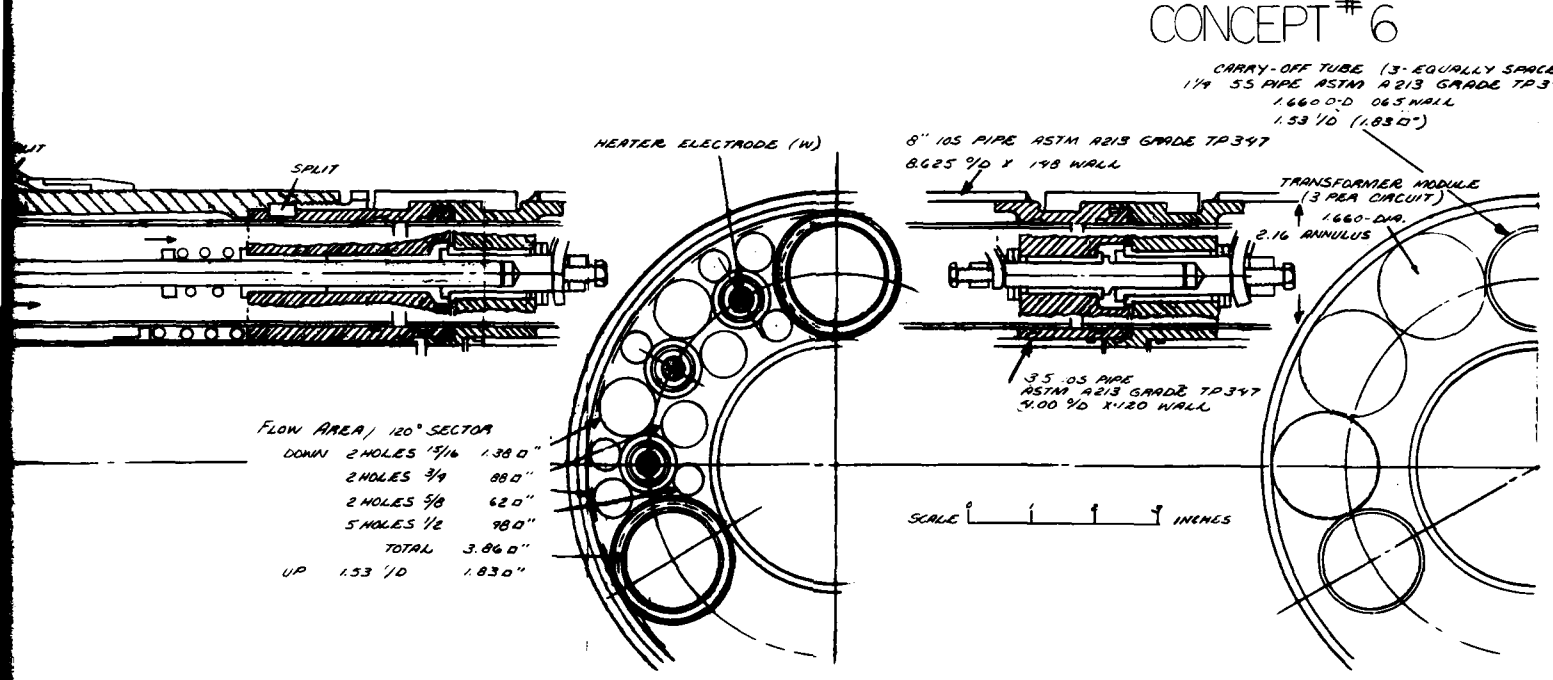

Figure 27. Concept No. 6 similar to Concept No. 5 but with rock flow into penetrator leading edge

Table 5

Graphite Data from Various Suppliers

Supplier	Graphite		Pyrolytic Graphite	
	Resistivity (ohm-in.)	Temp. Coef. $(X10^{-6})/^{o}F$	Resistivity (ohm-cm)	Temp. Coef. $(X10^{-6})/^{o}F$
A	5×10^{-4}	4.3	N/A	N/A
B*	45×10^{-4}	1.5 to 2	N/A	N/A
C			A Plane 200×10^{-6}	1
			C Plane 0.3	13

N/A Not Applicable

* Supplier does coat graphite with pyrolytic graphite

In addition, pyrolytic graphite exhibits good conductivity in the "A" and "B" planes which will allow for radial heat transfer in the penetrator body.

155. The present heater physical size under consideration is 1 inch in diameter and 10 inches long. Initial calculations and heater configurations are based on the LASL 84-mm penetrator design. Table 6 shows the comparison of heater designs based on the LASL penetrator and vendor supplied data. Column A represents data determined from the LASL 84-mm penetrator. Column B shows the calculated heater data for the same configuration for a 10-inch-long, 1-inch-diameter heater. Column C shows heater values using supplier "C" data. Column D shows heater data assuming that the entire heater is made of pyrolytic graphite from supplier "C."

156. To protect the tungsten within each heater compartment, a pyrolytic graphite sleeve will be used. In addition, a flow of helium gas will exist within the annulus between the heater and the sleeve to operate the heater in an inert environment. For any given distance between electrodes in a gas, there is some critical pressure at which discharge occurs at the minimum sparking potential of the gas. Thus, with a gap of 3 millimeters in air, spark-over occurs at a pressure of 1.5 millimeters at about 340 volts. For a gap of 1 millimeter, the discharge occurs at a pressure of 5 millimeters at the same voltage. At pressures above and below these minima, or critical pressures, the voltage necessary to produce breakdown of the gas increases with both increasing gap size and decreasing pressures. Therefore, the sparking potential of a gas is a function only of the product of the sparking distance and the pressure of the gas between the electrodes. If P, the pressure, and D, the gap length, are varied in such a way that the product PD remains constant, the sparking potential will remain unaltered, and the product PD is a constant for any gas. For helium, the minimum spark potential is 261 volts with PD at 27 mm Hg · mm.

157. Tungsten electrodes will be utilized between the heater and input power connector. Tungsten comes in various forms which include "black," "clean," and "ground." For the heater electrodes, the "clean" form will be utilized with the terminating ends "ground" to mate the interfacing components. Lengths of up to 48 inches that are available will satisfy the penetrator requirements.

Table 6

Comparison of Heater Designs

(Per Heater)	A	B	C	D
Heater Diameter	10.6 mm	25.4 mm	25.4 mm	25.4 mm
Heater Power	3.4 KW	56 KW	140 KW	212 KW
Heater Voltage	52 V	149 V	373 V	564 V
Heater Current	65.3 A	375 A	375 A	375 A
Heater Flux	1.16 MW/m^2	2.75 MW/m^2	6.9 MW/m^2	10.4 MW/m^2

Stem transformer

158. To minimize large transmission losses for a system length of 5000 meters, a design goal of installing step-down transformers in the stem behind the penetrator was investigated. By using transformers near the penetrator, a much higher power supply source voltage could be used, thus reducing the transmission line wire size for a given amount of power. The diameter space allowed for the transformers was 3.25 inches. This became a very difficult problem but continuing investigation into the transformer design indicated that a transformer could be built to power the heaters. The first approach was to determine what the configuration would be using typical 60-hertz power. To meet the diameter envelope established, each transformer phase would have to be 59 feet long. Since nine heaters are used and one three-phase transformer could be placed in a stem section, the stem length needed to accommodate just the transformers would be approximately 180 feet long. Figure 28 shows the 60-hertz transformer configuration. If the frequency of the power system could be increased, the stem transformer size could be reduced. (See Part VI for the recommended design.)

Power transmission

158. If the electrical current requirements are approximately 375 amperes as given in Table 6, the total current requirement would be 3375 amperes to achieve about 1.25 MW. To transmit currents of this magnitude for 5000 meters would result in extremely high transmission losses in addition to using large cable diameters. To keep transmission losses to a minimum and cable sizes practical, a higher transmission voltage will be utilized.

159. The design goal for the power requirements for each heater zone (3 heaters per zone) is 450,000 watts.

160. To determine the transmission line wire size, the following calculation was used:

$$P \quad \sqrt{3} \; V \, I \cos \theta$$

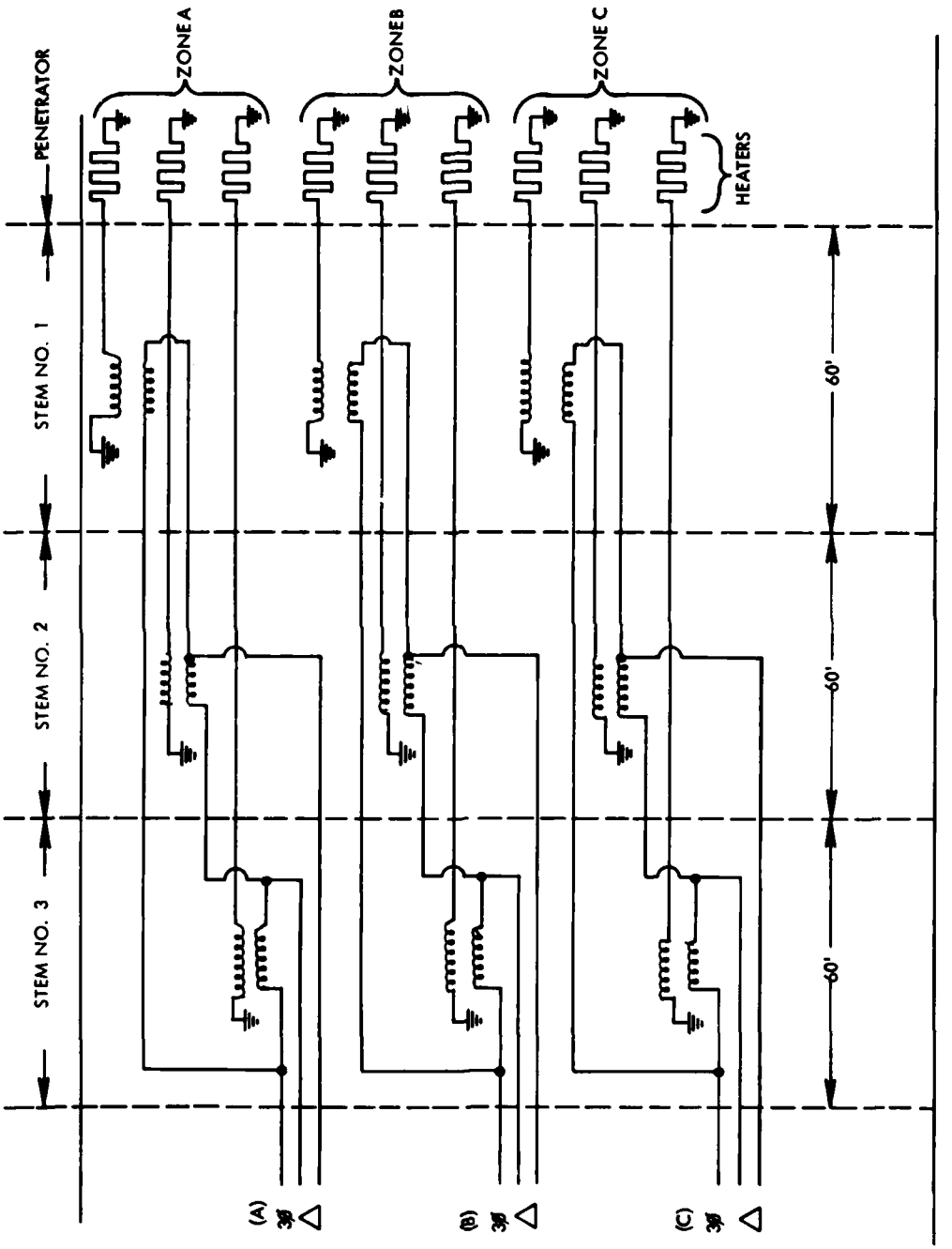

Figure 28. 60-Hz transformer configuration

where

P	Power in watts (450, 000)
I	Current in amperes
V	Voltage in volts (13, 800)
Cos θ	Power Factor

Assume Cos θ to be 0. 9

$$I \quad \frac{450,000}{\sqrt{3}\,(13,800)\,(0.9)} \quad 21 \text{ Amperes}$$

$$V.\ D. \quad \frac{K\,I\,L}{A}$$

where

V. D.	Voltage Drop in the line
I	Line current (21 amperes)
L	Line length in feet (16, 368)
A	Wire cross-sectional area in circular mils
K	Constant for copper wire (10. 4)

Assuming that the maximum line drop will not exceed 5 percent,

Voltage Drop (V. D.) 0. 05 (13, 800) 690 volts

$$A \quad \frac{K\,I\,L}{V.\,D.} \quad \frac{(10.4)\,(21)\,(16,368)}{690}$$

A 5180. 8 circular mils

AWG No. 12 wire 6, 530 circular mils

AWG No. 10 wire 10, 380 circular mils

161. To allow for resistance changes caused by increasing temperature and system operation at a frequency higher than 60 Hz, and for connector resistance between stems, a transmission wire size of AWG No. 10 was considered.

162. The power required to charge this line was then considered. Tables and equations were used from Reference 8 and the following charging KVA determined:

d = diameter of conductor, No. 10 = 0.102 inches

T = conductor insulation thickness = 0.234 inches

$$\frac{T}{d} = \frac{0.234}{0.102} = 2.33$$

G_1 from tables ≈ 1.75

$G_2 = G_1 \times$ Sector factor $= 1.75\ (0.961)$ 1.682

Charging current $= I = 0.63\ \frac{(E)}{G_2}$

where E is in Kilovolts = 13.8 kV

$$I = \frac{0.63\ (13.8)}{1.682} = 5.11 \text{ amperes/1000 ft}$$

Charging KVA for 3 ϕ = 3 (5.11) (13.8)/1000 ft

= 211.556 KVA/1000 ft

Charging current at 680 Hz = $\frac{680}{60}$ (211.556)

= 2397 KVA/1000 ft

Charging KVA for 5000 meters at 680 Hz =

KVA = 2397 (16.368) = 39,234 KVA

163. Since the charging KVA is 40 times greater than the load requirements, the generator capacity would be exceeded. Therefore, the characteristic impedance of the transmission line must be matched to the load to assure a practical generator size. The transmission line characteristic impedance will determine the transmission voltage that will be used. By selecting an available cable, the sending end voltage can be determined. It is expected that the characteristic impedance at 680 Hz will be between 45 and 120 ohms for a Number 6 cable. The transmission voltage will fall between 2600 and 5000 volts, which is within the capability of the heater generator.

Power supplies

164. Since the earth melting penetrator is to be used in remote locations where power from a public utility may not be available, only self-contained trailer mounted units

were considered. A number of options were considered with regard to the number of units that would be required.

165. Figure 29 shows the first option that was considered. One generator, sized to meet the entire heater load requirement, would be used to power a common bus. Three breakers would be used to control the various heater zones. This option was deleted because maintenance or generator failures that would require the generator to be shut down would stop the penetrating process.

166. Figure 30 shows the second option that was considered. Three smaller generators would be used, each supplying power through a breaker to the zone heaters. Although a failure of one generating system would only delete one heater zone, the system would have to be shut down because the penetrator would not continue to drive in a straight path. Therefore, the second option was also deleted.

167. Figure 31 shows the third option that was considered. Each of the generators is sized such that any two generators can supply power to all three heater zones. Paralleling and load sharing controls are also provided. With this configuration, any generator can be shut down for maintenance without stopping the process system. With generators operating at frequencies ranging from 600 to 700 Hz, extensive equipment would be required for paralleling, load sharing and automatic synchronizing of the machines. This option was also deleted in favor of Option 4 shown in Figure 32. In Figure 32, each generator is sized to operate two heater zones. The problems associated with paralleling, load sharing, and synchronizing are removed by adding a second set of circuit breakers, which are controlled such that any generator can be removed for maintenance or repair without process shutdown.

168. Figure 33 shows a typical mobile substation. The front end of the trailer contains the high-voltage switchgear, lightning arresters and high-voltage fuses. The center portion of the trailer contains the main transformer with its hand operated tap changer and associated configuration switches. The rear portion of the trailer contains the auxiliary transformers, circuit breaker, and control panel.

169. Figures 34 and 35 show a typical trailer mounted diesel-generator set and switchgear control panel that is available for 60 Hz operation. This unit is available from Melley Energy Systems, Inc. Another supplier of diesel generators is Onan.

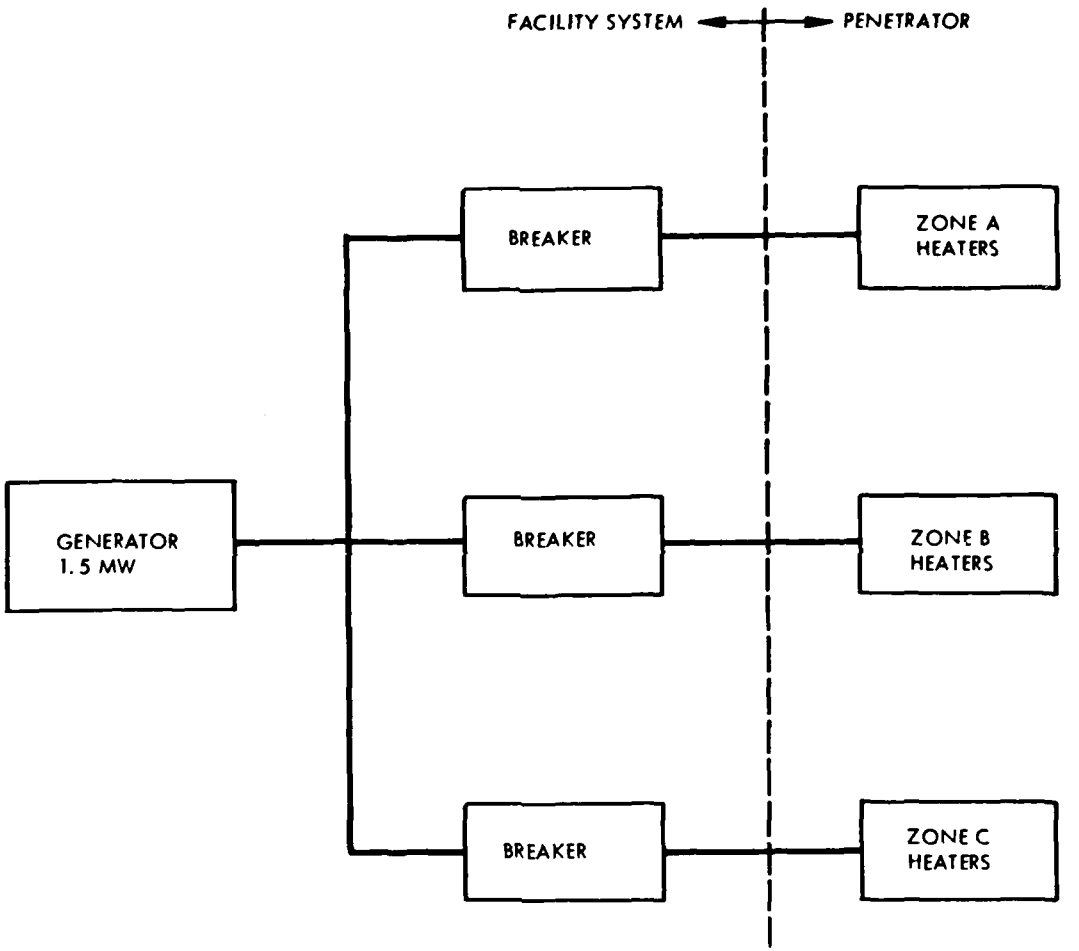

Figure 29. Power supply Option 1

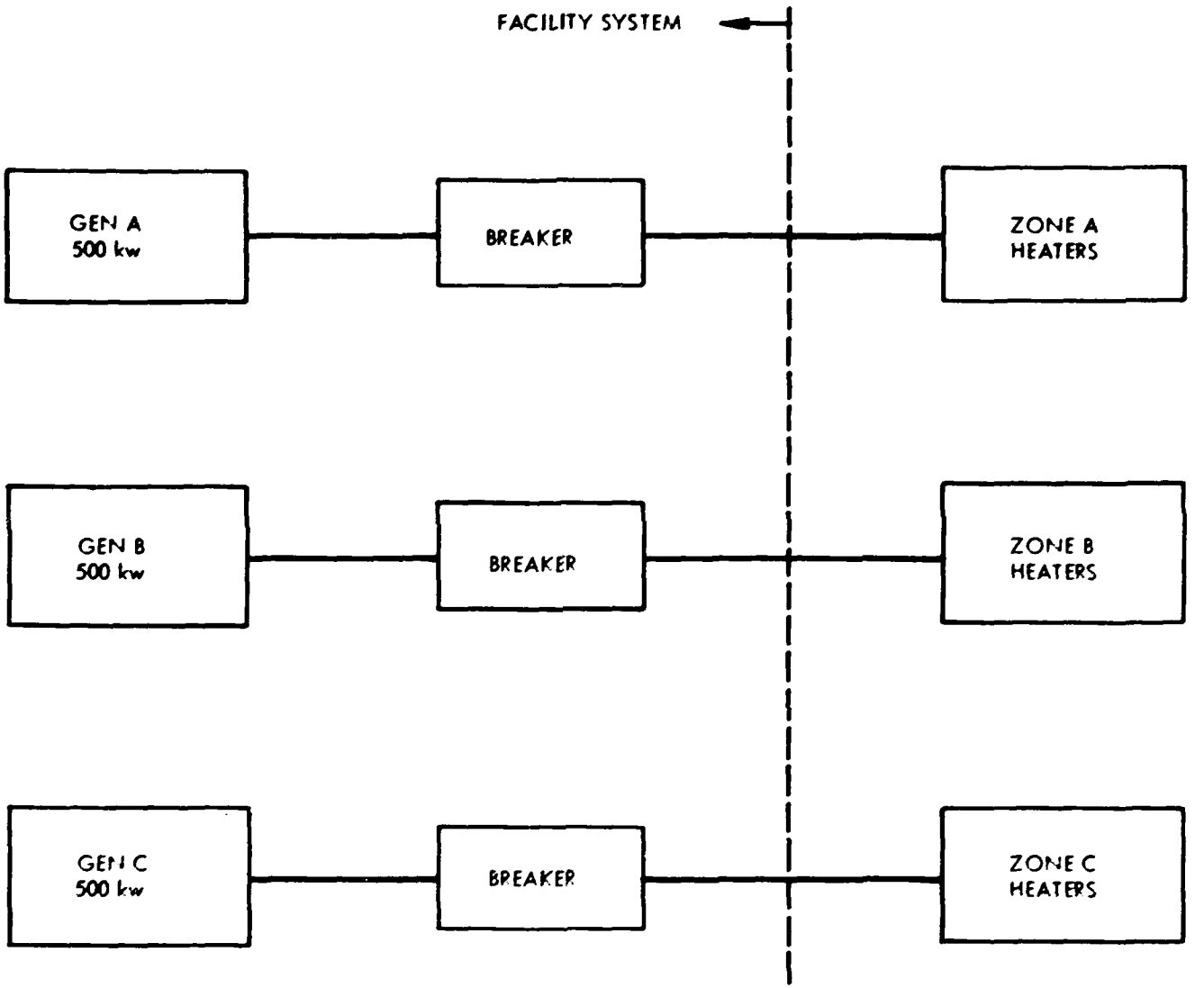

Figure 30. Power supply Option 2

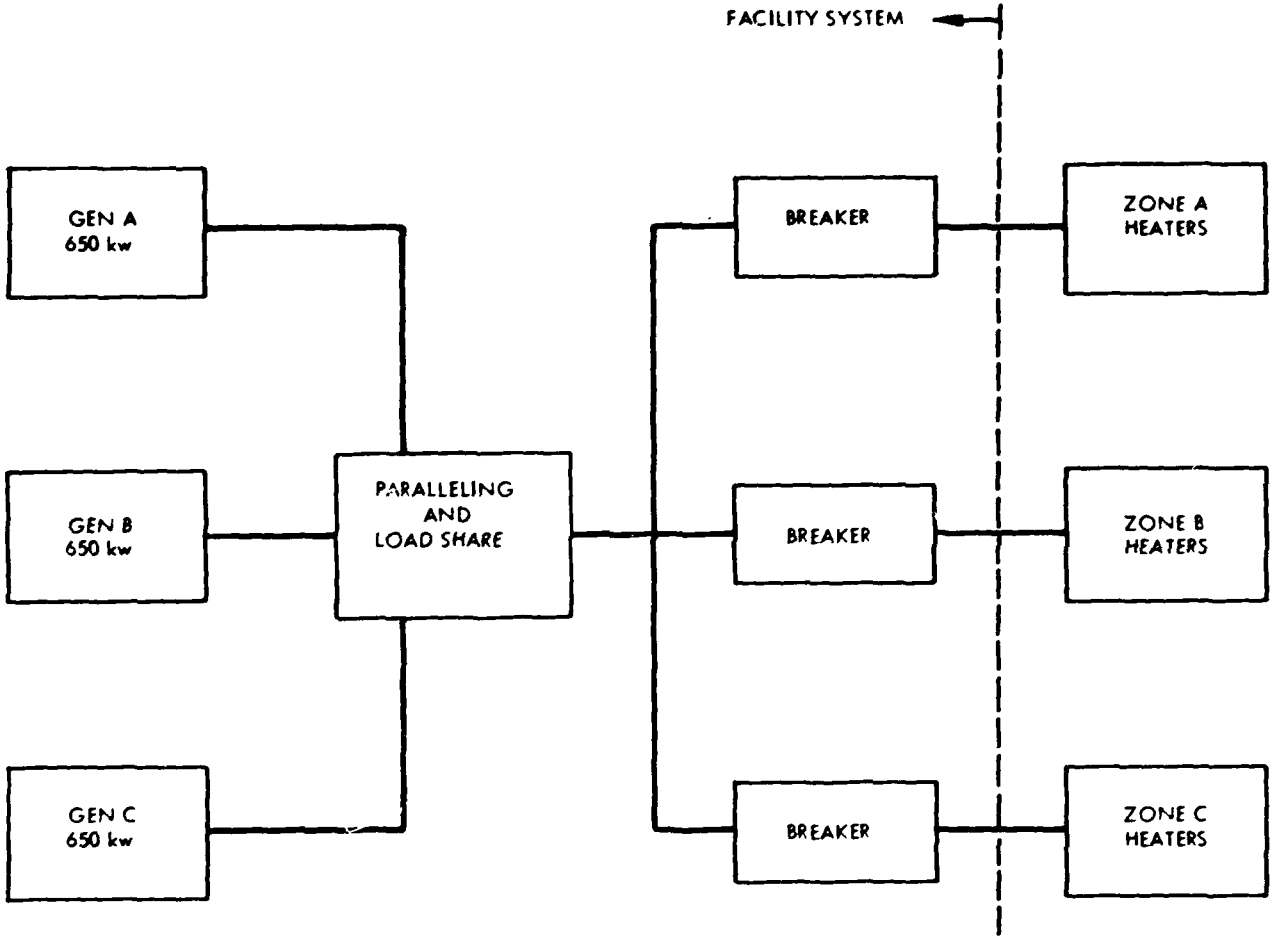

Figure 31. Power supply Option 3

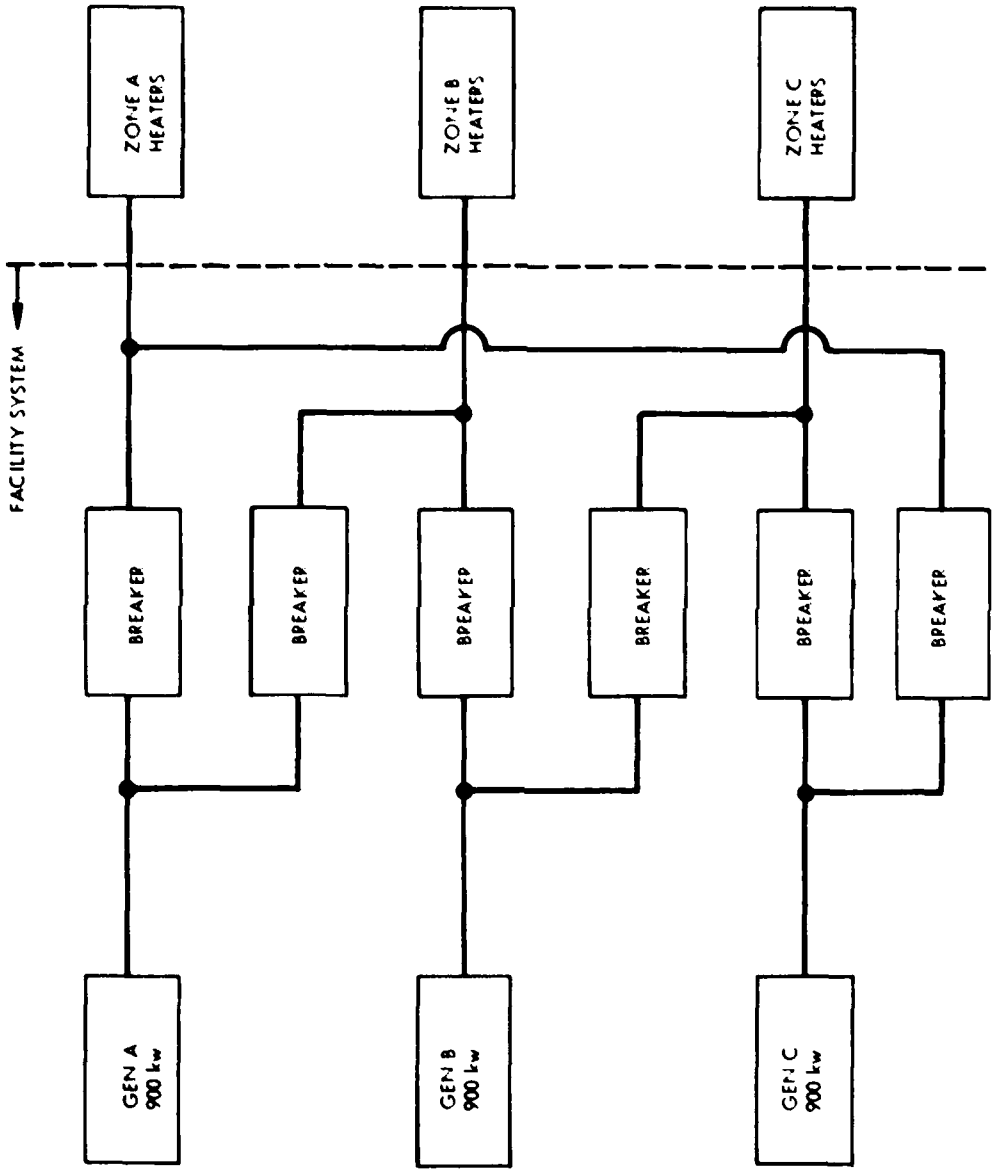

Figure 32. Power supply Option 4

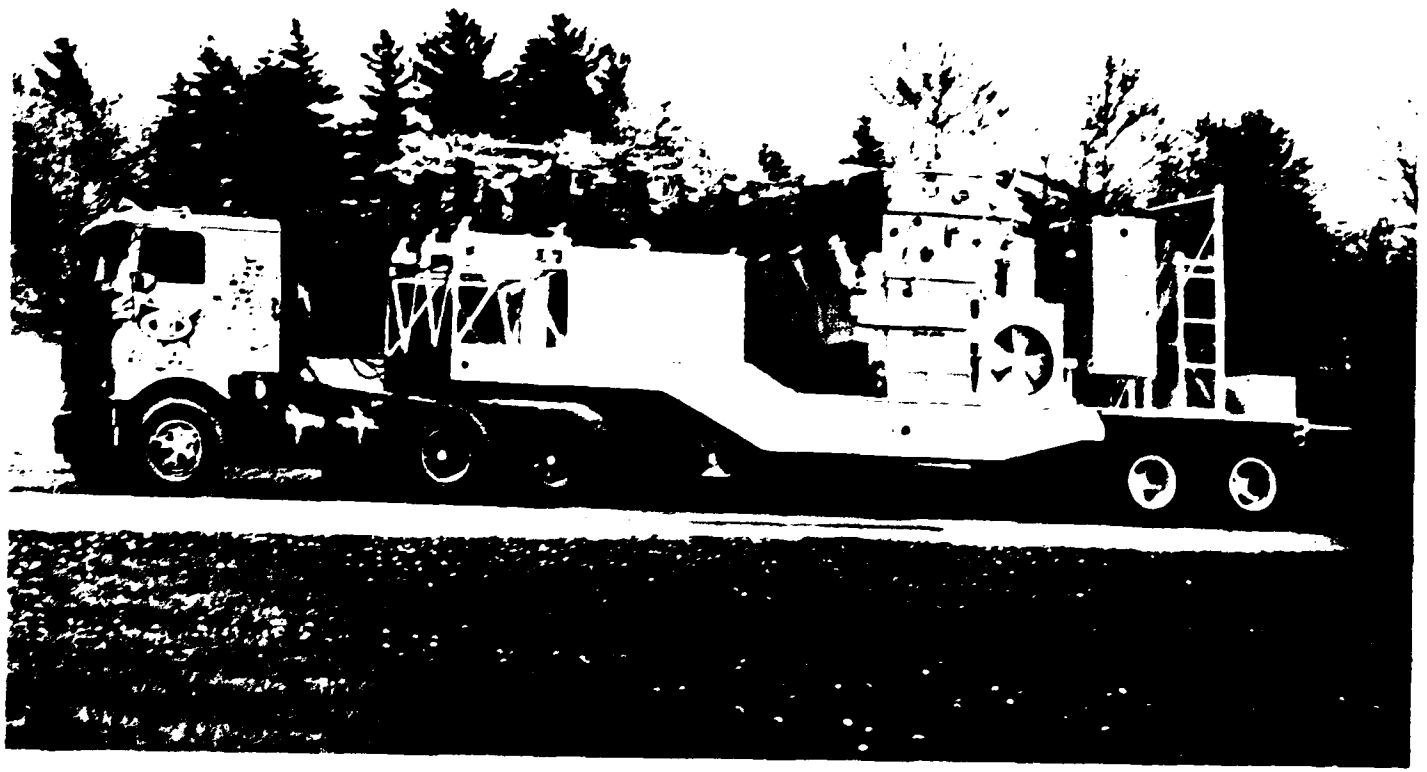

Figure 33. Typical mobile substation

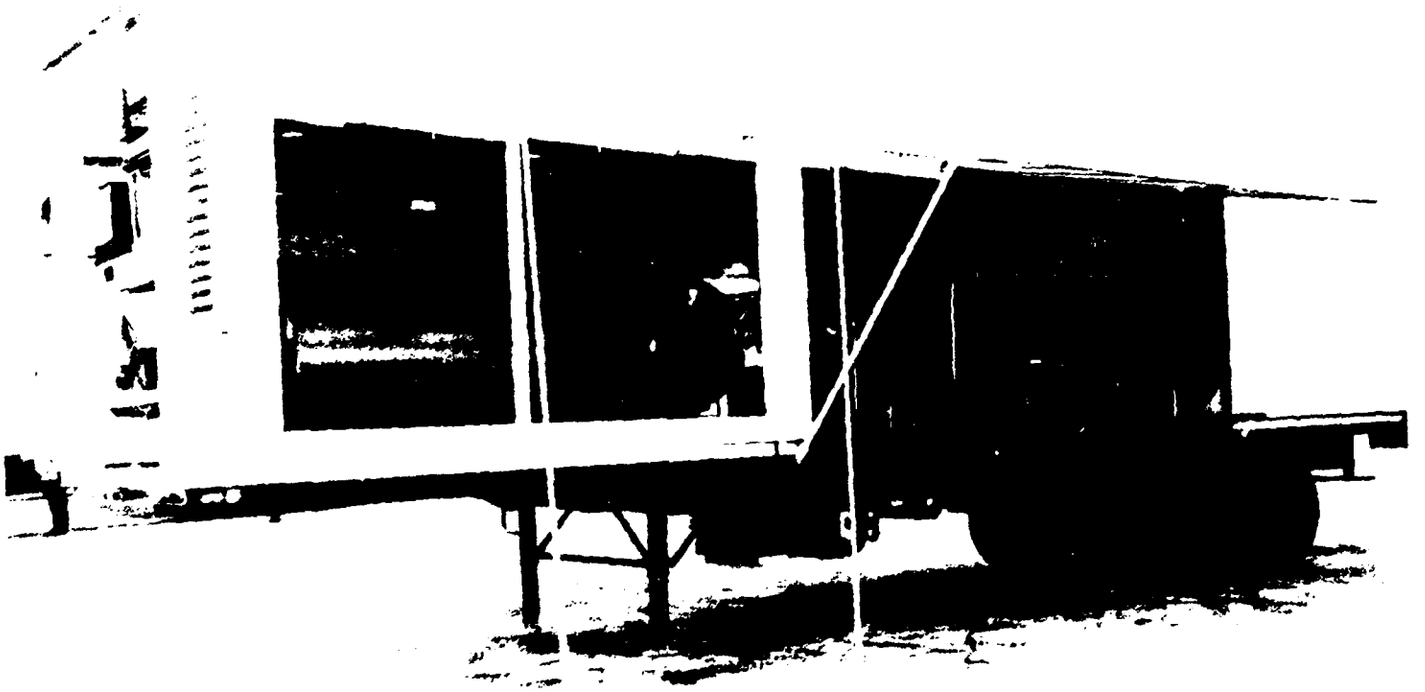

Figure 34. 1040-kW Desert-Pak - LH - front 3/4, view, access doors and filter panels open

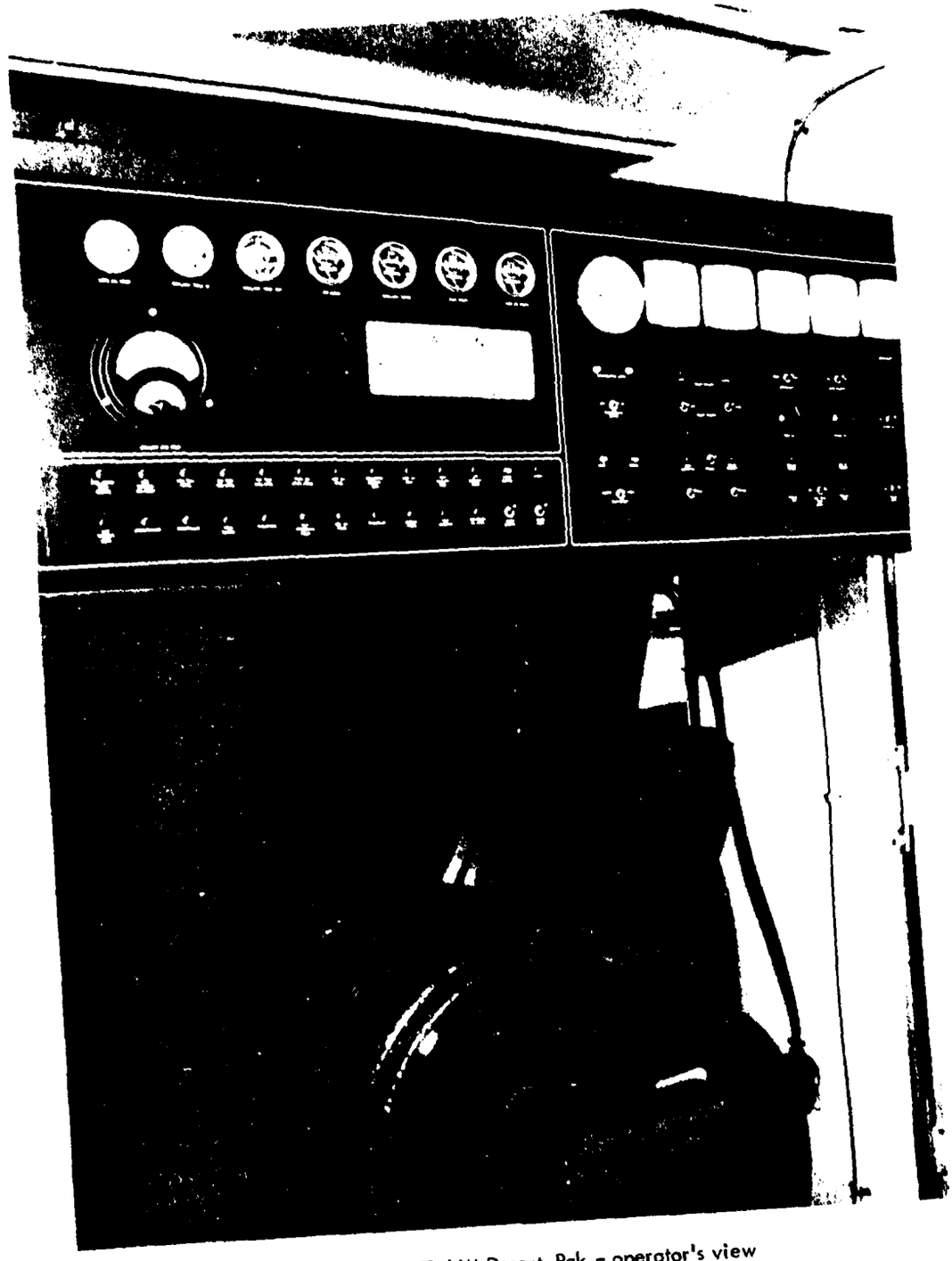

Figure 35. 1040-kW Desert-Pak - operator's view of unit mounted switchgear

Guidance

170. The problem of accurate guidance through the earth is complicated by the inhomogeneous, hostile, and unpredictable medium. Guidance of the earth melting probe must be approximately 5 feet in 5000 feet or $\pm$ 0.1 percent; data gathering must be nearly continuous. If the guidance system is in the probe, then the guidance package must be insulated from temperatures from 2000 to 2500 K. Magnetic fields caused by the 1000-ampere AC power for the melting element will be huge. However, drift in the system must be negligible since the probe will be in the hole for extended periods of time, and the entire package can be no more than 3-1/2 inches high. If the guidance system is a locator device, it must be relatively unaffected by mountainous terrain and unknown inhomogeneities in the earth. The possibility of encountering such unknowns as conducting materials, faults, and small diameter vugs must be accounted for by the system.

171. Guidance systems will be judged in light of these potential problem areas. Final evaluation will be determined by system performance in a horizontal bore hole into a mountain.

172. Several guidance systems are to be considered. A thorough treatement of most of them is given in Reference 9.

173. This text will be a summary of the applicability of the various guidance systems to the problem of the earth melting probe. Ciavatta treats seven systems; two others will be added. In an ideal situation, an above-ground mapping scheme would chart the path of the penetrator by use of radio or sonar waves and the position of the penetrator would be determined exactly. However, the state-of-the art in this field has not achieved the sophistication to allow such detailed mapping.

174. Two surface antenna schemes have been worked out, one by Bell Labs in 1968, and the other by the British Leader line system. In both systems, wires are laid out over the intended path and the tunneler is guided by sensing the magnetic fields of the wire. Neither system was every fully developed for underground use and neither accounts for rugged terrain. Also, inhomogenities such as metal ores or faults would cause unacceptable errors.

175. The underground radio homing device was not developed to the hardware stage, but rather used a radio or sonic transmitter in the probe to signal a receiver at the

destination point. The antenna located the probe by one of two methods: relative field strength, or travel time for pulse. While no data relative to the expected accuracy of this system are available, it was not considered a primary method and was afforded a low priority.

176. Seismic position detectors have several advantages over other systems in that the technology for detecting seismic sources through the earth is sufficiently advanced. Earthquake and rock burst monitoring systems are capable of a high degree of accuracy, given the dimensions of the problem. However, while Dudenhaven quoted an accuracy of 20 feet in less than 2 miles has been quoted, these locations involve sources capable of much greater magnitude than can be expected from the earth probe. Large magnitude sources greatly increase the signal to noise ratio. The level of accuracy offered by present systems does not satisfy the original requirements of the guidance system. Furthermore, the more complex the geology and seismic activity an area exhibits, the greater the reduction in seismic locator system accuracy.

177. Although the light beam guidance system appears applicable to straight line hole applications, it must be rejected because the proposed earth probe does not provide an unobstructed path for the laser beam to follow. Drill casings, wire, melted rock, and core effectively block the hole.

178. The inertial guidance system offers one possible solution to the accuracy problem. One example of such a navigation system, the Singer-Kerfott F-16 system (SKN-2416), has an accuracy of about 0.1 percent. In addition, the inertial system could give continuous pitch, yaw and roll data. The system is environmentally sensitive but could be cooled to the necessary 200°F and pressure protected by the introduction of cooling units and shielding. The effect of the magnetic fields is presently unknown, and while the unit may be unaffected, it possibly could only be used during the shutdown time as drill pipe is added. Unfortunately, the Singer-Kerfott system has a minimum height of 8 inches because of the gimbaling of the gyros. However, the N-73 or micron system, designed and built by Rockwell to achieve low cost and extremely small size, used electrostatic gyros and electromagnetic accelerometers. Tests have been completed at Holliman Air Force Base, but all other information on this system is classified. A usable system of the proper accuracy and size exists, but presently is a classified article.

179. Another possibility involves an arrangement of electrolytic levels and a compass that would give pitch and roll and direction or yaw. The levels are simple devices capable of much greater accuracy than necessary to this application. The lower limit of accuracy quoted by Rockwell as 1/360,000 degree far exceeds the requirements of this application and equipment is simple, representing a relatively minor expense. While an immense magnetic field would render a compass useless during operation, periodic power shutdown during pipe additions could provide accurate yaw data. The compass could be either magnetic or gyro although Singer-Kerfott's smallest gyro compass is about 5-1/2 inches high; repackaging could reduce the size. Further, Draper Labs in Cambridge, Massachusetts, is considering its 1-inch gyro as a compass and Rockwell has an electrostatic gyro comprised of a 1-cm ball spinning in an electrostatic field and shielded by its own magnetic field. While these are not off-the-shelf items, they may develop into a much smaller generation of direction devices.

180. The length of pipe would be used to determine the depth of penetration and, given an equation of motion, a computer could provide updated position data when the power is shut down to add pipe. This arrangement represents the cheapest available working system, assuming successful interface and test. However, the electrostatic gyro compass would also be need to provide continuous yaw data.

181. Therefore, only the inertial navigation system gives continuous real time data on roll, pitch, and yaw within the desired accuracy. Here the major obstacle was size and, although a smaller system exists, data on drift and environmental tolerances are classified.

PART V: COST EVALUATION

182. The original intent of this cost evaluation was to perform a cost/benefit trade study on the designs in the previous section and compare them with conventional drilling techniques. In accordance with the reduction in the scope of this task as directed by the contract, the rationale for selecting the reference design and some preliminary cost estimates for the entire system will be given.

Design Selection

183. The core barrel and wireline retrieval system was judged to be an unnecessary complication to the system, both at the penetrator and at the portal. At the penetrator, some means is required to positively ensure separation of the core increment to be extracted in the core barrel from the core material entering the barrel and still attached to the undisturbed rock mass. At the portal, winding machinery for withdrawing the core barrel and a system to facilitate removal of the core, reinsertion of the barrel, and the return of the barrel to the penetrator would be required. It was, therefore, decided not to require retrieval of core samples during the hole forming operation, but rather to retrieve the core together with the stem at the completion of the hole forming operation. This decision is also felt to have a beneficial effect on the continuity of the rock melting process by limiting the need for access to the stem at the portal. For these reasons, the core extraction provisions of Concept No. 1 were rejected early in the selection process.

184. The cooled inner diameter arrangement of Concept No. 2 required that additional air be supplied for cooling, which would not be available for pneumatic transport of the rock. Also, the additional heat removal in this region of the melting zone implied increased power requirements for a given advance rate. Since electrical power and air flow rate requirements were high and elimination of the cooled inner diameter arrangement promised a reduction in these requirements, Concept No. 2 was rejected. The "thermally

undisturbed" region of the core was judged not to be significantly reduced by the elimination of these cooling provisions because of the effectiveness of the low conductivity of the rock in confining the heating to the periphery of the core.

185. The annular carry-off passage arrangement examined in Concept No. 3 was judged to be detrimental from the pressure drop standpoint. The low effective hydraulic diameter resulted in increased frictional losses. In addition, the necessity for supporting the inner diameter of the stem required that structural members traverse the annular passage, introducing an additional source of pressure drop and impedance to the particulate constituent of the flow. The separate circular carry-off tube arrangement, on the other hand, presented a continuous, smooth, and undisturbed flow path of relatively large hydraulic diameter to the return air and suspended rock particles, resulting in reduced pressure drop and probability of plugging.

186. Although the annular heater arrangement provided increased circumferential uniformity of heating to the penetrator head and improved support stability, the need to provide the independent load components of three separate three-phase, electrical circuits required that it be segmented into a minimum of nine elements. The three separate circuits, each capable of independent power modulation, constitute the minimum steering provisions capable of providing directional control in both elevation and azimuth. As a result, the support stability advantage of the annular configuration conferred by its curvature was largely eliminated. A simple circular cyclindrical geometry was therefore adopted for each of the nine heater elements, providing comparable support stability in all directions and simplifying the manufacture of the heater elements. Some departure from perfect circumferential heating uniformity resulting from the nine separate circular heating elements was judged to be acceptable in view of the gross departure from circumferential heating uniformity, which would be deliberately imposed on the penetrator during steering corrections.

187. The provision made in Concept No. 6 for augmenting the heat flow to the penetrator leading edge by mass transport of the rock was deemed to be a potentially useful design feature and was therefore retained in the selected concept.

As a result, the arrangement defined in Concept No. 6 was selected for further refinement. Refinements made to date have included the addition of a circumferential collector groove at the penetrator leading edge to collect molten rock flowing from the extended surface and channel it to the three axially drilled holes connected with the carry-off tubes. In addition, improvements have been made to the stem end connections to maximize the available air flow path areas. A positive helium inerting gas flow system to the heater cavities has been incorporated. Also, details of the thermocouple instrumentation of the penetrator head have been developed. The smoothness of the periphery of the stem at the convections has been improved by increasing the diameters of the split ring connections. The selected design configuration incorporating these improvements is illustrated in Figure 36 and described in Part VI.

188. Although it is presently anticipated that propulsion of the penetrator head will be achieved by applying compressive force to the stem at the portal, a self-contained downhole propulsion module has been defined conceptually and is described in Part VI, *Mechanical and Structural*. As presently conceived, the propulsion module would be used together with another propulsion module of identical design in a close-coupled assembly near the penetrator head. Alternatively, a pair of modules might be separated by one or two lengths of stem sections. It is also conceivable that a pair of propulsion modules could be used at quarter-mile intervals along the stem to control the local advance rate, prevent stick-slip motion perturbations, and minimize the changes in compressive load in the stem caused by friction at the stem/rock interface.

189. Several options of the electrical system design were already selected in the previous section (Part IV), as in the power supply options in which the selection was based on system safety and reliability for existing hardware. In the EMP guidance design, only one system appears to meet the requirements and fit within the allotted volume.

Cost Summary

190. A cost estimate was developed for the items to be described in Part VI, Reference Concept Description. These costs were derived primarily from telephone conversations with potential vendors and are presented in 1977 dollars. Stem and assembly costs

are based on in-house manufacturing capability. Summaries of the mechanical and electrical system costs are given in Tables 7 and 8. A total cost for the system (assuming no Government Furnished Equipment is slightly less than $4 million. The two primary items involve 3 miles of stems and the heater generator for about $1 million each. Costs do not include trailers for housing personnel, fuel and water trailers, control room trailer, communication system, or general facility interconnections. In addition, tractors for trailers are not included.

Table 7

Mechanical System Cost Summary

Penetrator and Transition Sections	
Penetrator head - tungsten (forged)	$ 50,000
Transition tube - molybdenum	5,000
Smaller molybdenum pieces and tubes	1,000
Tungsten electrodes	900
Pyrographite insulation	2,000
Misc. small machined parts	3,000
Carry-Off tubes (molybdenum and SS brazed)	3,000
Graphite heaters and receptors	5,000
Instrumentation	1,000
Total penetration and transition	$ 70,900
Stem	
Aluminum (20' long)	$ 2,300
Total cost - 5000 m (820 units)	1,900,000
Aluminum (40' long)	2,540
Total cost - 5000 m (410 units)	1,040,000
Stainless steel (20' long)	4,600
Stainless steel (40' long)	5,000

Table 8

Electrical System Cost Summary

Description	No. of Units	Total Cost
Heaters	9	$ 5,350
Primary compressor power supply	2	561,110
Facility power supply	1	200,000
Stem transformers	3, 3 ø	125,000
Heater generator	(Nonrecurring) (Based on 3 units)	521,000
	1st unit	200,000
	2nd unit	170,000
	3rd unit	150,000
a) Regulator for above generator	1st unit	2,000
	2nd unit	1,000
	3rd unit	1,000
Prime mover and trailer	(Nonrecurring)	20,000
	3	270,000
Switchgear	(Nonrecurring)	200,000
	3	260,000
Guidance	1	125,000

PART VI: SELECTED PENETRATOR DESIGN

Mechanical and Structural

General

191. The selected earth melting penetrator configuration is illustrated in Figure 36. Its present configuration represents the most recent development of the concept selected from a number of arrangements developed earlier in the program and discussed in Part IV. The most recent changes, made since the Bimonthly Progress Report of July 1, have been relatively minor and have been mainly concerned with improving the flow path configurations for the molten rock, the helium purge gas, and the air used to transport the removed rock. As a result, the inerting of the heater cavities has been made much more positive and the flow area available for the incoming transportation air has been substantially increased. In addition, the diameter of the split clamps used to joint stem sections has been increased to present a smoother external configuration, and the complete inventory of power transformer sections is now accommodated within one stem section. The design illustrated in Figure 35 incorporates these latest changes.

Penetrator

192. The penetrator head is made of tungsten. Tungsten has been selected for its high melting point of 3410°C, which is 800°C above that of molybdenum. High advance rates required of the earth melting penetrator necessitate operation at the highest possible temperatures. Actual operating temperatures, however, will probably have to be considerably below these melting points. The melting points of tungsten-carbon eutectic and moly-carbon eutectic, 2710°C and 2200°C, respectively, represent more realistic ultimate limits in view of the intimate contact between the penetrator head and graphite heater and insulator components. The 500°C advantage possessed by tungsten should provide a strength advantage for operation at the highest temperature levels. However, the corrosion/erosion resistance of the tungsten in a molten rock environment may be inferior to that of molybdenum. Experimental testing is needed to properly evaluate the relative merits of the materials.

For the purpose of the design study, the use of tungsten has been assumed. This selection represents a conservative approach since the manufacturing problems associated with tungsten are more severe than with others, like molybdenum.

193. Manufacture of the tungsten penetrator head involves the initial pressing and and sintering of 92 percent density blanks, which must then be further densified by forging. Since available press size is limited, the penetrator head will consist of laminations diffusion bonded together. This concept was discussed with Northwest Industries of Albany, Oregon who are familiar with this technology. This company has the capability of machining tungsten using single point tool methods and has worked in the LASL penetrator program. In preliminary phone conversations, total cost of manufacturing a penetrator head was estimated to be roughly $50,000 for tungsten and $35,000 for molybdenum. By way of comparison, an estimate of $27,000 was obtained from Sylvania of Towanda, Pennsylvania, for a completely machined 9-inch penetrator in 92 percent density tungsten (no final forging). However, the strength of this material would almost certainly be inadequate.

194. The penetrator head has axial fins machined in its exterior surface. A large diameter hole is machined along its centerline. The central hole accommodates inserted tungsten, pyrographite, and molybdenum rings that together function as the core former. The rings are held in position by a spring-loaded molybdenum tube and end ring. Insulation tubes made of pyrolytic graphite are interposed between the molybdenum tube and the penetrator head to minimize the conduction of heat radially inward to the core.

195. Twelve holes are machined axially in the penetrator. Three of the holes are equally spaced at 120° intervals and provide a flow path for molten rock, from a circumferential groove machined in the penetrator leading edge, to the rock nozzles of the three carry-off tubes. The other nine holes are arranged in three equally spaced groups of three holes between the rock flow holes and accommodate the nine resistance heaters.

196. Each resistance heater consists of a cylindrical stack of pyrographite and graphite discs held in position by a compressive force transmitted through a spring loaded tungsten electrode. The resistance heater is surrounded by a receptor cylinder of fine grain graphite which is a close fit in the tungsten penetrator head. An annular clearance space, sufficiently large to prevent arcing, is maintained between the heater stack and its receptor. Concentricity of the heater in its receptor is maintained by pilotting the heater in a

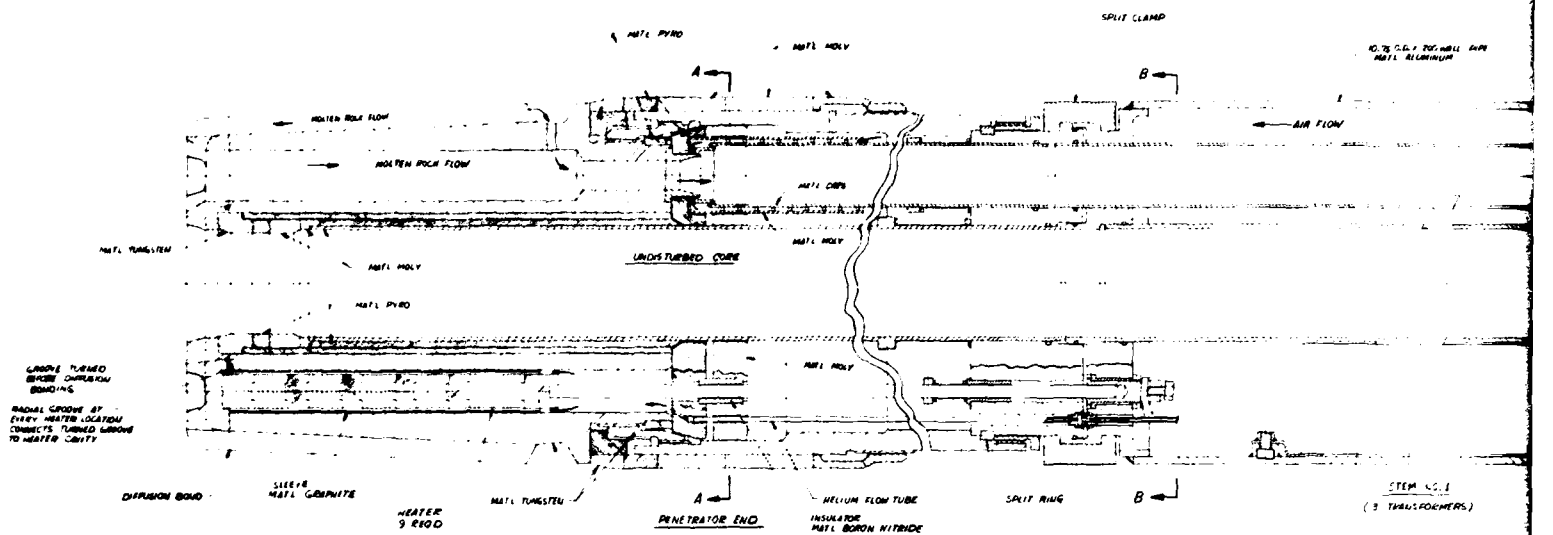

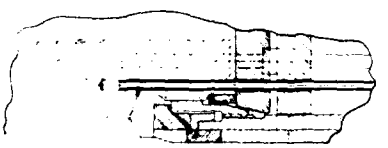

THERMOCOUPLE TUBE — SECTION E-E

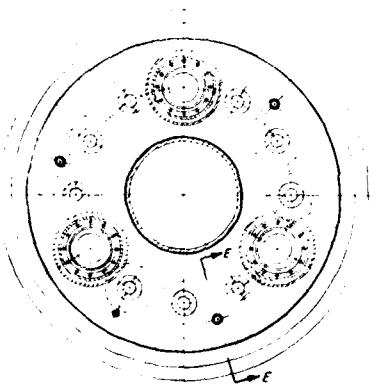

SECTION A-A

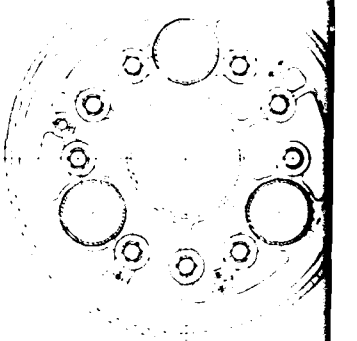

SECTION B-B

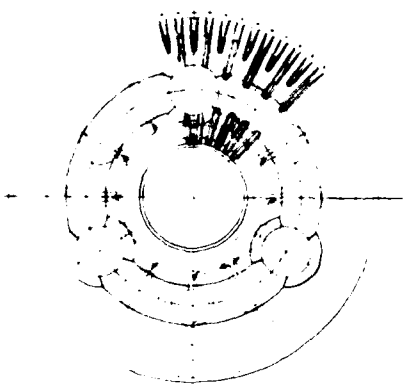

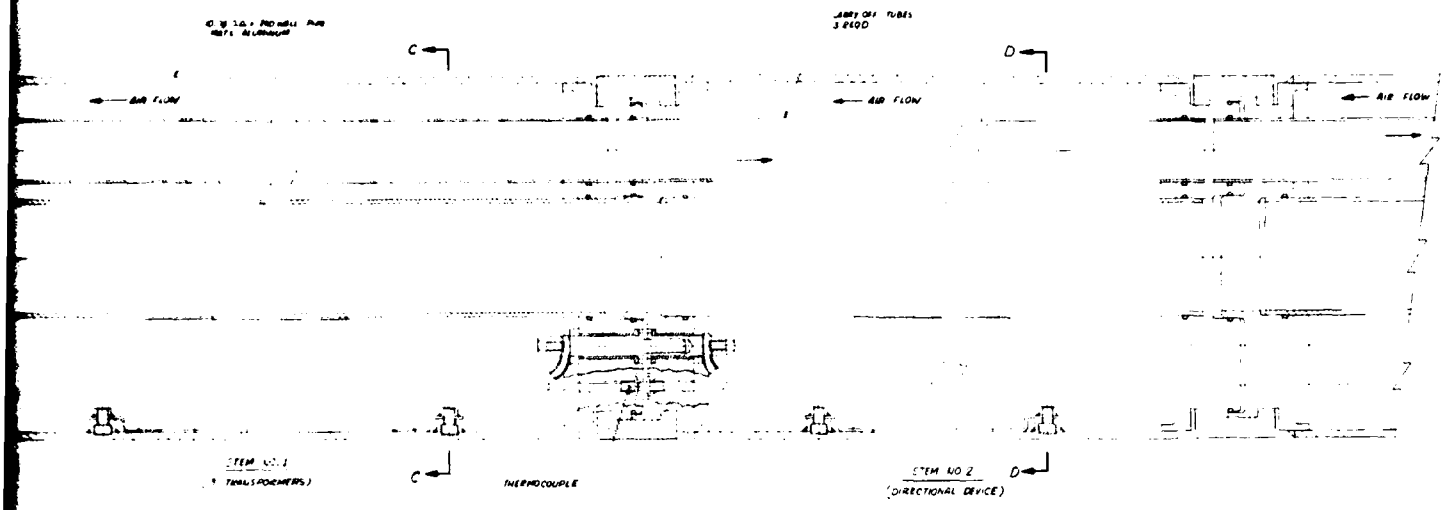

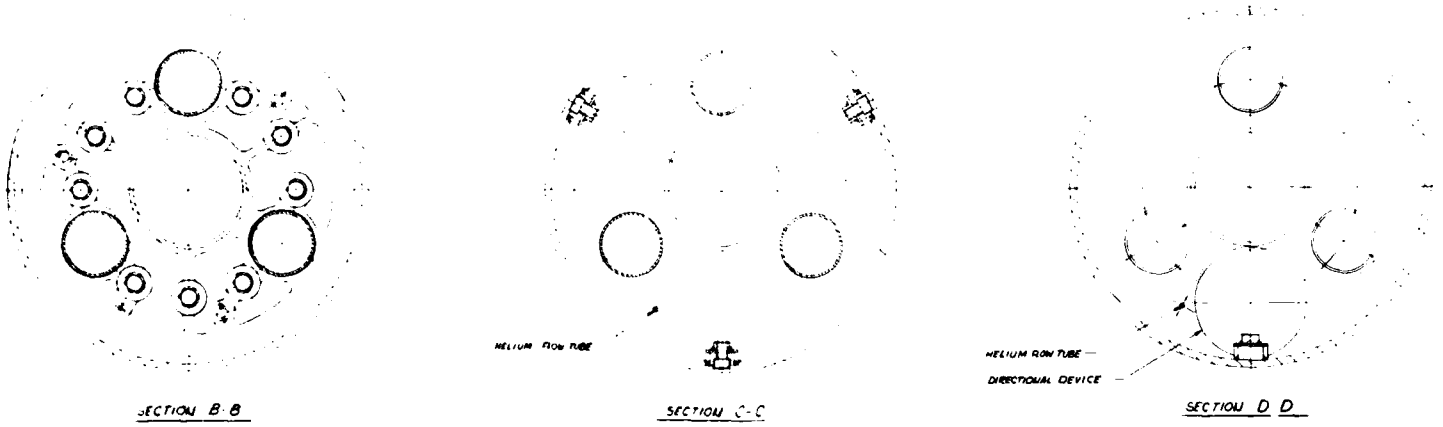

SECTION B-B

SECTION C-C

SECTION D-D

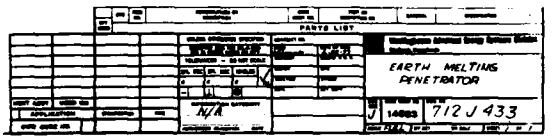

Figure 36. Earth melting penetrator

machined receptacle at the leading edge of the penetrator. Concentricity of the tungsten electrode is maintained by a boron nitride insulator bushing that locates the electrode and that, in turn, is supported in a molybdenum ring located in the molybdenum transition tube assembly which forms the tungsten penetrator to the stem.

197. The transition tube assembly consists of a molybdenum tube of sufficient length to provide the necessary thermal isolation of the stem from the penetrator. A short length of threaded tube joins the transition tube to the penetrator head and serves to minimize heat conduction to the transition tube. A pyrographite ring transfers compressive force to the penetrator from the transition tube and limits heat transfer, while another ring inside the transition tube also serves to limit heat transfer to the stem. A series of rings made of tungsten, graphite, and molybdenum around the transition tube where it joins the penetrator head function as a hole former. The transition tube is joined, at the end remote from the penetrator, by means of a split ring and ring nut arrangement to a stainless steel end fitting. The end fitting provides for the attachment of the adjacent stem section by means of a split clamp arrangement, and accommodates insulation bushings that locate the heater electrodes. The end fitting also supports the termination of the carry-off tubes. That portion of the end fitting not required structurally is machined away to provide a flow path for the air flowing along the stem to the carry-off tube entrances.

198. Each carry-off tube consists of an inner stainless steel tube, extending from the rock nozzle to the transition end fitting, and a shorter molybdenum outer tube joined to it through a spiral wire. The spiral wire forms a spiral passageway along which the air enters the carry-off tube. At the rock nozzle, the air enters the inner diameter of the carry-off tube at high velocity, impinging on the molten rock and breaking it up into small particles. The air then transports the rock particles along the carry-off tube to the portal.

199. Three thermocouples are accommodated in drilled holes in the penetrator head, one to each 120° sector. This number represents an absolute minimum and will probably have to be increased to achieve the necessary control reliability. The thermocouple leads terminate at the transition endfitting in a miniature connector that allows the lead to be continued through the stem sections to a control box at some suitable location. The control box modulates power to the penetrator sectors in accordance with the requirements of the guidance system and thermocouples.

200. Helium gas is fed to the heater cavities of the penetrator head through a single small-diameter line with sealed connectors at each stem joint. The helium enters one of the heater cavities from the delivery tube and flows along the heater periphery toward the penetrator leading edge. The helium then enters a machined groove connecting the heater cavity to a circumferential groove turned in one of the laminations prior to the diffusion bonding process. The circumferential groove conveys the inerting helium to the other heater cavities. The helium is ultimately exhausted into the transition region.

201. No particular problems are foreseen in the manufacture of the transition components since similar components have been fabricated for the LASL penetrator program.

202. Required length of the transition section has not yet been determined. The use of a stainless steel stem section immediately adjacent to the transition would probably allow its length to be minimized. The possible alternative arrangements need to be investigated from a heat transfer standpoint and the best arrangement selected.

Stem

203. The stem consists of an assembly of standard stem sections joined end to end by split clamps. Specially modified stem sections accommodate transformer modules, guidance equipment, and control boxes. Standard stem sections from which most of the stem length is constructed are made of aluminum. The stem section immediately adjacent to the penetrator and transition section may be made of 18-8 stainless steel to provide improved temperature capability.

204. The standard stem section is fabricated from standard sizes of extruded aluminum pipe. An outer casing, of 10.75-in.-diameter x 0.200-in.-thick pipe is welded at each end to a machined aluminum end fitting. The end fittings are machined to provide support for a central 3.5-in.-diameter x 0.120-in.-thick pipe and three 1.900-in.-diameter x 0.065-in.-thick pipes equally spaced around the central pipe. The three smaller pipes carry the particulate rock and transport air to the portal. The larger central pipe accommodates the rock core. Rubber O-rings are used to seal the smaller tubes to the end fittings and to seal the stem sections to each other.

205. The end fittings also provide support for nine male and female electrical connectors three thermocouple connectors and the connectors for the single helium line. The electrical convertors provide electrical continuity for the nine wires of the three separate three-phase circuits. The nine wires traverse the length of the stem section and are bolted to female connectors at one end and male connectors at the other end of the stem. The connectors permit simple

plug-in connection of stem to stem. The connectors are supported from the end fittings in insulating bushings made of some suitable plastic material. It should be noted that the wires between the transformer modules and the penetrator head carry low voltage-high amperage current while the wires between the transformer modules and the portal carry high voltage-low amperage current. The nine transformer modules are arranged in groups of three between the three carry-off tubes of a single stem section. Each group of three modules is constructed as a single 3.25-in. -diameter tube supported from the outer casing of the stem through brackets welded to the transformer and bolts inserted from the outside of the stem.

206. The end fittings are machined away, wherever possible, (while providing the necessary support for connectors, etc.) to provide the largest possible flow path area for the incoming air. Incoming air flows from the portal to the penetrator head in the spaces inside the outer casing and outside the central pipe. The returning air, transporting the rock particles, travels to the portal inside the three smaller tubes. Pressure drop in the air causes the outer casing to be stressed in tension and the central pipe and three smaller pipes to be compressively loaded. Maximum hoop stresses are experienced at the portal and, as presently designed, the stem is capable of withstanding an air pressure at entry of approximately 500 psi. This capability could be increased by the use of pipes of thicker section that would, in turn, increase the weight of the stem and, as a consequence, the required thrust force.

207. Axial compressive stresses in the stem outer wall resulting from the propulsion force, estimated to be approximately 69,000 lb, are approximately 10,000 psi. No stress or stability problems are anticipated to result from propulsion forces.

208. Each stem section is estimated to cost approximately $2300 if made in a 20-ft length. Thus, total stem cost for a 5000-meter hole would be roughly $1,900,000. If the stem is made in 40-ft lengths, the cost per section would increase to $2540 and the total cost for a 5000-meter hole would be reduced to approximately $1,000,000. The longer stem lengths are obviously preferable from the standpoints of both cost and pressure drop. However, the cost and performance advantage must be considered in relation to the inconvenience of transporting and handling the longer sections. It may be possible to make a case for several design "weights." Light section, short lengths could be used for short holes with progressively heavier and longer sections for long holes. A cost summary of the penetrator head and stem components is given in Part V. The hardware costs for a 5000-meter hole appear to be

dominated by the stem costs. Moreover, at least 80 percent of the stem cost is incurred in the machining of end pieces and connector details. A detailed manufacturing engineering study would appear to be warranted before proceeding further into the detail design phases to attempt to reduce machining costs. The small pieces such as electrical connectors can be considered high production items (3650 items for the 40-ft stem design) and could probably justify the procurement of some production tooling.

Propulsion module

209. A propulsion module concept is illustrated in Figure 37. The design employs a circumferential sleeve that can grip the wall of the hole through an inflatable boot and be propelled along the stem in either direction by a system of ball screw jacks. The propulsion module, thus, has the capability of propelling the stem in the melting direction while the gripping mechanism is energized. At the end of its travel, the inflatable boot is deflated and the gripper sleeve is rapidly returned to its starting position to repeat its gripping and propulsion cycle. Propulsion modules are planned for use in pairs, both units driving together but returning separately to hold position. However, the mode of operation is flexible and can be varied to suit the particular conditions encountered. Modules could be used singly at regular intervals along the stem or in pairs at widely separated locations. When used in pairs, some separation of the two units may be beneficial in traversing unconsolidated rock formations.

210. Three ball screw jacks are employed to exert the propulsive force and are evenly spaced around the annulus between the inner and outer diameters of the stem section between the carry-off tubes. The largest possible ball screw jacks, consistent with the space limitations, are employed to achieve the maximum thrust capability. For the purpose of developing a properly sized and potentially practical design, the ball scew nuts were selected from the Saginaw catalog. * A 2.000 BCD unit with a lead of 0.265 in. and 10-1/2 turns of balls was stated to have an operating load capability of 11,502 lb for 1,000,000 inches of operating life. This operating life is representative of about five holes 5000 meters in length. Thus, the three screw jacks working together have a thrust capability of 34,506 lb, and two of the propulsion modules working together should be capable of exerting a propulsive force of 69,000 lb. This is approximately equal to the force required to overcome the friction

* The particular units used in the design were obtained from the listing of CTS custom thread ball bearing screw assemblies given on page 2 of Section A-3 of the Saginaw catalog.

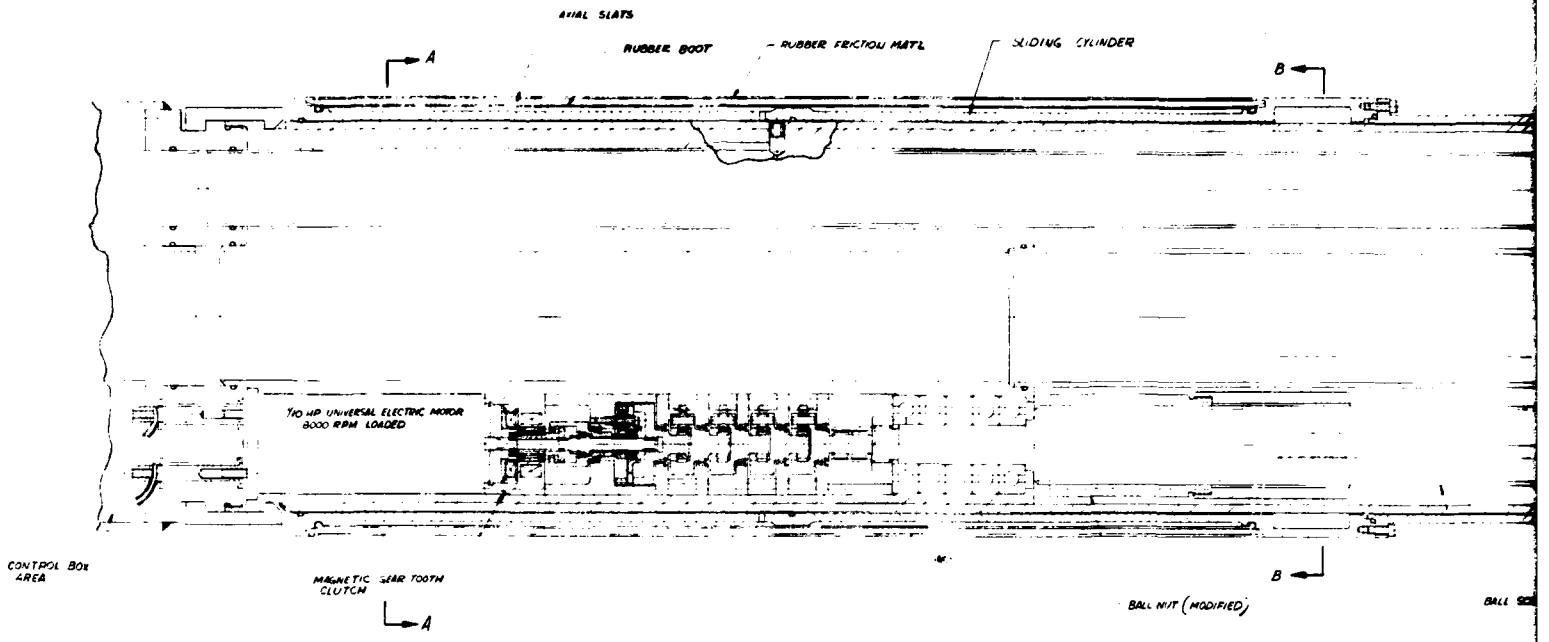

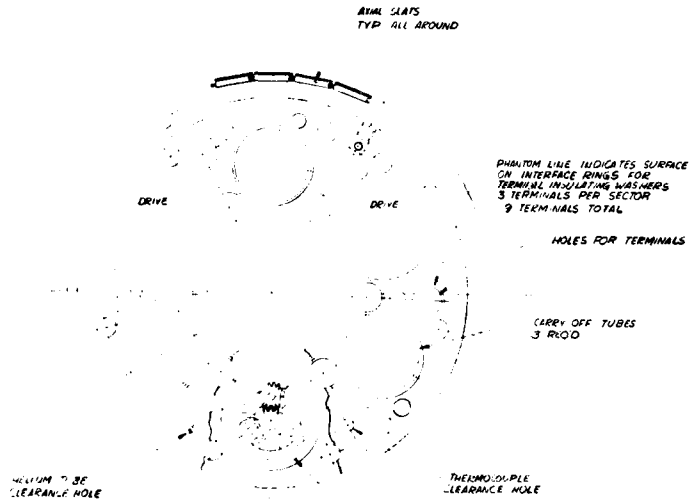

SECTION A-A

DRIVE MECHANISM
3 REQD

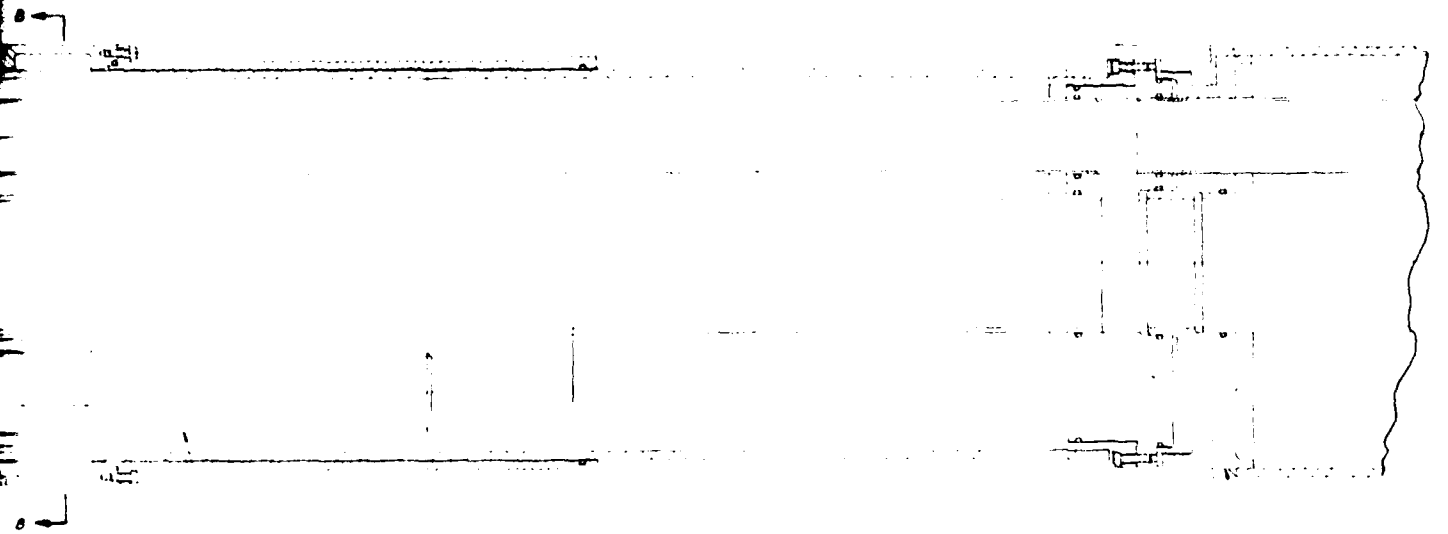

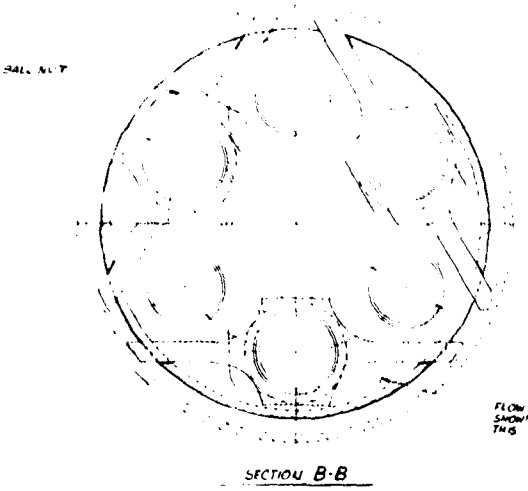

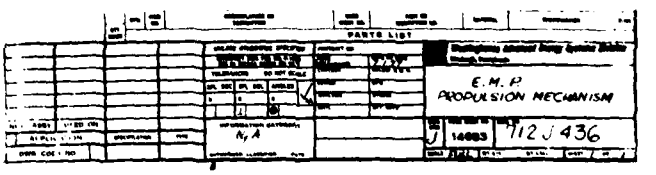

Figure 37. EMP propulsion mechanism

(assuming $\mu = 0.25$) exerted by the weight of 5000 meters of stem and the contained rock core.

211. The thrust of the ball screw is transmitted to the stem through a stack of five duplex 62-mm-OD x 25-mm-ID x 17-mm-wide ball bearings. The stacked configuration results in a load capacity of the stack approximately three times that of a single bearing, on the basis of the life of the first bearing to fail, and provides sufficient life, based on bearing minimum life, to form three 5000-meter holes.

212. The ball screw is driven, through a five-stage planetary reduction gear, by a 1/10 HP universal electric motor. Four of the stages drive in through the sun gear and out through the planet carrier, the annulus gear being fixed. The reduction ratio of each stage is four for a total reduction of 256. The fifth, high speed stage has a 3:1 ratio and drives in through the sun and out through the annulus gear, the planet carrier being fixed. Thus, when driving through this gear, the direction of rotation is reversed and the overall reduction ratio is 768. This gear ratio is used when propelling the penetrator and, under these conditions, the universal motor generates its full power at approximately 8000 rpm. The ball screw is then turned at approximately 10.4 rpm, a speed calculated to produce an advance rate of about 1.15 mm/sec, leaving some margin to allow time for return of the slider.

213. The electric motor drives the reduction gear through a quillshaft whose axial position is controlled by a magnetic actuator. Axial motion of the quillshaft allows it to disengage the motor drive from the sun gear of the three-stage reduction/reversing gear and drive directly into the four-stage fixed annular gear set. Under these conditions, the direction of rotation is reversed and the overall reduction ratio is reduced from 768 to 256. This mode of operation is used to return the sliding gripper boot to its original position after the completion of a driving cycle. Under these conditions, the universal motor is relatively unloaded and its operating speed increases to about three times its unloaded rpm. This speed increase, together with the three-fold reduction in gear ratio, returns the slider in about 11 percent of the time taken in the driving direction. Thus, the time required to return the slider does not form a substantial portion of the operating time and is essentially compensated for by a small excess of operating speed under load. (1.15 mm/sec versus 1 mm/sec design goal).

214. The electrical connections to the universal motors are made in the form of male and female plug components to allow easy connection of the propulsion module to a

special stem section containing the appropriate control boxes. Provision must also be made in the connector area to provide continuity for the main EMP power supply cables, helium line, and instrumentation. All of these details have not been worked out on Figure 36 because of time limitations, but no particular problems are anticipated in accommodating them.

215. The ball screw nut transmits its driving force to a beam whose outer ends engage with a groove turned in the inside diameter of the slider. The beam ends pass through axial slots machined in the outer diameter of the stem. The straight beam allows the large ball screw load to be transmitted to the slider without imposing any bending moment on the ball screw. The offset moment in this arrangement is carried internally by the straight beam.

216. The slider member is extended axially beyond the groove to carry O-ring seals that engage the stem beyond the extremities of the axial slots. Thus, the stem remains hermetically sealed, despite the drive mechanism and slots.

217. High pressure air is supplied to the space between the slider and stem between a pair of O-rings that move with the slider but are separated such that they always straddle the supply port. Thus, movement of the slider in no way interferes with the air supply. A drilled passage in the stem is led to a plug connector which engages with a similar device in the special stem section accommodating the control box. In this manner, high pressure air, tapped from the air flowing in the stem annulus, is fed to the slider pneumatic gripper boot when demanded by the control system.

218. The gripper boot consists of an assembly of axial slats inserted into circumferential grooves at each end of the slider. The slats carry rubber friction material on their outer surfaces. A continuous rubber tubular member, sealed to the slider at each end, is used to energize the gripper boot. When the high pressure air is admitted to the space inside the rubber tubular member, it expands, forcing the slats to move outward and grip the wall of the hole. The frictional propulsive force is transmitted along the slats, as compressive force, to the slider and from the slider to the screw jacks.

219. The length of gripper boot engaged with the hole wall must be sufficient to transmit the propulsive force without overloading the glass hole liner. If the limiting tensile strength of the glass liner is assumed to be 2000 psi, the allowable radial pressure is 130 psi (assuming a liner thickness of 0.39 inch). Approximately 8 inches of gripper boot length are required to transmit the 34,500-lb propulsive force, assuming a coefficient of friction

of 1. In the design illustrated in Figure 37, approximately 24 inches of gripper length have been provided, permitting coefficients of friction below 1 or radial pressures below 130 psi. It is envisaged that the control system would employ a pressure reducing valve to ensure that the pressurizing air pressure is held safely below the fracturing pressure of the glass liner (130 psi).

Electrical

Heaters

220. The penetrator will be powered from nine heaters placed in three groups of three heaters each. Each heater group is powered from one three-phase transformer whose secondary winding is wired to a wye configuration. One heater is terminated between one phase to neutral of the transformer secondary. To provide a total heating capacity from 1 to 1.5 MW, it is suggested that a prototype heater be fabricated and tested to insure that the power requirements per heater and the helium pressure established for the required heater voltage can be achieved. This would clarify the discrepancies defined in Part IV, Electrical System. The heater would be fabricated from discs of pyrolytic graphite and fine grain graphite. Various configurations of disc combinations would be tested to achieve the power required.

221. The thermal expansion of the heaters must also be considered. As shown in Table 5, the temperature coefficient of pyrolytic graphite in the C plane is $13 \times 10^{-6}/^{\circ}F$. If the entire heater length of 10 inches were made of pyrolytic graphite, then the thermal expansion for a maximum of $5000^{\circ}F$ would be:

$$\text{Thermal expansion} = 13 \times 10^{-6} \frac{\text{in.}}{\text{in.} \ ^{\circ}F} (10 \text{ in.}) (5000^{\circ}F)$$

$$= 0.65 \text{ inches}$$

222. The thermal expansion of the heater as well as the tungsten electrode is accommodated as shown in Figure 36. A spring is used to force the electrode to the heater and maintain compression of the heater discs. As the heater expands, the spring is compressed

and the mating portion of the electrode is driven into the power inlet connector. Sufficient space in the mating connector is provided for maximum system expansion. The tungsten electrode is insulated from system common with boron nitride sleeves.

223. The pyrolytic heater discs are available from Pfizer; the fine grain graphite discs from Ultra Carbon or Pure Oil; pyro sleeves from Ultra Carbon; tungsten electrodes from Sylvania.

Stem transformer

224. As was indicated in Part IV, Electrical System, the stem section to house the transformers using a 60-Hz power system would be approximately 180 feet long. Before decisions could be made to power the heaters with a higher frequency source, an investigation was made into the availability of higher frequency generators (Part IV, Stem Transformer).

225. By using a power source frequency of 680 Hz, the overall transformer stem length could be reduced from 180 ft to 30 ft. By using a 30-ft section, the transformer stem section would be compatible with the entire system stem lengths for ease of shipment and minimum coolant pressure losses through the stem end plates. The transformer primary and secondary would be wound around micro-laminations. The transformer would be made up of small sections about 15 in. long and 3.25 in. in diameter. Each of these small sections would be stacked in series like cells in a flashlight until the proper operating voltages were required for the primary. All of the secondaries would be connected in parallel to a common bus for that phase. Three such transformer stacks would be connected primary delta - secondary wye for a three-phase system for three heaters. Three three-phase transformers would be required for the nine heaters. As with the heaters, it is recommended that a single phase of the transformer be built and tested to verify the transformer design. The transformer design is available from Westinghouse.

Power transmission

226. It is suggested that a minimum wire size of AWG No. 6 be used for the transmission line. To allow for the maximum cross-sectional area within a given stem section for coolant flow, cable insulation material used on the transmission wire should be considered. The overall cable diameter can be reduced by using "Kapton" as an insulating

material over the cable conductors. "Kapton" is a DuPont product and several cable manufacturers produce cables with "Kapton" insulation.

Power supply

227. Figure 33 shows a typical mobile substation. All trailers used within this system shall contain outline lights and reflectors that comply with applicable highway regulations of the Interstate Commerce Commission. It is expected that all equipment mounted on trailers for this system will meet the vehicle size and weight limits for all 50 states. Only two areas pose a potential problem for road clearance. These are the District of Columbia and the state of West Virginia. These two areas define their maximum clearances at 12.5 feet. Should the final design of equipment fall within this limit, the equipment could be used in these two areas also.

228. As indicated in the discussion of stem transformers, a power frequency of 680 Hz will be used for this system to reduce the stem transformer size as well as other auxiliary equipment. Generators to provide the power requirements for this system at 680 Hz are expected to be 18 inches in diameter and 48 inches long with an estimated weight of 1600 pounds. To produce this frequency, the generators may have to be turbine driven. A number of suppliers of the prime mover include the following: Stewart and Stevenson Services, Inc.; AVCO, Lycoming Engine Group; AiResearch; Solar International; and General Electric.

229. Of the above, Stewart and Stevenson is the most experienced for this application and has the capability for handling the power supply system, including trailer mounting. The generator is available from Westinghouse and involves only a modification to a unit being built for the Navy.

230. Since the heater power supply system is to operate at 680 Hz, a separate power supply would be required for facility needs. These include power for lighting (indoor and outdoor), fans, pump motors, convenience outlets, power tools, compressors, trailers to house personnel, cooking facilities, heating and air conditioning, welding machines, etc. It is expected that the vast majority of facility power will be required to operate the primary compressor for the stem coolant. Compressor power requirements can be in the range of 1 MW. To provide for power supply failures, two units of the type shown in Figure 33 will be required for the compressor. Figure 38 shows a typical unit that would

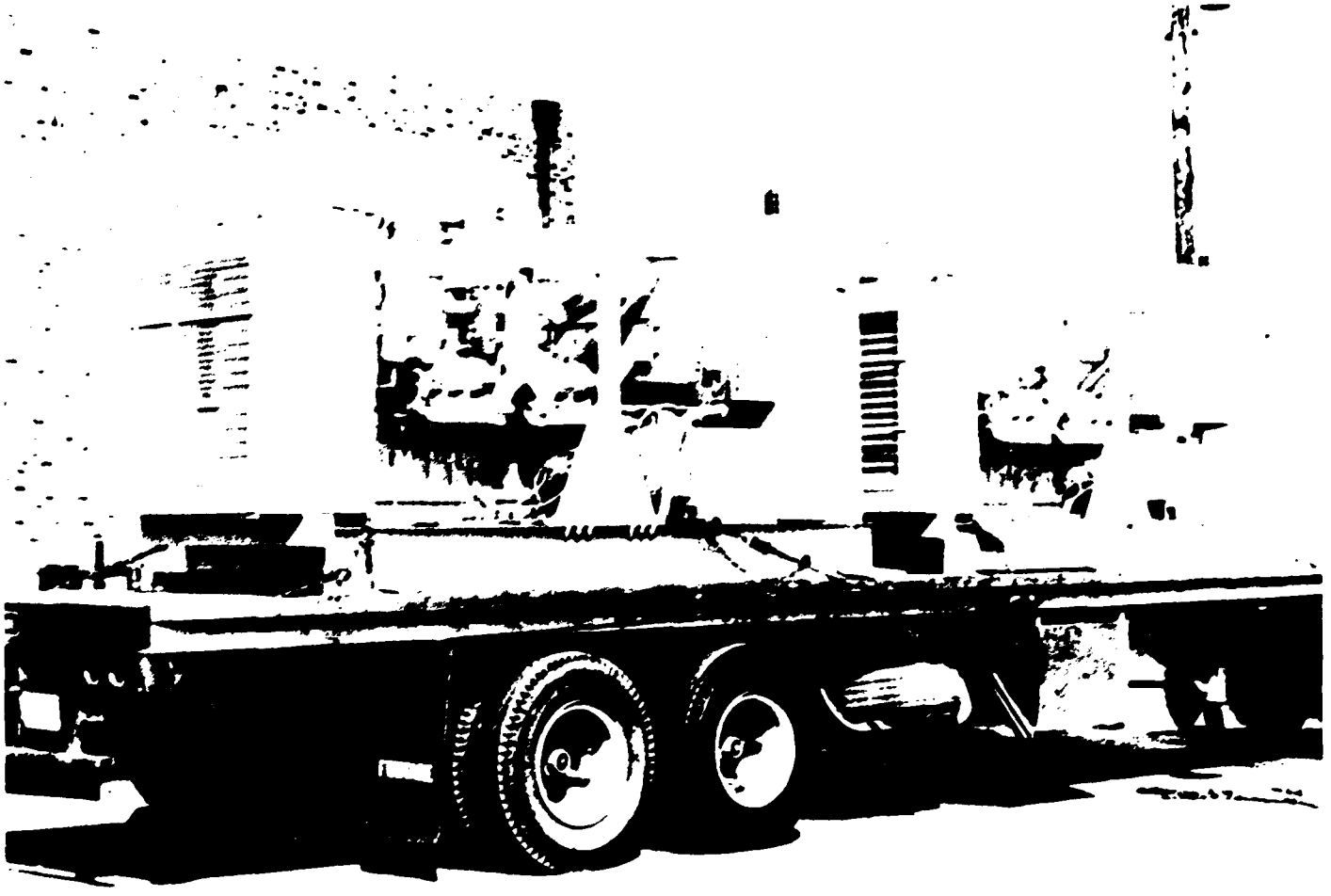

Figure 38. 300-kW precise power gensets supplied to NASA - - Kennedy Space Center

be required for the rest of the facility. Although the figure shows two units, it is expected that only one unit would be required. If the smaller unit were to fail, it would be possible to tap into the compressor power supply temporarily. The smaller unit is suggested for the rest of the facility since there will be times when the process is not operational, and it would not be practical to run the large unit for facility needs alone. Diesel fuel can be provided from standard fuel hauling trailers. The facility water supply could also be provided by water carrying trailers. Figure 39 shows the system block diagram for the entire facility.

Thermal/Hydraulic

Power and temperature

231. Power and temperature were calculated for the reference design configuration in all geologic models using the same techniques as described in Part IV, System Performance Analysis. The maximum power requirement of 909 kW is shown in Figure 40 for the CALCI model at 1.39 mm/sec (5 m/hr) velocity. Of this, 303 kW appears as chemical energy in the evolution of CO_2 and 73 kW is lost to the surrounding rock. For the MASIG calculation, there are no chemical reactions and the maximum amount of heat input is 685 kW, of which up to 600 kW can be recovered in the air coolant stream.

232. The calculated surface temperature of the penetrator is given in Figure 41 for all five models. As described in Part IV, the temperature calculation is subject to the significant uncertainty associated with the unknown liquid thermal conductivity. In general, temperatures are less than those of Figures 12 and 13 since the design configuration is a finned surface providing more than 60 percent greater heat transfer surface area than the simple planar surfaces of those figures. The maximum temperature at 1.39 mm/sec of 2800 K (4580°F) in UNCON is still excessive, because of the low thermal conductivity of the model. Increasing the length of the penetrator substantially reduces the temperature by up to 300 K as shown by the dotted line for UNCON in Figure 41.

233. A two-dimensional heat transfer model of the circular cross section of the earth melting penetrator tungsten head was developed. The current model version shown in Figure 42 is equipped with only 38 nodes* to minimize the complexity of the problem and to

* Heat transfer analyses commonly use several hundred nodes.

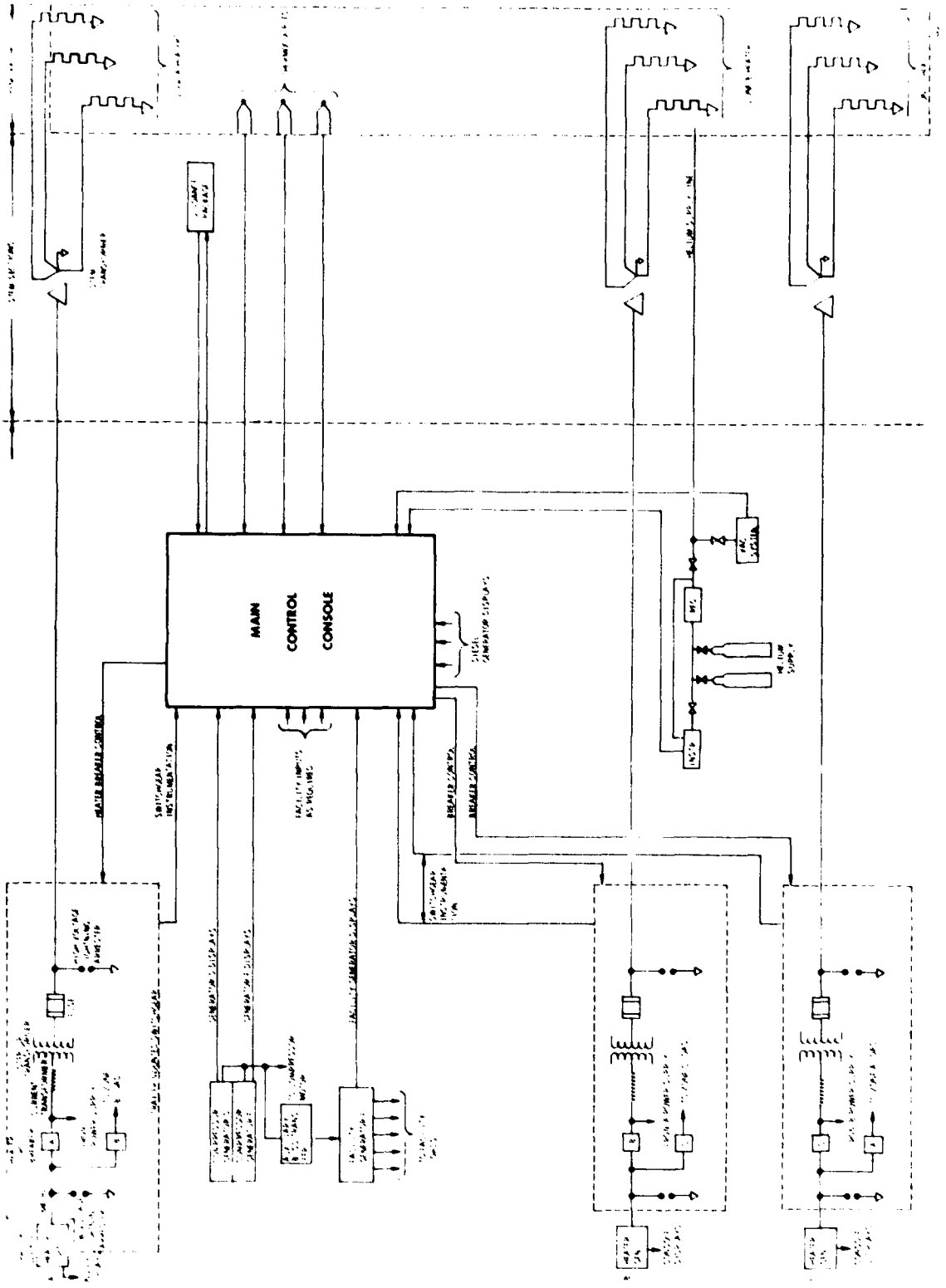

Figure 39. System block diagram

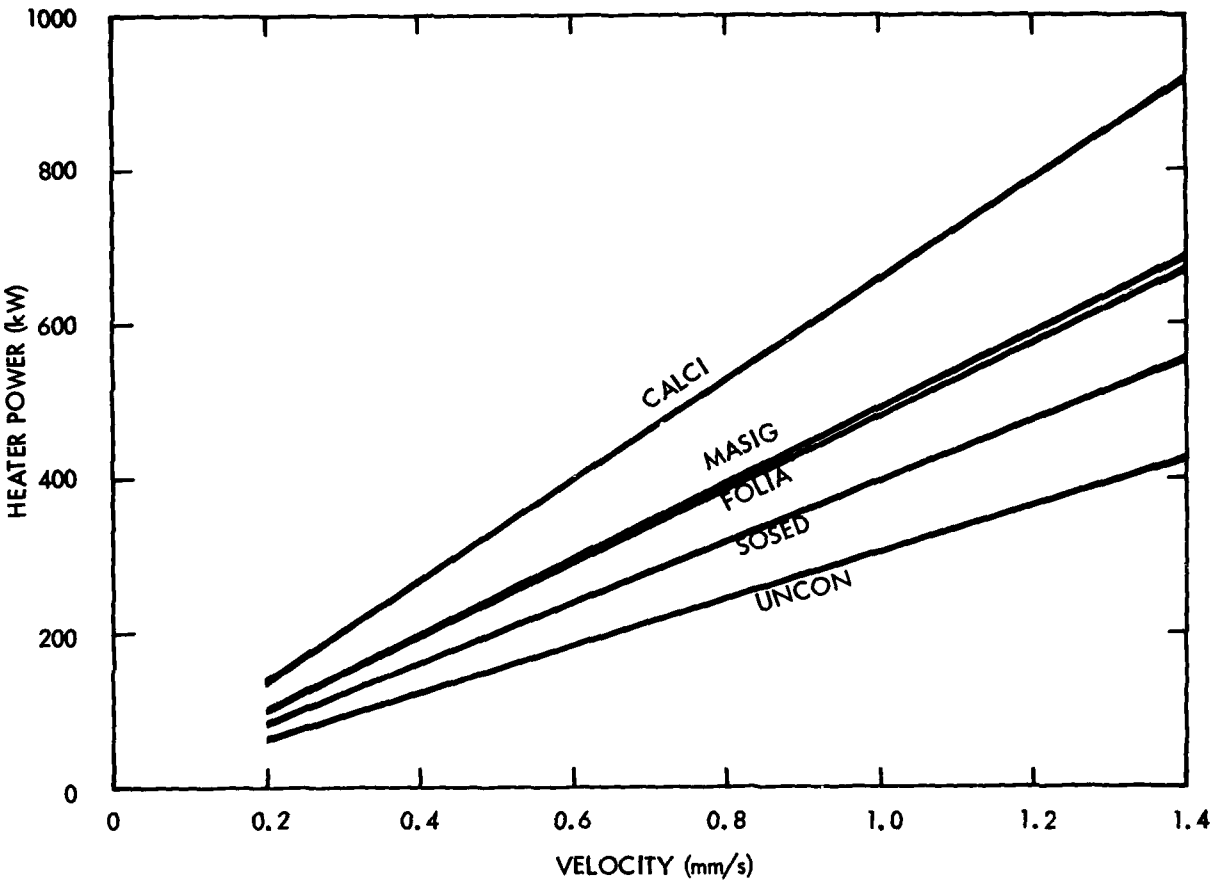

Figure 40. Heater power for the design configuration

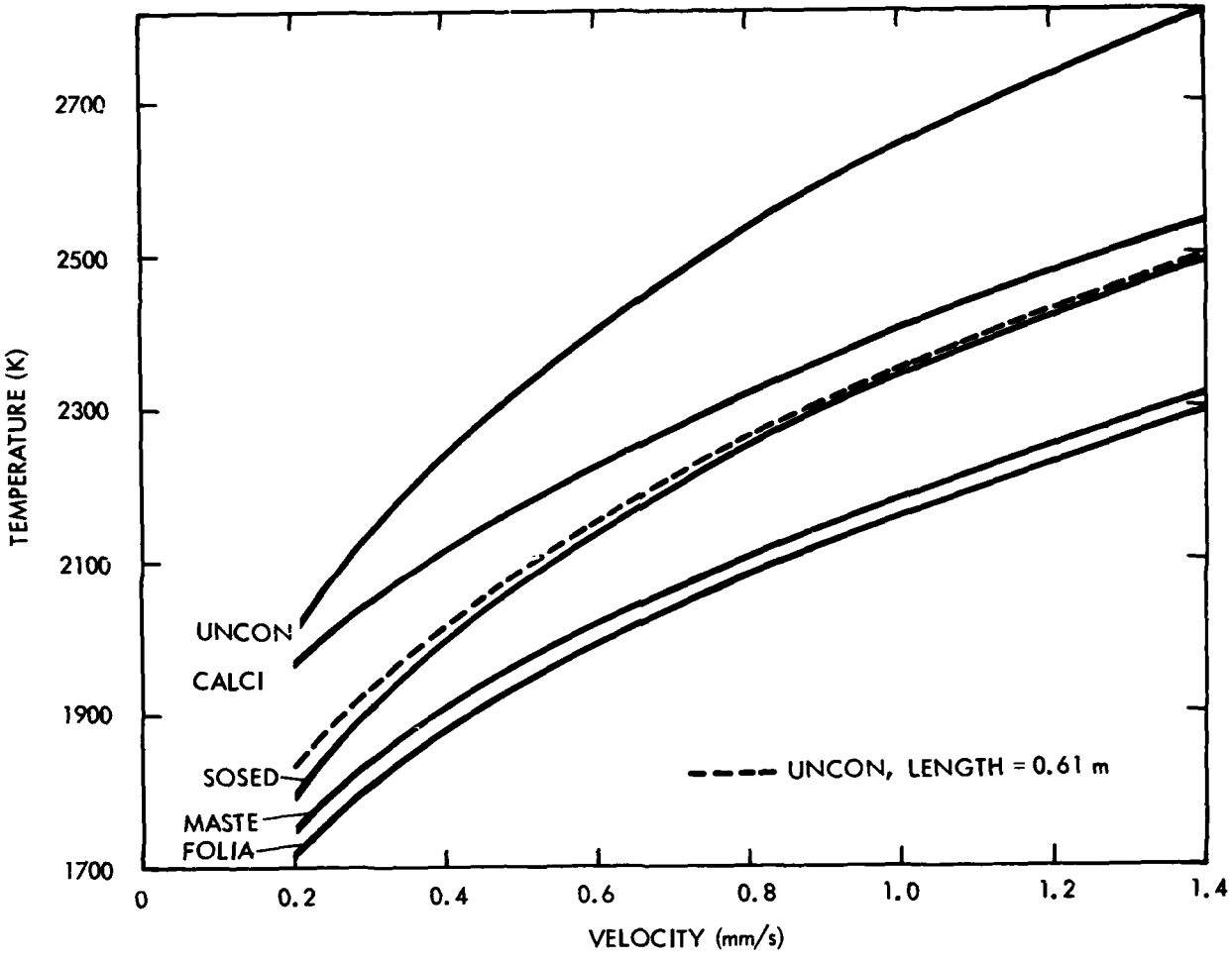

Figure 41. Penetrator surface temperature for the design configurations

accelerate the acquisition of results. The purpose of analyses with this model is to provide a two-dimensional reference temperature distribution prediction for the current conceptual EMP design.

234. The first calculations have been completed using the Figure 42 model. The material nodes (1 through 38) were assumed to be tungsten having a constant thermal conductivity of 20 BTU/hr ft ^{o}F. Nodes 9, 12, 13, 16, 19 and 20 model the penetrator heaters. They have been assigned volumetric heat generation rates of 1.26 BTU/in.^{3}-sec to simulate penetrator operation at 0.10 MW. Calculations performed with this preliminary model confirm earlier hand calculations, which indicated that large radial-direction temperature differentials could exist in the penetrator as currently designed. Under the assumed boundary conditions, which are noted in Figure 42, nodes 1 and 38 are the points of highest and lowest tungsten temperature, respectively. For the heat generation rate and material property conditions identified above, the predicted temperature difference between those nodes was 1890^{o}F. This differential is clearly unacceptable considering the low penetrator power level applied in the calculations. These preliminary results are being reported here to identify a potential thermal problem in the current EMP design and to note that detailed two-dimensional heat transfer analyses of the penetrator have been initiated. Improvements and refinements planned for the heat transfer model will increase the number of material nodes, account for heat transfer to the undisturbed core region, permit temperature-dependent material properties, model the cylindrical shape of the penetrator heaters and melt removal tubes more effectively, etc. Future thermal analyses will employ the model to further assess the adequacy of the penetrator design and to evaluate potential design modifications.

Air coolant supply

235. The purpose of the air coolant supply is threefold: provide coolant for internal parts (e.g., guidance package); cool the glass liner until it becomes self supporting; and provide floatation for extrudite cooling and removal.

236. In the requirements definition, air was specified as the preferred coolant, water was less desirable because of its potential limited availability at the drilling site, and other coolants such as pure nitrogen which has zero site availability in quantities

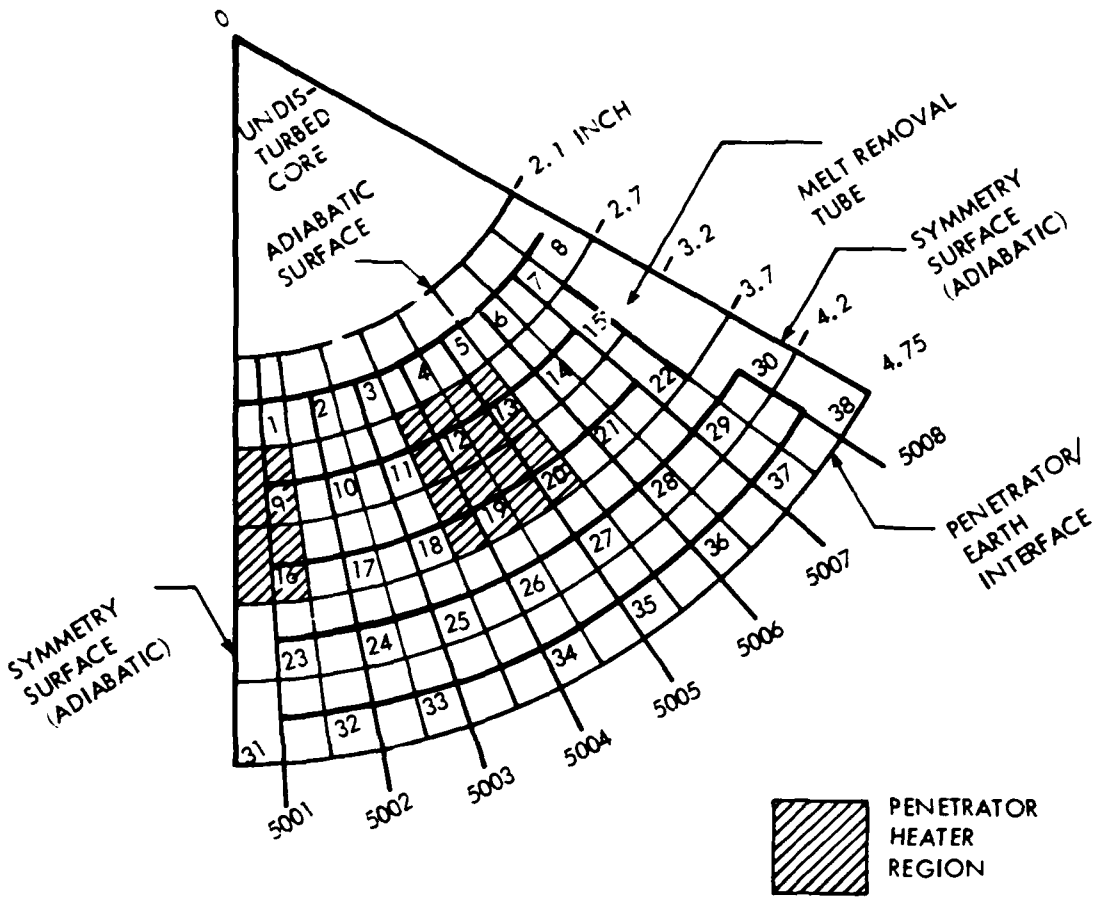

Figure 42. EMP heat transfer model

needed. Calculations to determine the amount of air needed and the piping pressure drops were made. The coupled energy/momentum solution for counterflow streams of air over three miles long is indeed complex. For the conceptual design of this report, scoping calculations were made to identify problem areas.

237. Assuming the maximum allowable pipe temperature is 400°F for the aluminum stem configuration, and the maximum power which can be extracted of 600 kW as explained in the previous section, the maximum air flow requirement is approximately 8 lb/sec (6300 SCFM). For the flow of water at pressures greater than 250 psia, only 2 lb/sec (14 gpm) is needed. If steel pipes were used, air flow rates of 3 to 4 lb/sec could be used because of higher allowable material temperatures.

238. Pressure drop calculations were made to determine feasibility of supplying this quantity of air to the end of a 5000 m hole. In most of the following calculations, incompressible flow equations were assumed, and make the results applicable only to small pressure drops. A series of steps are necessary to complete the evaluation, the first being the wall friction pressure drop in the pipe.

239. For the fL/D_H friction losses down the stems to the penetrator tip (5000 meters), pressure drop can be calculated by

$$\Delta P_f = \frac{2 \frac{fL}{D_H} W^2}{g_c \rho A_F^2}$$

where

- f - Fanning friction factor, unitless
- L - total length of penetrator, in.
- D_H - hydraulic diameter, in.
- W - coolant flow rate, lb/sec
- g_c - gravitation constant, $\frac{\text{lb m}}{\text{lb f}} \cdot \frac{\text{in.}^2}{\text{s}^2}$
- ρ - average density of coolant, lb/in.^3
- A_F - stem flow area, in.^2
- ΔP_f - friction pressure drop down stem, lb f/in.^2

The hydraulic diameter by definition is

$$D_H = \frac{4 A_F}{W.P.}$$

where

W. P. - wetted perimeter, in.

For the current penetrator design

$$A_F = A_s - A_R - A_W - A_c$$

where

A_s	-	Solid cross-sectional area stem	- 83.3 in.^{2}
A_R	-	Cross-sectional area of 3 coolant return pipes	- 8.5 in.^{2}
A_W	-	Cross-sectional area of helium flow tube and nine power wires	- 0.5 in.^{2}
A_c	-	Cross-sectional area of core	- 9.6 in.^{2}

$A_F = 64.7$ in.^{2}

and

$$W.P. = \pi (D_s + 3 D_R + D_W + D_c) \qquad (4)$$

where

D - Respective pipe or wire outside diameter.

Therefore

$$D_H = 4 \frac{(64.7)}{68.7} = 3.8 \text{ in.}$$

240. The Fanning friction factor above was estimated based on using a hydraulic Reynolds number calculated by

$$Re_H = \frac{D_H W}{A_F \mu}$$

where

W equals coolant flow rate.

241. For air and water coolant flows of 2 ⟶ 16 lb/sec, Re_H numbers were $0.5 \times 10^5 \longrightarrow 8 \times 10^5$. Using a roughness factor of ~ 0.004, Fanning friction factors were of the order of ~ 0.005.

242. The overall total penetrator stem length for the fL/D_H calculation above is

$$L \leq 5000 \text{ meters or } 1.97 \times 10^5 \text{ in.}$$

243. Substituting the above parameters, the total stem friction pressure drop down to the penetrator tip as a function of coolant flow and density is

$$P_f = 3.2 \times 10^{-4} \frac{W^2}{\rho}$$

244. Figure 43 shows the stem pressure drop using this equation. For air flow of 8 lb/sec at an average of 300°F and 500 psia, the pressure drop is only 20 psi.

245. In the reference EMP design, the penetrator stems are connected in series. Each stem length is 20 ft long and has a support plate at each interface. There are 820 interfaces for the maximum 5000 meter length. The purpose for these plates is twofold:

a. To give structural rigidity to the stem section.

b. To support the weight of the retractable core, coolant/debris return pipes and power lines.

246. To allow for coolant flow down to the penetrator tip, each support plate has 35 flow holes. As a result, there are a significant number of contraction and expansion flow losses. Since the thickness of these plates is small compared to the upstream and downstream flow diameters, a sharp-edged orifice loss calculation is made to conservatively estimate the total pressure drop for 820 plates.

247. The pressure drop across one plate is

$$\Delta P_o = \left(\frac{W}{C_d S_o}\right)^2 \left(\frac{1 - (S_o/S)^2}{2\rho g_c}\right)$$

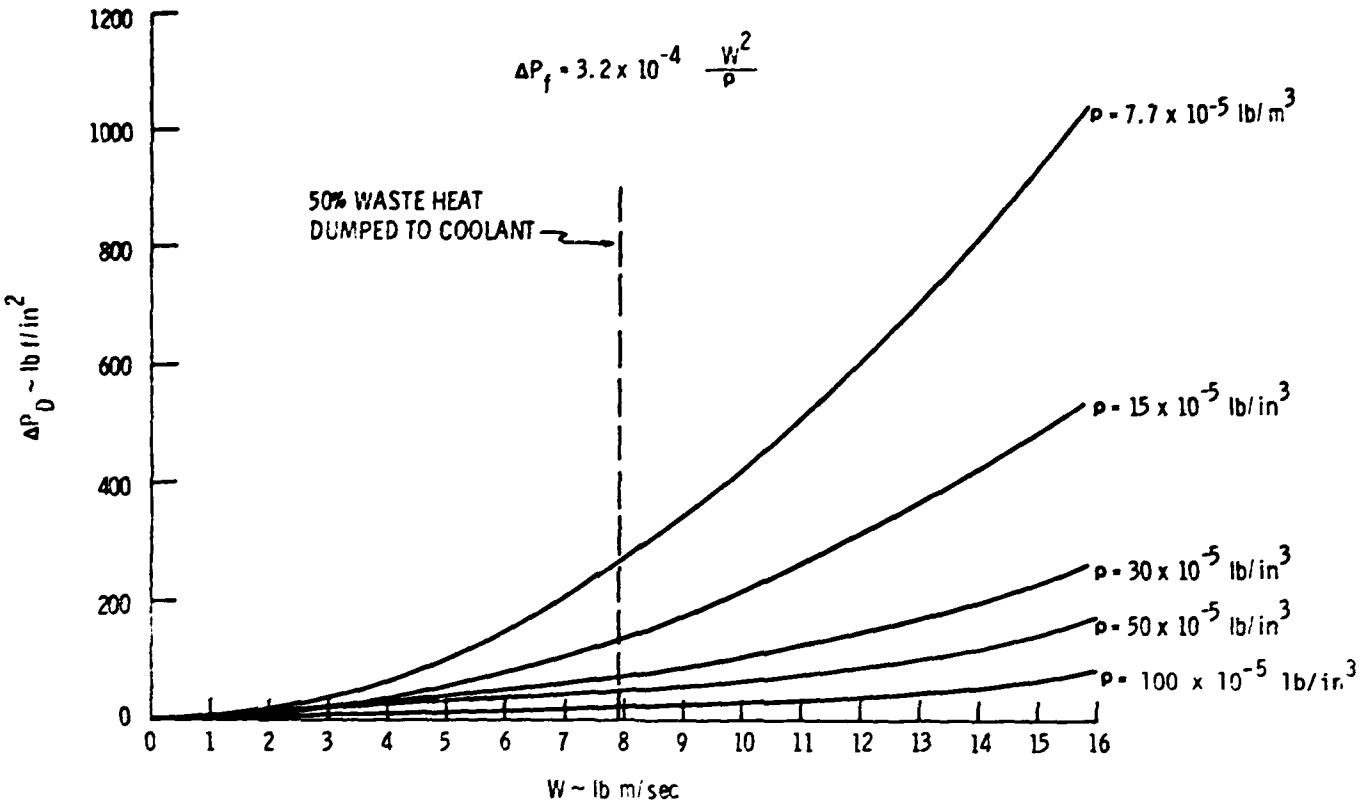

Figure 43. Total friction pressure drop down penetrator stem vs coolant flow rate. Note: The density of water is ~ 3.6×10^{-2} lb/in.^{3}. The pressure drop for water is negligible.

where

W	-	Flow rate, lb/sec
C_d	-	Orifice discharge coefficient, unitless
S_o	-	Orifice flow area, $in.^2$
S	-	Upstream flow area, $in.^2$
ΔP_o	-	Pressure drop across one plate, psi

248. For high Reynolds number C_d approaches about 0.61; the plate flow area hole is 1.100 $in.^2$; and the upstream flow area is 64.7 $in.^2$. Substituting into the equation the pressure drop for coolant flow of 7.9 lb/sec and density at 200°F and 400 psia is 1510 psia. The impossibility of this value indicates the need for a design revision.

249. The support plate design of Figure 36 contains 11 $in.^2$ of flow area which may be possible to enlarge to nearly 18 $in.^2$. If this flow area and the 40 ft long stems are selected (making 410 plates rather than 820), the pressure drop is substantially reduced. With these dimensions, the pressure drop equation is

$$\Delta P = 0.00442\ W^2/\rho$$

Figure 44 is a plot of this equation for densities ranging from 100°F and 25 psia (7.7×10^{-5} $lb/in.^3$) to 200°F and 850 psia (200×10^{-5} $lb/in.^3$). With the results of Figures 42 and 43, surface air compressor outlet pressures of 750 - 1000 psia are needed to supply the adequate air flow cooling, provided the pressure drop in the pneumatic mucking tubes is not excessive.

250. There are two air flow return paths to the surface - the pneumatic mucking tubes carrying the solidified lava, and the liner coolant path formed by the annulus between the stem and the liner wall. Previous heat flow analysis indicated an air flow rate of 1 lb/sec. is necessary. The reference design shows a 0.25 in. annulus (8.64 $in.^2$ flow area). Using a compressible isothermal equation at 300°F and 500 psia at the penetrator head, the flow passage chokes. The annulus must be increased to greater than 0.43 to avoid choking over its 5000 in. length.

251. The pneumatic mucking system fluidizes the solidified lava in the remaining portion of the air, carrying it to the surface inside three 1.8 diameter tubes. For the flow of air as a carrying gas with rock solids, there are several modes of flow possible, depending

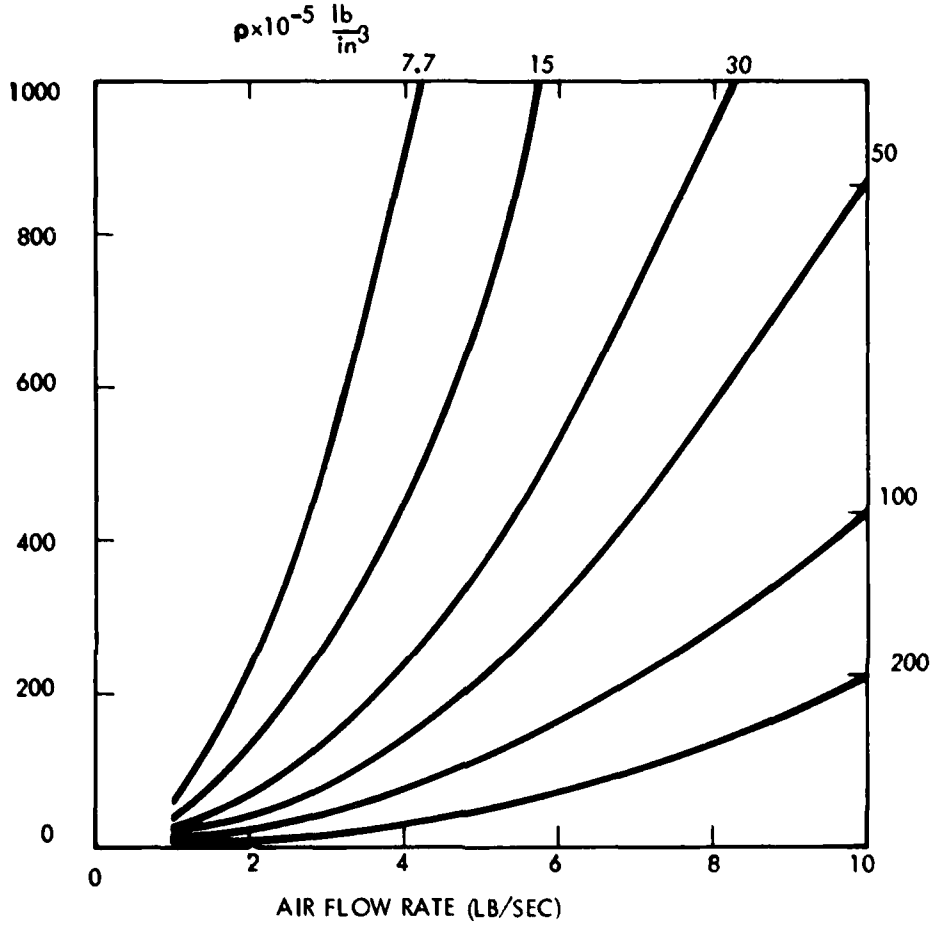

Figure 44. Stem support plate pressure drop for maximum flow area configuration and 410 plates

depending upon the density of the rock solids, solids-to-air weight ratio and air velocity. With low-density rock solids, or low solids-to-air ratios, and high air velocities, the solids may be fully suspended and fairly uniformly dispersed over the return pipe cross section. In a horizontal pipe with low solids-to-air ratios and low air velocities, the solids may bounce along the bottom of the pipe. With high solids-to-air ratios and low air velocities, the rock solids may settle to the bottom of the pipe and form dunes with the rock particles moving from dune to dune (Reference 10).

252. Assuming a minimum penetration rate of 5 m/hr and a cylindrical melt-out of the rock material, the solid mass flow rate for granite is 0.64 lb/sec. Using an air flow rate of 7.9 lb/sec, the solid-to-air weight ratio is 0.08 for granite. These are very low ratios compared to those used in conventional pneumatic conveying. In practice, the actual conveying velocities used in systems with low solids-to-gas weight-rate ratios (< 10), i.e. conventional pneumatic conveyors (References 11 and 12, are generally over 50 ft/sec. The air coolant velocity is ~ 170 ft/sec which is more than ample to convey small particles of rock material. For high solid-to-gas weight-rate ratios (> 50), the actual gas velocities used are generally less than 25 ft/sec and are approximately equal to twice the actual solids velocities (Reference 10).

253. For low rock solids-to-air weight ratio, the minimum carrying velocity can be estimated by the following equation proposed by *Dalla Valle* (Reference 13), based on conveying tests with particles less than 0.32 in. in size. Using air as the carrying gas:

$$v_c = 270 \left(\frac{\rho_s}{\rho_s + 62.3} \right) D_s^{0.40}$$

where

v_c - Minimum carrying velocity, ft/sec

ρ_s - Density of the solids particles, lb/ft^3

D_s - Diameter of largest particle to be conveyed, ft

254. The density of granite is approximately 186 lb/ft^3, respectively. From the above equation, for particles as large as 0.32 in. the minimum carrying velocity required is 48 ft/sec.

255. For one return pipe, the minimum carrying mass flow rate is therefore

$$W_c = A_p v_c \rho_A$$

where

A_p - cross-sectional flow area of a return pipe, ft^2

ρ_A - average density of air in return pipe, lb/ft^3

W_c - minimum carrying mass flow rate for air, lb/sec

$W_c = 0.73$ lb/sec

256. The total minimum air mass flow needed for all three return pipes is 2.19 lb/sec at the average density of air used in the return pipe for conditions of ~225 psia and ~250°F.

257. For upflow of gases and solids in vertical pipes, the minimum carrying velocity for low solids-to-gas weight-rate ratios can be estimated by the following equation proposed by Dalla Valle in Reference 13:

$$v_c = 910 \left(- \frac{\rho_s}{\rho_s + 62.3} D_s \right)^{0.60}$$

258. Substituting values for granitic rock material and using a particle diameter of 0.32 inches gives 78 ft/sec.

259. In Reference 15 for low solid-to-gas weight-rate ratios less than 10, $v_G - v_s$ in a vertical pipe is about equal to the free fall terminal velocity of the particles. Also, in Reference 15 for the case of spherical particles, the terminal velocity can be calculated by

$$v_t = \frac{4 g_c D_s (\rho_s - \rho_G)}{3 \rho_G C}^{0.5}$$

where C - drag coefficient, dimensionless

ρ_G - gas density

260. In Reference 15, a plot is presented of drag coefficient versus Reynolds number. In the Newton's Law region which covers the Reynolds-number range of 1000 to 200,000 drag coefficient C has an approximately constant value of 0.4 for spherically shaped particles. For a particle diameter of 0.32 inches, the terminal velocity is 25 ft/sec.

261. The above fluidization requirement is less than the thermal requirement needed for solidification. A pressure drop analysis of 7.9 lb/sec air flowing in three tubes of 1.8 in. diameter indicates that the flow is choked for pressure levels of 1000 psia, the highest pressure level considered reasonable for this application.

262. A number of conclusions can be drawn from the preceding air flow calculations. Up to 8 lb/sec of air or 2 lb/sec of water is needed to solidify the molten rock before the fluidized mucking system can remove it. Within the present geometric constraints of 12 in. diameter and a 3 mile hole, the water pressure drop and pressure level (to prevent boiling) are not a problem since only 500 psia pump pressure is required. The air flow pressure requirement is substantially different, that is, there is insufficient flow area at reasonable pressure levels to provide 7.9 lb/sec. The engineering solutions to this problem are not immediate. A more detailed analysis of the coupled heat transfer/pressure drop relationships including compressible flow with heat exchange between the counterflow air streams, the drill string and the glass liner could show a lower flow rate and area requirement.

263. If the 8 lb/sec is still required and the flow area is insufficient after a more sophisticated analysis, the remaining options are water cooling or a change in the more constraining requirements. For example, an increase in allowable diameter to 14 in. would provide nearly double the available flow area. These design/requirement trade-off sequences must be addressed in the first period of a preliminary design phase.

PART VII: DEVELOPMENT PROGRAM

264. With the completion of the Phase I Conceptual Design Study of an Earth Melting Penetrator to be used as a geoprospecting tool, the details of subsequent phases can be prepared. The development program consists of three more phases spanning the next 5 fiscal years and is depicted in Figure 45.

Phase II - Prototype Penetrator Demonstration

265. The objective of Phase II is to demonstrate a prototype penetrator in the field. The penetrator, consisting of the penetrator body, heaters, transformers, and associated hardware to permit field demonstration of the "hot end" of the system, will be designed and two assemblies fabricated. Operational performance will be evaluated through demonstration of penetration rate; hole and core formation; response to guidance through differential heating; starting, stopping, and retraction evaluations; general compatibility of the penetrator with earth; and internal electrical, thermal, cooling, and extridite removal.

Tasks associated with this phase include:

Task 1 Heater Tests
Task 2 Penetrator Design
Task 3 Penetrator Fabrication and Assembly
Task 4 Field Test Plan
Task 5 Field Tests
Task 6 Program Management and Integration

266. The objectives of these tasks are as follows:

Task 1 - heater tests

267. A heater will be fabricated, based on the conceptual design of Phase I and the detailed design of Task 2, to verify satisfactory heater performance. The heater will be assembled into a refractory body and the completed test assembly used to melt earth

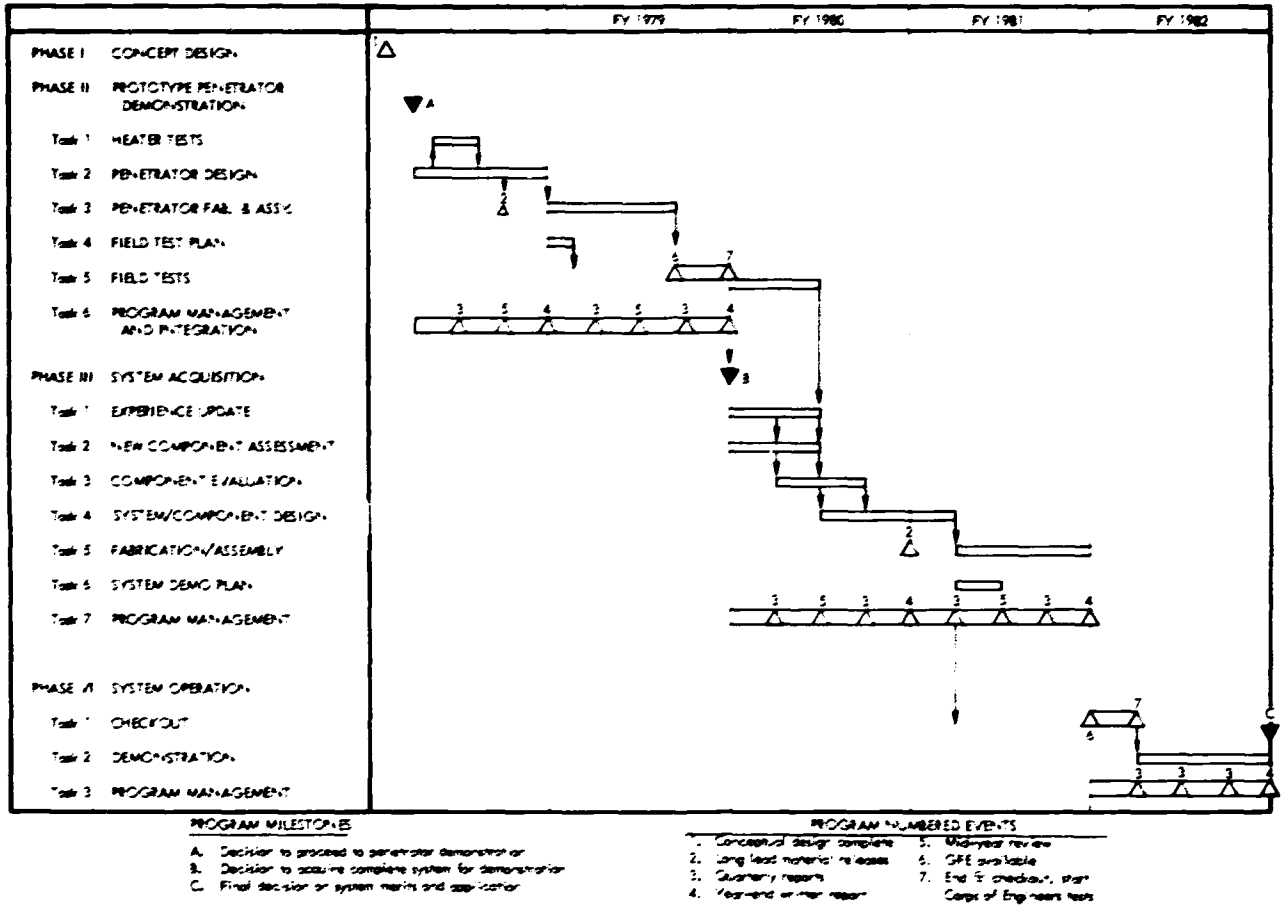

Figure 45. Development plan – geoprospecting with earth melting penetration technology

material, simulating the heat sink and demonstrating compatibility of the refractory body with the earth.

Task 2 - penetrator design

268. Detailed design of the prototype penetrator as previously described will be the objective of Task 2. Specifications of field support equipment recommended for government supply will be developed and will include such items as those required to supply electrical power, fluids, and gases to the penetrator.

Task 3 - penetrator fabrication and assembly

269. Work in Task 3 will involve procurement, fabrication and assembly of the hardware designed in Task 2.

Task 4 - field test plan

270. In Task 4, details of the test phase will be developed. Included will be test sequence logic and procedures for operation of the penetrator.

Task 5 - field tests

271. During Task 5, field test demonstrations will be performed. A test checkout will be performed at Westinghouse prior to delivery to the Corps of Engineers. This test will require some government supplied equipment. It is recommended that the Corps of Engineers cooperate in this test as part of its orientation to penetrator operation. The penetrator will then be turned over to the Corps of Engineers for evaluation with technical assistance from Westinghouse. In addition, an evaluation of logging instruments can be performed in glass-lined holes and compared with performance in conventional holes upon request by the Corps of Engineers.

Task 6 - program management and integration

272. Task 6 provides program administration details such as schedule and cost monitoring, progress reports, and customer interface. In addition, technical integration is included to assure that the penetrator design requirements remain consistent with the overall system requirements of the follow-on phases and that technical integration with the government supplied equipment for the field tests is maintained.

273. This phase represents a significant step in earth melting penetrator technology because of the scale-up from Los Alamos feasibility experiments. The time span is 2-1/4 years, with the effort divided between these years to satisfy fiscal year funding constraints. To maintain reasonable costs while achieving the field testing stage, LASL experience, off-the-shelf components or adaptation of same, and a restricted development effort will be employed. While the level of confidence is still considered acceptable, this approach does introduce some risk to the program in that the penetrator assembly involves high technology and is best evaluated as an assembly. At this point, the risk incurred is anticipated in the area of achieving specific design performance objectives such as penetration rate. Experimental results derived from performance demonstration may be used to update design in subsequent phases.

274. At a logical program decision point near the end of Phase II, continuation or termination of the program can be considered and determined.

Phase III - System Acquisition

275. The objective of Phase III is the acquisition of a complete system for checkout and field demonstration in Phase VI. This effort, of course, assumes a successful Phase II program and the decision to proceed. Current plans envision the following tasks as appropriate to Phase III:

Task 1 Experience Update
Task 2 New Component Assessment
Task 3 Component Evaluation
Task 4 System and Component Design
Task 5 Fabrication and Assembly
Task 6 System Demonstration Plan
Task 7 Program Management

276. Objectives of these tasks are detailed in the following paragraphs.

Task 1 - experience update

277. The design and experimental experience obtained from Phase II penetrator tests will be factored into an updated design of the penetrator to improve performance.

Task 2 - new component assessment

278. Components not involved in the Phase II program will be evaluated prior to their integration into the design. Components such as guidance, control, and grippers are in this category. It is anticipated that some test evaluations in the next task will be required as a result of these assessments.

Task 3 - component evaluations

279. Component tests to evaluate critical parameters of components resulting from Task 2 assessments and from Phase II test results are included here. Effects of a "hostile" environment on a guidance component, electrical circuit, or material are candidate areas for evaluation.

Task 4 - system/component design

280. During this task, the system design will be completed. Components of the system will be designed or specifications prepared for procurement. The designed and procured components will be interfaced and integrated. Additional government support equipment beyond that determined in Phase II will be specified. This task should benefit significantly from the penetrator design effort of Phase II.

Task 5 - fabrication and assembly

281. During this task, the system will be fabricated, procured, and assembled and assembly test performed to ready the system for operational tests in Phase VI.

Task 6 - system demonstration plan

282. A System Demonstration Plan will be required to define the test plan objectives and sequence logic of tests. Included will be procedures for the operation of the penetrator system.

Task 7 - program management

283. This task will provide the program supervision and customer contact for technical, schedule, and cost control and reporting.

284. The output of this phase will be one complete geoprospecting EMP system and selected spare parts for use in Phase VI. This phase is shown in Figure 42 to span 2 years.

Phase IV - System Operation

285. Phase IV is the test phase for the hardware acquired in Phase III. Its relationship to the total program is shown in Figure 45 and is expected to be 1 year in duration consisting of the following tasks:

Task 1 Checkout

Task 2 Demonstration

Task 3 Program Management

286. Objectives of these tasks are detailed in the following paragraphs.

Task 1 - checkout

287. Task 1 involves a brief test program conducted by Westinghouse at the Corps of Engineers site to check out the initial operation of the system and procedures. It is expected to consist of an integrated test with Corps of Engineers personnel to insure orderly transfer of equipment and provide training.

Task 2 - demonstration

288. Task 2 is an extended test period under the direction of the Corps of Engineers with technical support from Westinghouse. It, in fact, represents the significant system demonstration to which the total program has been directed. Demonstration is to take the form of a prototype field operation to prove the worthiness of the technology for geoprospecting applications.

Task 3 - program management

289. Task 3 provides the program supervision and customer contact for technical, schedule, and cost control and reporting as well as source engineering support for the Corps of Engineers field demonstrations.

290. At the end of Phase IV, another logically scheduled program milestone will allow for a decision regarding the deployment of the earth melting penetrator (EMP) as a geoprospecting system.

Estimated Contract Resources

291. The estimated resources by phase and task and by fiscal year are presented in Table 9. The costs are estimated based on 1977 dollars, do not include escalation, and should therefore be considered approximate.

Table 9

Estimated Program Resources

	BASIC RESOURCES				COSTS BY FY*					PHASE TOTAL
	ENGR	DFTG	TECH	MATL+	1978	1979	1980	1981	1982	
	MAN MONTHS									
PHASE II										
Task 1	2.5	1.0	2.0	5	39.3					
Task 2	12.0	6.0	-	5	130.8					
Task 3	2.0			150		213.8				458.6
Task 4	0.5					4.2				
Task 5	3.0		3.0			20.1	16.8			
Task 6	8.0					33.6				
PHASE III										
Task 1	1.5						12.6			
Task 2	3.0						25.2			
Task 3	3.0			75			123.2			735.2
Task 4	13.0	6.0	3.0	6			113.4	54.4		
Task 5	3.0		3.0	250				364.4		
Task 6	1.0							8.4		
Task 7	8.0							33.6		
PHASE IV										
Task 1	3.0		6.0						48.6	
Task 2	3.0								25.2	99.0
Task 3	3.0								25.2	
	FISCAL YEAR TOTAL				170.1	271.7	291.2	460.8	99.0	1292.8

*Cost estimates listed in thousands of dollars

+Material costs do not include surface support equipment (GFE), 5000 m of stems or downhole electronics (see Tables 7 and 8).

REFERENCES

1. Black, D. L., et al., "Basic Understanding of Earth Tunneling by Melting," Westinghouse Astronuclear Laboratory, Pittsburgh, Pennsylvania, WANL-TME-2841, Vol. II, October 1973.

2. Hetényi, M., Beams on Elastic Foundation, University of Michigan Press, 1946.

3. Fisher, H. N., "Thermal Analysis of Some Subterrene Penetrators," Journal of Heat Transfer, August 1975, pp 485-490.

4. Murase, T., McBirney, A. R., "Thermal Conductivity of Lunar and Terrestrial Igneous Rocks in their Melting Range," Science, Vol. 170, 1970, pp 165-167.

5. Lawson, A. W., Jamieson, J. C., "Heat Transfer in the Earth's Mantle," Journal of Geology, Vol. 66, 1958, p 540.

6. Blackett, P. M. S., Lectures on Rock Magnetism, The Weizmann Press of Israel, Jerusalem, 1956.

7. Nagata, T., Rock Magnetism, Revised Edition, Maruzen Co., Ltd., Tokyo, 1961.

8. Knowlton, A. E., ed., Standard Handbook for Electrical Engineers, McGraw-Hill, New York, 1957, Section 14.

9. Ciavatta, A., System Requirements and Analysis of an Experimental Guided Tunneler, ERDA E(49-18)-2127.

10. Earth Melting Penetrator - Current Design, Drawing Number 712J433.

11. Wen, C. Y. and H. P. Simons, American Institute of Chemical Engineers J., 5, pp 263-267, 1959.

12. Krasicki, B. R., "Fluid Hydraulic Evaluations for ℵ AESD EMP," Westinghouse Advanced Energy Systems Division, Pittsburgh, Pennsylvania, DRM No.: DA-0386, August 10, 1977.

13. Hudson, W. G., Chemical Engineering, 61 (4), pp 191-194, 1954.

14. Zenz, F. A. and D. F. Othmer, "Fluidization and Fluid particle Systems," pp 220-222, 322, Reinhold, New York, 1960.

15. Dalla Valle, Heating, Piping Air Conditioning, 4, pp 539-641, 1932.

16. Hinkle, H., Ph. D Thesis, Chemical Engineering, Georgia Institute of Technology, Atlanta, 1953.

17. Perry, J. H., "Chemical Engineers Handbook," 4th ed., McGrant Hill Co., New York, 1963.

In accordance with letter from DAEN-RDC, DAEN-ASI dated 22 July 1977, Subject: Facsimile Catalog Cards for Laboratory Technical Publications, a facsimile catalog card in Library of Congress MARC format is reproduced below.

Black, D L
Feasibility study of an earth melting penetrator system for geoprospecting tunnel right-of-ways / by D. L. Black, Westinghouse Advanced Energy Systems Division, Large, Pennsylvania. Vicksburg, Miss. : U. S. Waterways Experiment Station ; Springfield, Va. : available from National Technical Information Service, 1978.
155 p. : ill. ; 27 cm. (Technical report - U. S. Army Engineer Waterways Experiment Station ; S-78-17)
Prepared for Office, Chief of Engineers, U. S. Army, Washington, D. C., under Contract No. DACW 39-76-C-0163.
References: p. 154-155.

1. Drilling. 2. Earth melting penetrators. 3. Feasibility studies. 4. Geophysical exploration. 5. Penetration. 6. Penetrators. 7. Right of way. 8. Rock melting penetrators. 9. Soil penetration. 10. Subsurface exploration. 11. Tunnels. 12. Underground openings. I. United States. Army. Corps of Engineers. II. Westinghouse Electric Corporation. Advanced Energy Systems Division. III. Series: United States. Waterways Experiment Station, Vicksburg, Miss. Technical report ; S-78-17.
TA7.W34 no.S-78-17